A Role of *Pox neuro* in the Developing *Drosophila* Brain: Determination of Large-Field Neurons Essential for Ellipsoid Body Formation and of Ventral Projection Neurons

Dissertation

zur

Erlangung der naturwissenschaftlichen Doktorwürde

(Dr. sc. nat.)

vorgelegt der

Mathematisch-naturwissenschaftlichen Fakultät

der

Universität Zürich

von

Shilpi Minocha

aus

Indien

Promotionskomitee

Prof. Dr. Markus Noll

(Vorsitz und Leitung der Dissertation)

Prof. Dr. Reinhard F. Stocker

Prof. Dr. Konrad Basler

Werner Boll

Zürich, 2010

CONTENTS

Summary

The wealth of genetic and molecular tools available for the detailed analysis of gene function in *Drosophila* has been instrumental in the understanding of the genetic basis of various fundamental biological processes. Thus, *Drosophila* has been used extensively to investigate various aspects of neural development and neural morphology. The *Drosophila* brain is characterized by an enormous diversity and specificity of neurons and exhibits the basic architecture common to most insect brains with a cortex of cell bodies surrounding central neuropil structures and a complex axonal and dendritic circuitry. This organization may originate from the fact that many neurons in the *Drosophila* brain are unipolar, allowing all synapses to occur in a core. However, relatively little is known about the mechanisms that give rise to such complex brain structures and their associated functions.

The *Pox neuro* (*Poxn*) gene, a member of the *Drosophila* Pax gene family, encodes a transcription factor with a DNA-binding paired domain. It is expressed in discrete domains throughout brain development. We have dissected the neuronal projection pattern of the Poxn-expressing neurons during brain development. (In the following we call these neurons that express *Poxn* in the wild type *Poxn*-neurons, also in *Poxn* mutants). A mojority of Poxn-expressing cells in the developing brain are primary neurons that are born during embryogenesis and establish a pioneering scaffold in late embryonic and early larval stages, which might then be utilized by the later appearing *Poxn*-neurons to extend their neurites along these pre-established routes in third instar larvae and pupae. Most of the *Poxn*-neurons are immature at the end of the larval stages and undergo the final steps of differentiation during the first half of pupariation. A majority of these neurons persist through metamorphosis to perform their functions during adulthood.

During metamorphosis, the axons of the neurons in the dorsal Poxn-expression domain form the ellipsoid body neuropil by 45 hours after puparium formation. In the *Poxn* mutant brain, the prominent topology of the ellipsoid body is degenerate and transformed into several globular structures.

The projections of the *Poxn*-neurons in the ventral cluster pass through a few lateral glomeruli in the larval antennal lobe, through the presumptive precursor of the adult antennal lobe in the larval brain, and then target the lateral protocerebral regions through the middle antennocerebral tract (mACT). These neurons target the adult antennal lobes in all stages of pupal development and these connections persist in the adult brain, where they form dendritic termini in the antennal lobes, send axonal projections through the mACT, and arborize in the lateral horn, a higher olfactory center of the adult brain. The location of the cell bodies as well as the morphology of the neural projections qualifies the majority of these neurons as ventral projection neurons. Most of the adult antennal lobe glomeruli, including the sexually dimorphic glomeruli, are targeted. In the adult brain of *Poxn* mutants, these neurons are still present but exhibit aberrant projection patterns. Their innervations of the adult antennal lobes in larvae and adults are dramatically reduced, including the sexually dimorphic glomeruli, and none of the axons appear to pass through the mACT. As a consequence of the latter aberrations, the lateral horn is no longer targeted.

In conclusion, the *Poxn* function in the developing *Drosophila* brain is not important for the survival of these two clusters of cells, representing large-field and ventral projection neurons, as their number remains the same in *Poxn* mutants, but is crucial for proper fate determination, which results in the precise targeting of specific neuropil structures and the correct formation of the ellipsoid body neuropil. Hence, in *Poxn* mutants we expect the functions fulfilled by the *Poxn*-neurons to be largely

impaired and the neural network in which these neurons are embedded to be substantially affected.

Zusammenfassung

Die Fülle genetischer und molekularbiologischer Werkzeuge, die für die detaillierte Analyse von Genfunktionen in der Fruchtfliege *Drosophila melanogaster* zugänglich sind, ist sehr wichtig für das Verständnis der genetischen Basis verschiedener biologischer Prozesse. Deshalb wird *Drosophila* auch extensiv als Modellorganismus für die Erforschung verschiedenster Aspekte in der Entwicklung und Morphologie des zentralen Nervensystems eingesetzt. Das Hirn von *Drosophila* zeichnet sich durch eine enorme Vielfalt und Spezifität seiner Neuronen aus und zeigt die grundsätzliche Architektur, welche die meisten Insektenhirne auszeichnet. Ein Cortex von Zellkörpern umgibt die zentral gelegenen Neuropilstrukturen, die sich aus einem komplexen Netzwerk von Axonen und Dendriten zusammensetzen. Diese Struktur lässt sich vermutlich auf den Umstand zurückführen, dass viele der Neuronen im Hirn von *Drosophila* eine unipolare Morphologie aufweisen und damit das Auftreten der Synapsen in solchen zentralen Sektoren fördern. Über die Mechanismen, welche zu solchen komplexen Hirnstrukturen und den damit assoziierten Funktionen führen, ist immer noch relativ wenig bekannt.

Das *Pox neuro* (*Poxn*) Gen, ein Mitglied der Pax-Genfamilie kodiert für einen Transkriptionsfaktor, der eine DNA-bindende *Paired*-Domäne trägt. *Poxn* ist während der gesamten Hirnentwicklung in diskreten Domänen exprimiert. Wir haben das Projektionsmuster der Poxn-exprimierenden Neuronen - einfachheitshalber (auch in *Poxn* Mutanten) *Poxn*-Neuronen genannt - während der gesamten Hirnentwicklung analysiert. Ein Grossteil dieser Zellen wird während der Embryogenese im sich entwickelnden Hirn geboren und etabliert ein Pioniergerüst von Projektionen während den späten Embyonal- und frühen Larvenstadien, welches dann durch die später auftretenden *Poxn*-Neuronen im

späten dritten Larvenstadium und im Puppenstadium genutzt wird, um ihre Neuriten entlang dieser vorgegebenen Routen auszubilden. Die meisten *Poxn*-Neuronen sind am Ende des Larvenstadiums noch nicht voll differenziert und durchlaufen die letzten Differenzierungsschritte während der ersten Hälfte des Puppenstadiums. Eine Mehrheit dieser Neuronen überlebt die Metamorphose, um ihre eigentlichen Funktionen in der adulten Fliege zu erfüllen.

Während der Metamorphose, etwa 45 Stunden nach dem Verpuppen der Larve, bilden die Axone der Neuronen in der dorsalen Poxn-Expressionsdomäne den Ellipsoidkörper. Im Hirn der *Poxn* Mutante ist die prominente Struktur des Ellipsoidkörpers degeneriert und hat sich in eine Anordnung von glubulären Strukturen gewandelt.

Die Projektionen der Neuronen in der ventralen Poxn-Domäne passieren nur wenige der lateralen Glomeruli des larvalen antennalen Lobus, durchdringen den mutmasslichen Vorläufer des adulten antennalen Lobus im larvalen Hirn und projizieren durch den medialen antennocerebralen Trakt (mACT) in Regionen des lateralen Protocerebrums. Diese Neuronen projizieren während der gesamten Puppenentwicklung in die antennalen Loben und die Verbindungen bleiben auch im adulten Hirn bestehen, wo sie dendritische Termini im antennalen Lobus und axonale Projektionen durch den mACT mit Verästelungen und Synapsen im lateralen Horn, einem höheren olfaktorischen Zentrum, bilden. Die Lage der Zellkörper, aber auch die Morphologie der neuralen Projektionen lassen für die Mehrheit dieser Neuronen eine Zuordnung zu den ventralen Projektionsneuronen zu. Die Dendriten dieser Neuronen kontaktieren eine Mehrzahl der Glomeruli des adulten antennalen Lobus, einschliesslich der sexuell dimorphen Glomeruli. Im adulten Hirn der *Poxn* Mutante sind diese Neuronen immer noch vorhanden, weisen aber ein stark abweichendes Projektionsmuster auf. Die Innervierung

des adulten antennalen Lobus durch diese Neuronen in Larven und adulten Fliegen ist dramatisch reduziert, und dieser Effekt betrifft auch die sexuell dimorphen Glomeruli in diesen Loben. Es werden auch keine axonalen Projektionen der betroffenen Neuronen durch den mACT beobachtet, und als Konsequenz davon sind auch keine Verästelungen im lateralen Horn sichtbar.

Zusammenfassend lässt sich sagen, dass die Funktion von *Poxn* im sich entwickelnden Hirn von *Drosophila* unwichtig für das Überleben der betreffenden Neuronen in den zwei Zellgruppen ist, die in der einen Domäne hauptsächlich Tangentialneuronen des Ellipsoidkörpers, in der anderen ventrale Projektions-neuronen darstellen, da die Anzahl der Neuronen nicht durch das Fehlen der *Poxn* Funktion negativ beeinflusst wird. Die *Poxn* Funktion ist jedoch unabdingbar für die richtige Differenzierung dieser Neuronen, welche präzise Projektionen in die spezifischen Neuropilstrukturen senden und sogar massgeblich den Ellipsoidkörper ausbilden. So ist zu erwarten, dass im Hirn der *Poxn* Mutante die Neuronen, in denen dieser Transkriptionsfaktor nun fehlt, funktionell stark beeinträchtigt sind und das neuronale Netzwerk, in welches diese Neuronen eingebettet sind, spezifische und substanzielle Funktionseinbussen oder Fehlfunktionen zeigt.

1. Introduction

During development *Drosophila melanogaster*, a holometabolous insect, displays successive change of form between larva, pupa, and adult by undergoing metamorphosis. During metamorphosis, the nervous system of the fly is extensively reorganized, and this affects the fate of different types of neurons (Truman, 1990; Levine *et al*., 1995; Consoulas *et al*., 2000). Many neurons are born during larval or pupal stages, and have a function in the larger and more complex nervous system of the adult fly, while some larval neurons die during metamorphosis. Another distinct class of neurons functions in both larvae as well as in the imago, but exhibits pronounced remodeling of dendrites and axons during metamorphosis (Consoulas *et al*., 2000; Tissot and Stocker, 2000; Marin *et al*., 2005). The development of the brain is divided into embryonic and postembryonic neurogenic phases. During embryogenesis, a set of neuroblasts generates small lineages of primary neurons and glial cells, which differentiate and give rise to a functional larval brain with distinct neuropil compartments (Truman, 1990; Younossi-Hartenstein *et al*., 2003, 2006). During postembryonic neurogenesis in the larva, certain neuroblasts resume their proliferative activity and produce lineages of secondary neurons, which differentiate in the pupa (Dumstrei *et al*., 2003; Marin *et al*., 2005) and form neurites that integrate, along with the remodeled projections of primary neurons, to give rise to the adult brain neuropil.

In the adult brain, the central complex (CC), located between the two supraesophageal hemispheres and enclosed by a thin glial lamella, is one of the most prominent neuropil structures described in hexapods (Homberg, 1987; Strausfeld, 1999; Loesel *et al*., 2002; Homberg, 2008). It is composed of four interconnected

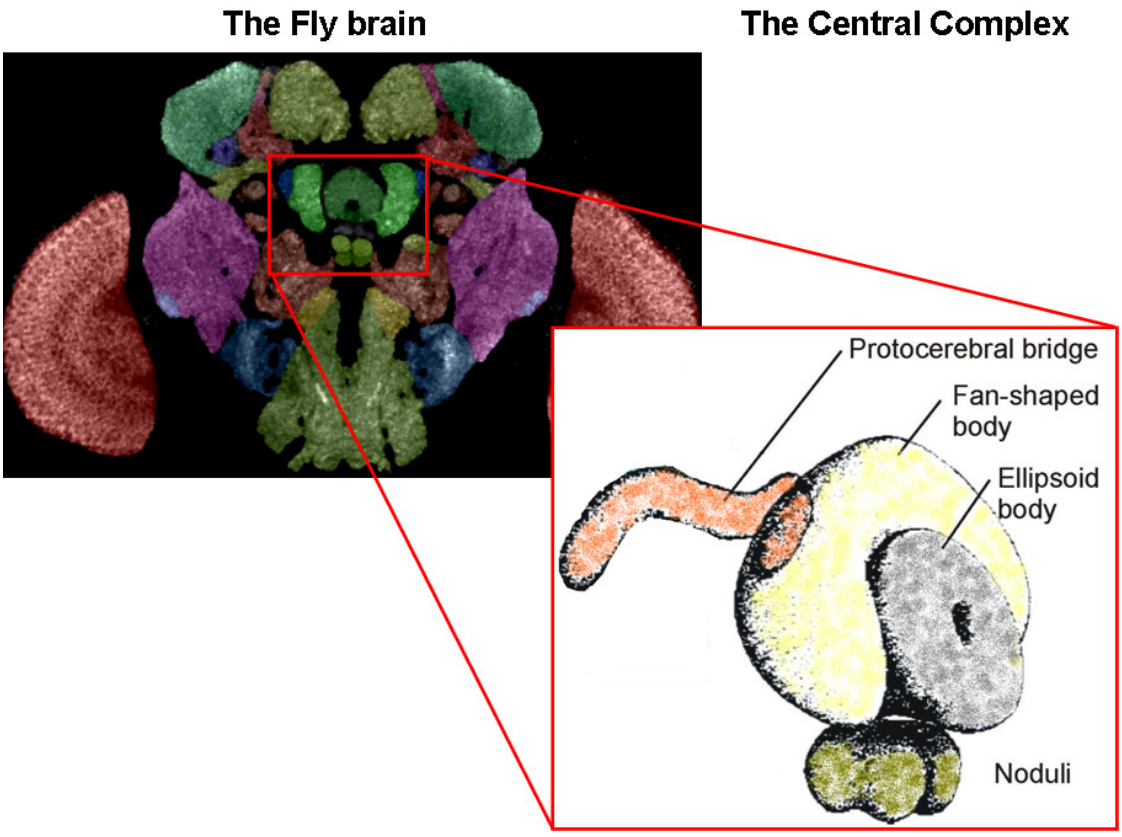

Figure 1. Location of the central complex within the *Drosophila* adult brain and its schematic representation. The central complex consists of the protocerebral bridge, the fan-shaped body, the ellipsoid body, and the paired noduli. Modified from Strauss and Heisenberg, 1993.

neuropils: the protocerebral bridge (pb), the fan-shaped body (fb), the ellipsoid body (eb) and the noduli (no) (Figure 1). Neurons participating in the neuropils of the CC are classified as tangential large-field neurons (LFN) and columnar small-field neurons (SFN). LFNs typically arborize within an individual neuropil of the CC, where they cover the whole neuropil or only a single layer of it, but extend their processes to other brain areas and are thought to provide the principal input to the CC (Figure 2A-C). The large-field neurons of the eb, also called ring (R) neurons, form dendritic arborizations in the lateral triangle (ltr) and ring-shaped axonal projections in the eb (Hanesch *et al*., 1989; Renn *et al*., 1999). R neurons have been classified as 4 types, R1-R4, based on their axonal projection patterns in the eb (Hanesch *et al*., 1989; Renn *et al*., 1999). SFNs are mostly intrinsic and interconnect small domains within or between the different neuropils of the CC (Figure 2D, E), but a subpopulation of SFNs also project to the accessory ventral bodies (Figure 2F) and is thought to provide output from the CC (Hanesch *et al*., 1989).

The CC might play an important role in the coordination of the two brain hemispheres because of its central location (Homberg, 1987; Hanesch *et al*., 1989). Many other roles of the CC have been postulated, like higher control of locomotion (Strauss and Heisenberg, 1993; Ilius *et al*., 1994; Martin *et al*., 1999; Strausfeld, 1999; Strauss, 2002; Poeck *et al*., 2008), control of courtship song production (Popov *et al*., 2003), regulation of courtship behavior (Popov *et al*., 2005), consolidation of long-term olfactory memory (Wu *et al*., 2007), visual learning (Liu *et al*., 2006), memory of spatial orientation (Neuser *et al*., 2008), orientation with the aid of polarized light (Vitzthum *et al*., 2002; Heinze and Homberg, 2007; Sakura *et al*., 2008), and ethanol tolerance (Scholz *et al*., 2000). It has been reported that the central complex is formed late in development and has only a rudimentary counterpart in the larval brain (Renn *et al*., 1999). By

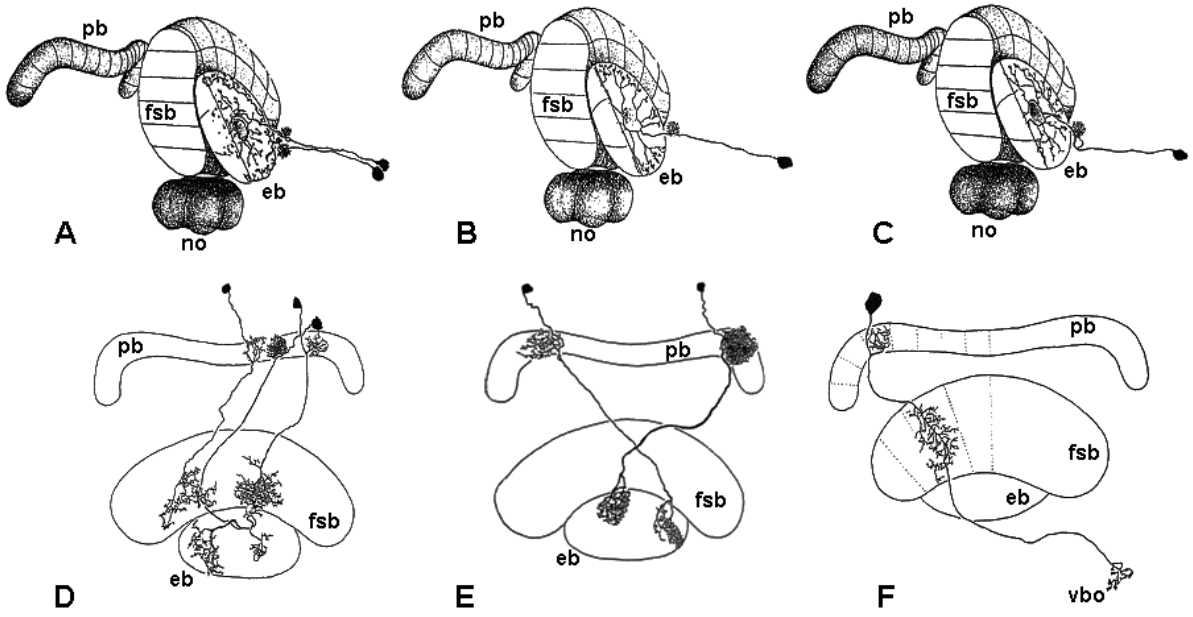

Figure 2. Schematic representation of different types of the eb large-field (Ring) neurons and small-field neurons. R1 to R3 neurons project to the eb via the eb canal and arborize outwardly. R1 axons arborize in an inner ring and extend to the posterior layer, while R2 axons arborize in an outer ring and are restricted to the anterior layer, and R3 axons arborize throughout both inner and midrings. Axons of the R4 neurons arborize in the outer ring and are restricted to the anterior eb. (**A**) An example of R1 and R4 neuron type. (**B**) An example of R2 neuron type. (**C**) An example of R3 neuron type. (**D**) A type of intrinsic columnar small field-neurons interconnecting different substructures of the central complex like pb, fsb, and eb. (**E**) Another type of intrinsic columnar small-field neurons connecting different substructures of the central complex. (**F**) A special class of extrinsic small-field neurons connecting pb, fsb, and contralateral vbo. Abbreviations: eb, ellipsoid body; fsb, fan-shaped body; no, noduli; pb, protocerebral bridge; vb, ventral body. Modified from Hanesch *et al*., 1989.

means of enhancer trap lines specific for adult eb neurons, the formation of this neuropil was shown to be complete by 48 hours after puparium formation (APF) (Renn *et al.*, 1999).

The brain consists of three documented major centers that play important roles in the processing and integration of olfactory stimuli: the antennal lobes, the mushroom bodies, and the lateral horn (de Belle and Heisenberg, 1994; Stocker, 1994; Ito *et al.*, 1998; Heimbeck *et al.*, 2001). *Drosophila melanogaster* exhibits robust behaviors in response to various odor stimuli present in the environment (de Bruyne *et al.*, 1999, 2001). Olfaction helps the flies to experience their environment and react to the various olfactory stimuli by translating them into appropriate behaviors. The qualitative and quantitative differentiation of these odors is important in many contexts, for example in the search of food sources and appropriate egg-laying substrates, the choice of suitable conspecific mating partners, and the avoidance of toxic substances (Stocker, 1994). The olfactory response in flies can be scored either by physiological or behavioral means (Carlson, 1996; Hallem and Carlson, 2004, 2006).

Volatile odorants are perceived by two pairs of primary sensory appendages, the third segment of the antenna and the maxillary palps (Figure 3A, B). They are covered by sensory hairs or sensilla that are innervated by olfactory receptor neurons (Stocker, 1994). The antenna harbors about 450 sensilla, the maxillary palp about 60 sensilla (Figure 3C). The antennal sensilla are divided into three classes: basiconic, coeloconic, and trichoid sensilla. The two maxillary palps, being the simpler olfactory organs carry only basiconic sensilla (Figure 3C). The sensilla are innervated by one to four olfactory receptor neurons (ORNs). The third antennal segment houses about 1200 ORNs, and the maxillary palp contains about 120 ORNs (Stocker, 1994). The ORNs are bipolar and

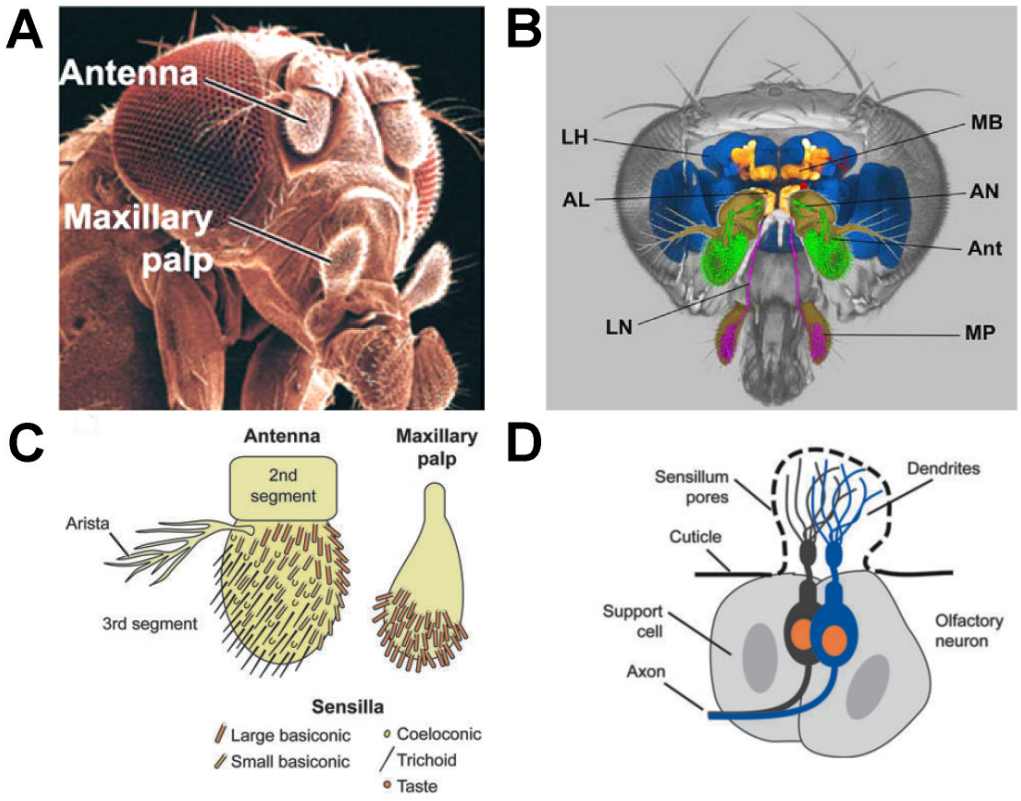

Figure 3. The olfactory system of the adult *Drosophila*. (**A**) The olfactory organs of the fly: the antenna and maxillary palp. **(B)** Various odorants are detected by the olfactory sensory neurons located on the antenna (Ant) and maxillary palp (MP). The OSNs send their axons via the antennal nerve (AN) and the labial nerve (LN) to the antennal lobe (AL). The information is then collected by projection neurons and relayed to the mushroom bodies (MB) and the lateral horn (LH). Modified from Lin *et al*., 2007. (**C**) Schematic representation of the antenna and maxillary palp displaying the three classes of olfactory sensilla. (**D**) Schematic representation of olfactory sensillum structure with two olfactory receptor neurons. A, C, and D are modified from Vosshall and Stocker, 2007.

extend a sensory dendrite into the shaft of the sensillum and an axon to the antennal lobe (Figure 3D), where it innervates a specific glomerulus. Each ORN expresses usually one (occasionally two) ligand-binding olfactory receptor (OR) and the broadly expressed receptor Or83b (Vosshall *et al*., 2000; Larrson *et al*., 2004) (Figure 4). The non-canonical receptor Or83b heterodimerizes with canonical ORs and is necessary for ciliary targeting and proper function of ORs in any ORN and thus acts as co-receptor. However, some coeloconic sensilla function independently of the Or83b receptor. They are generally those whose ORNs react to amines, ammonia, and water vapor (Figure 4), and they utilize ionotropic glutamate receptors (IRs) instead (Benton *et al*., 2009). In addition, the ORNs expressing carbon-dioxide sensitive gustatory receptors, Gr21a and Gr63a, do not express or require Or83b (Figure 4). All ORNs that express a unique combination of ORs target a single antennal glomerulus, and each glomerulus can be targeted by two or more ORN classes.

An OR-to-glomerulus map has been generated (Couto *et al*., 2005: Fishilevich and Vosshall, 2005), wherein details of all the glomeruli receiving projections from the ORNs expressing a given OR or GR are indicated (Figure 5). The three glomeruli that are innervated by *fruitless*-expressing neurons are indicated in pink in Figure 5 (Kondoh *et al*., 2003, Stockinger *et al*., 2005). There are two major types of neurons targeted by the ORNs in the glomeruli of the antennal lobe: (1) inhibitory or excitatory local interneurons, which provide connectivity among various glomeruli, and (2) projection neurons, which relay information from the antennal lobe to higher olfactory centers, i.e. to the mushroom body and lateral horn (Stocker 1994). Mushroom bodies are integrative centers that control learning in various paradigms, like sleep, courtship, and locomotor activity (Vosshall and Stocker, 2007). By contrast, the lateral horn is involved in

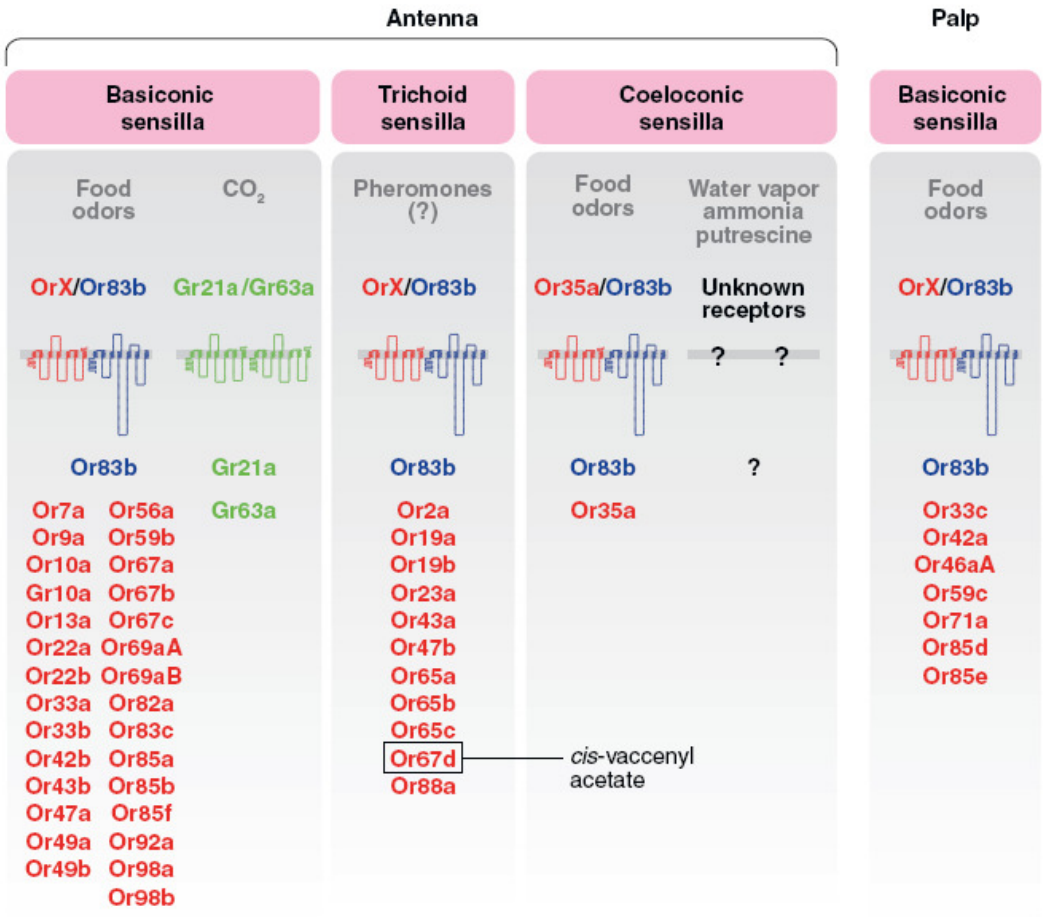

Figure 4. A list of olfactory (ORs) and gustatory receptors (GRs) expressed in the adult olfactory sensory organs, antenna and maxillary palp. Modified from Vosshall and Stocker, 2007.

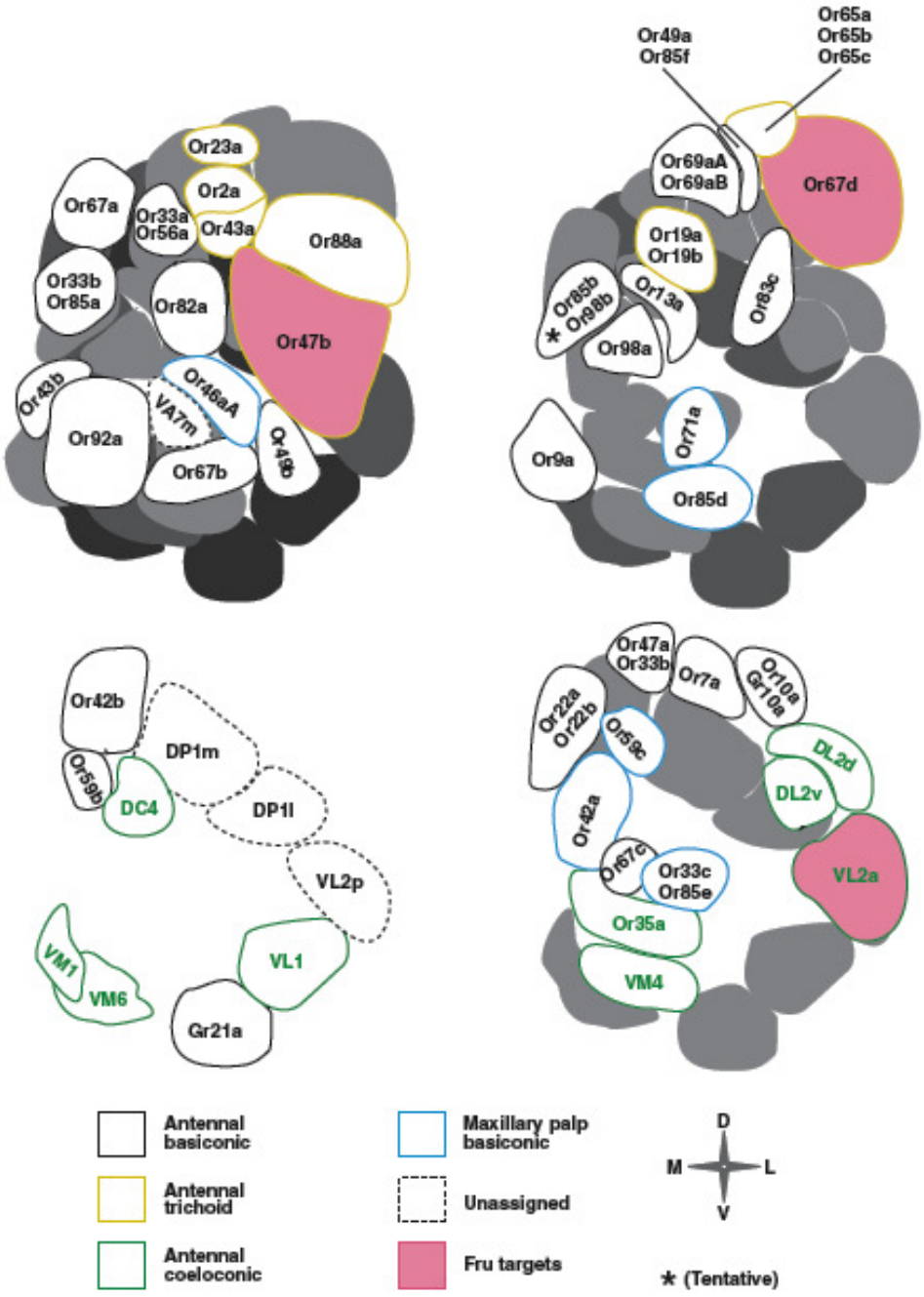

Figure 5. Molecular neuroanatomy of the adult antennal lobe. 46 different ORs were mapped definitively to the glomeruli of the AL, based on the projections they receive from ORs. Various glomeruli expressing a given OR or GR are indicated. The AL sections are from anterior to posterior, with depth-coding of black for posterior, gray for intermediate, and white for anterior sections. Modified from Vosshall and Stocker, 2007.

experience-independent odor recognition (de Belle and Heisenberg, 1994; Heimbeck *et al*., 2001). The projection neurons arborize in specific regions of the antennal lobe and send their trajectories either through the inner antennocerebral tract (iACT) to target the mushroom bodies and the lateral horn or through the middle antennocerebral tract (mACT) to directly target the lateral horn. The projection neurons (PN) are generated from three neuroblast lineages, giving rise to anterodorsal (adPN), lateral (lPN), or ventral projection neurons (vPN). The neural projections of the anterodorsal and lateral lineages synapse with the mushroom bodies and exhibit stereotypic terminal branching in the lateral horn, while those of the ventral lineage bypass the mushroom bodies and directly target the lateral horn (Figures 6 and 7). The projection neurons are born between early embryogenesis and late third larval instar, while the adult ORNs develop during pupal stages (Figure 8) (Jefferis *et al*., 2002; Lai *et al*., 2008). On basis of the *CD8::GFP* patterns driven by *repo-Gal4*, which labels glial cell membranes, the developing adult antennal lobe can already be recognized in the third instar larval brain in a position dorsal and posterior to the larval antennal lobe. The adult antennal lobe adopts the perfect glomerular structure in the developing adult brain by 50 h APF (Figure 9).

The studies presented here are focused on the brain functions of the *Pox neuro* (*Poxn)* gene, a member of the Pax gene family, which encodes a transcriptional regulator including a DNA-binding paired domain (Bopp *et al.* 1989; Noll, 1993). *Poxn* is a pleiotropic gene with many functions and is expressed in different tissues, including the central and peripheral nervous system (Bopp *et al*., 1989; Dambly-Chaudière *et al.*, 1992; Awasaki and Kimura, 1997, 2001; Boll and Noll, 2002). A *Poxn* null allele, $Poxn^{\Delta M22\text{-}B5}$, has been generated in our lab (Boll and Noll, 2002). Homozygous $Poxn^{\Delta M22\text{-}B5}$ flies are viable but males are sterile. In the PNS, *Poxn* plays a crucial role in the specification of

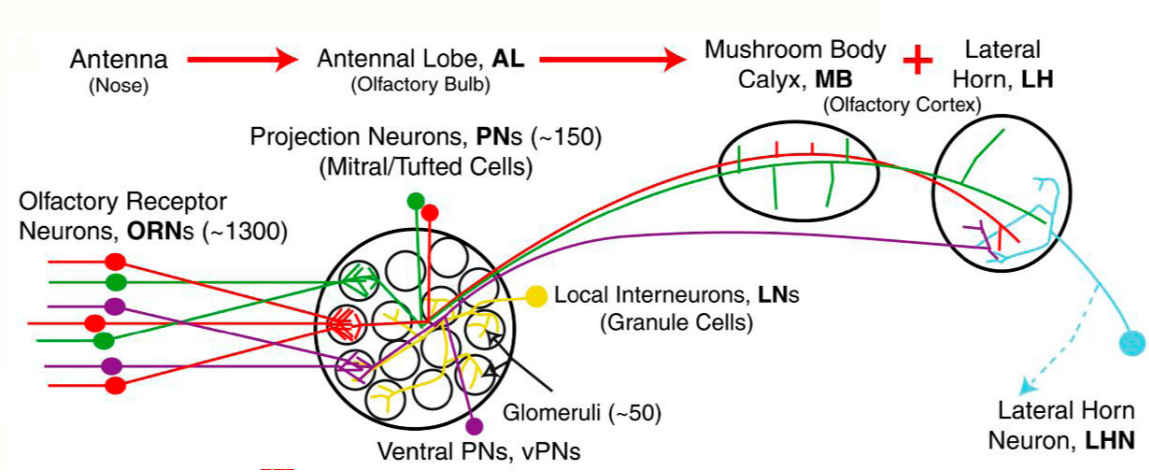

Figure 6. The neural architecture of the olfactory system in the adult. Olfactory information is transmitted from olfactory receptor neurons (ORNs) to projection neurons (PNs) in the antennal lobe (AL). PNs transmit this information further either directly to the lateral horn (LH) or via the mushroom body (MB) to the LH. In addition, local interneurons (LNs) interconnect different glomeruli in the AL. Vertebrate equivalents of neuronal structures are in parentheses. Modified from Jefferis *et al.*, 2007.

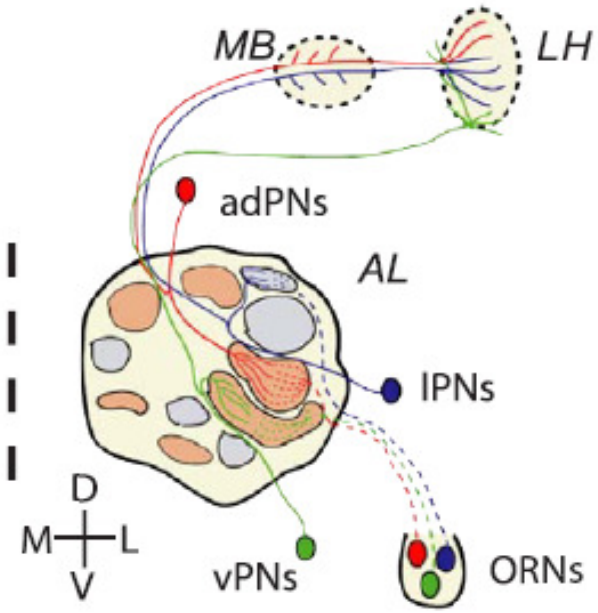

Figure 7. Schematic representation of the *Drosophila* antennal lobe. The olfactory receptor neurons, ORNs (first-order neurons), project their axons to different glomeruli in the antennal lobe (AL) and synapse with local interneurons and dendrites of projection neurons, PNs (second-order neurons). The PNs collect the information and extend their axons to the mushroom body (MB) and lateral horn (LH) according to their glomerular class. The PNs are derived from three neuroblast lineages, producing the anterodorsal (adPNs), lateral (lPNs) and ventral PNs (vPNs). adPNs and lPNs send information to the higher olfactory center LH via MB, whereas vPNs send information to the LH directly. Modified from Spletter *et al.*, 2007.

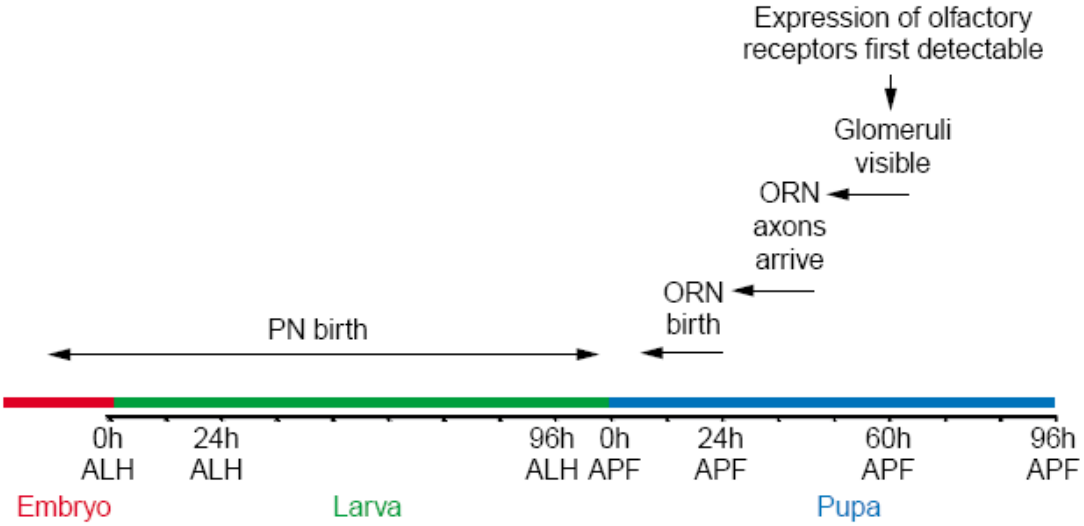

Figure 8. Schematic diagram showing the developmental events at various time windows of projection neuron and olfactory receptor neuron development. The projection neurons (PNs) are generated throughout embryonic and larval development, whereas most of the olfactory receptor neuron (ORN) neurogenesis seems to occur during early stages of pupal development. Additional abbreviations: ALH, after larval hatching; APF, after puparium formation. Modified from Jefferis *et al*., 2002.

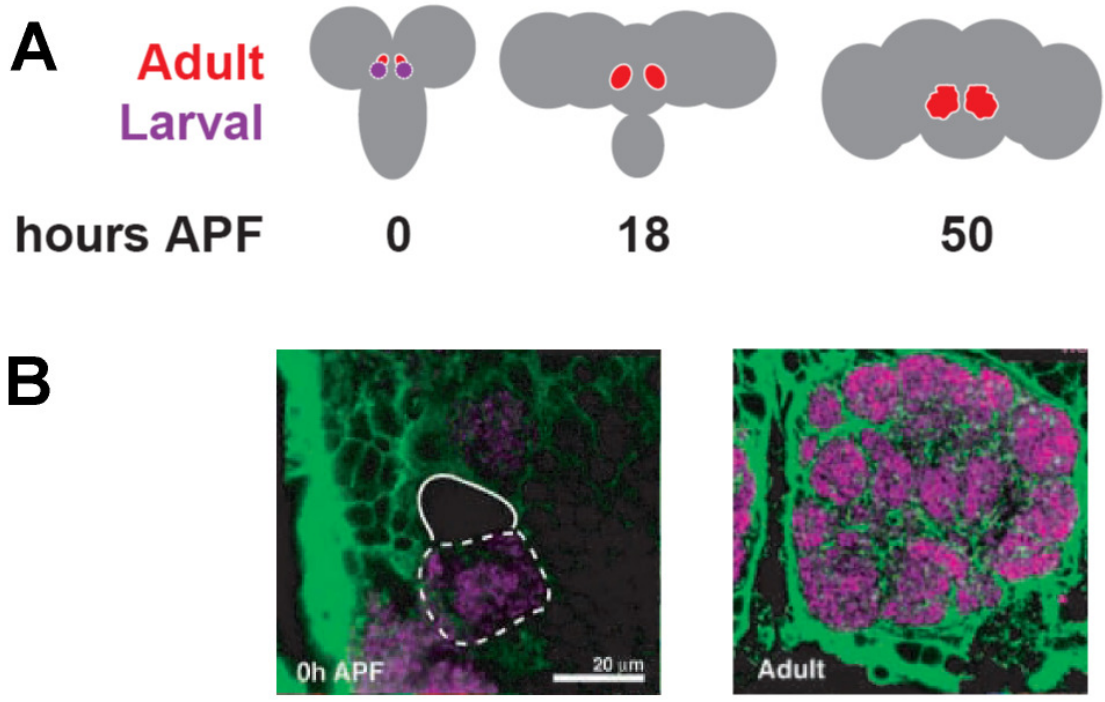

Figure 9. Time course of adult antennal lobe development and degeneration of larval antennal lobe during early stages of metamorphosis. (**A**) The larval antennal lobe degenerates by 18 h APF. The adult antennal lobe is shown in red and the larval antennal lobe is shown in purple. (**B**) Confocal images showing frontal views of the larval antennal lobe at 0 h APF on the left and the antennal lobe of an adult brain on the right, both labeled by *repo-Gal4* driving CD8-GFP expression, which marks glial cell membranes in green. Synapses are marked in purple by NC82. The continuous line marks the adult antennal lobe while the dotted line marks the larval antennal lobe. The antennal lobe adopts the perfect glomerular structure visualized in the adult brain by 50 h APF. Modified from Jefferis *et al.*, 2004.

poly-innervated external sensory organs in both larvae and adults (Dambly-Chaudière *et al.*, 1992; Awasaki and Kimura, 1997, 2001; Boll and Noll, 2002). In *Poxn* mutants, chemosensory bristles on wings, legs, and labellum are transformed into mechanosensory bristles (Boll and Noll, 2002). *Poxn* is also instrumental in the development of adult appendages where it plays a role in the segmentation of legs and antenna, but also in the proper formation of the wing hinge and male genitalia. Furthermore, *Poxn* has multiple functions that govern male courtship and copulation behavior (Krstic *et al*., 2009), which are evident in *Poxn* mutants not only from defects in the PNS and male genitalia but also from the absence of *Poxn* expression in the developing brain and the embryonic ventral cord that can be correlated with behavioral courtship phenotypes of the mutant male (Boll and Noll, 2002).

The Poxn protein is first detected in two bilaterally symmetric groups of cells in the brain of stage 12 embryos and continues to be expressed throughout brain development (Figure 10A-C). In the adult brain, Poxn is detected in two clusters of neurons in each brain hemisphere, a dorsal and a ventral cluster. The major target of neurons in the dorsal cluster (DC) is the ellipsoid body neuropil and the lateral triangles (Figure 10D). The majority of these neurons has been shown, in a previous study from our lab (Schmid, 2005), to overlap with subpopulations of large-field neurons (LFNs), labeled by several enhancer trap lines (Renn *et al*., 1999). All these enhancer trap lines labeling sets of LFNs, previously used to describe the development of the eb neuropil (Renn *et al*., 1999), have been shown to depend on the *Poxn* function in the developing brain (Schmid, 2005). The neurons of the ventral cluster (VC), however, display a completely different projection pattern. They target the antennal lobes (Boll and Noll, 2002) and the lateral horn but not the central complex (Figure 10D).

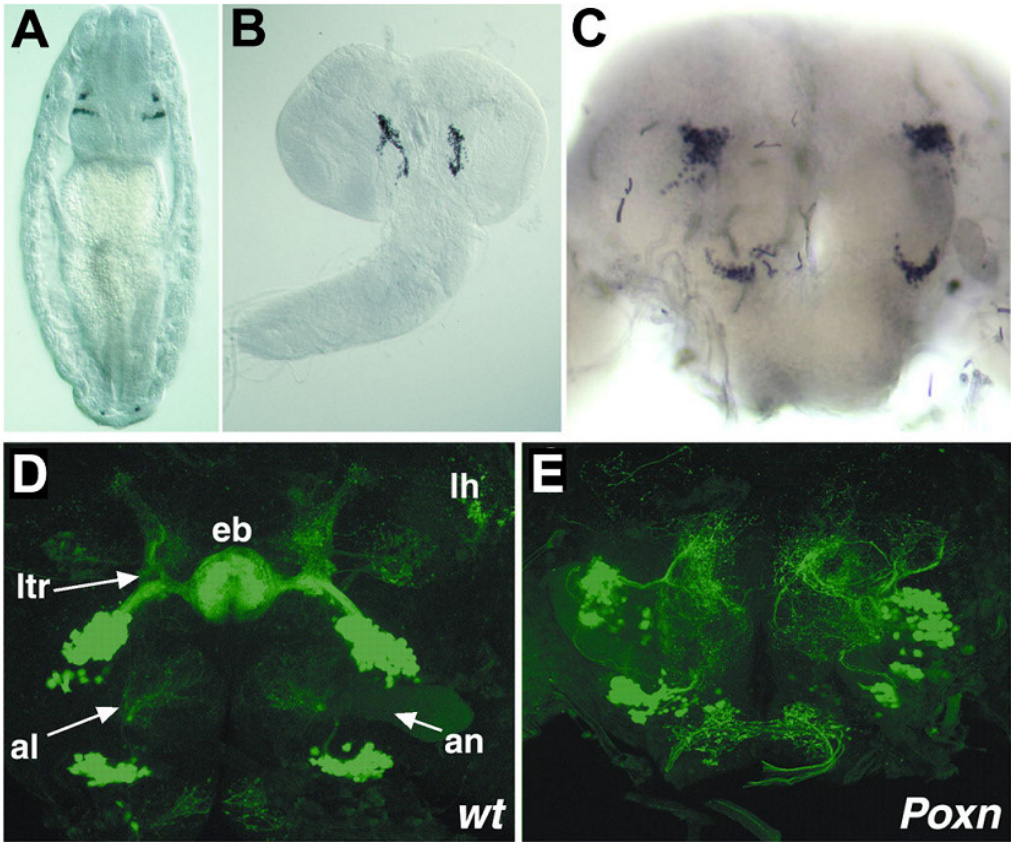

Figure 10. Poxn expression patterns in the developing brain. (**A-C**) Bilaterally symmetrical Poxn expression patterns, visualized by immunohistochemical staining with rabbit anti-Poxn antiserum, in brains of a stage 16 embryo (whole mount, dorsal view) (A), a third instar larva (B), and an adult male (brain whole mount, frontal view) (C). (**D**) Wild-type (*wt*) GFP-expression pattern of Poxn-expressing neurons and their projections in the brain (frontal view) of a w^{1118}; *Poxn-Gal4-13-1 UAS-GFP* male. The main target areas of the two *Poxn* clusters are the antennal lobes (al), ellipsoid body (eb), lateral triangle (ltr), and lateral horn (lh). an, antennal nerve. (**E**) GFP-expression pattern of *Poxn*-neurons and their projections in the brain (frontal view) of a *Poxn* mutant w^{1118}; $Poxn^{\Delta M22\text{-}B5;}$ *Poxn-Gal4-13-1 UAS-GFP* male. The *Poxn*-neurons are still present in the *Poxn* mutant, but the arborizations are dramatically disturbed and main target areas are not targeted anymore. (D) and (E) have been recorded by confocal fluorescence microscopy and are displayed as maximum projection from a z-stack of CLSM sections. Modified from Boll and Noll, 2002.

In the *Poxn* null mutant $Poxn^{\Delta M22\text{-}B5}$ (Boll and Noll, 2002), the neurons of both clusters are still present, the projection pattern visualized by *UAS-GFP* driven by *Poxn-Gal4*, however, is completely disturbed, and the structure of the ellipsoid body is not formed by axonal projections of the dorsal *Poxn*-neurons (Figure 10E). Therefore, I analyzed in this thesis the role of the dorsal *Poxn*-neurons in the formation of the ellipsoid body neuropil during development in greater detail.

Since in the *Poxn* mutant brain the two salient olfactory neuropil regions, the antennal lobe and the lateral horn, are no longer targeted by the neurons of the ventral cluster, I further aimed to analyze the developmental and functional aspects of the ventral *Poxn*-neurons, which by morphology resemble ventral projection neurons, in the olfactory system of *Drosophila*.

2. Materials and Methods

2.1. *Drosophila* strains and genetics

The following fly stocks were used:

w^{1118}; *P{W6 Poxn-CD8::GFP}3-3* (from Werner Boll),

w^{1118}; $Poxn^{\Delta M22\text{-}B5}$/*CyO*; *P{W6 Poxn-CD8::GFP}3-3*,

w^{1118}; $Poxn^{\Delta M22\text{-}B5}$ *P{W6 Poxn-Sbl107}*; *P{W6 Poxn-CD8::GFP}3-3* (from Werner Boll),

w^{1118}; *P{W6 Poxn-Gal4}13-1 P{*y^{+}*UAS-GFP}/TM6B* (Boll and Noll, 2002),

w^{1118}; $Poxn^{\Delta M22\text{-}B5}$ *P{W6 Poxn-SuperA}158/CyO*; *P{W6 Poxn-CD8::GFP}3-3*,

UAS-Flp; *tub-Gal80*^{ts}/+; *Act5C>polyA>lacZ.nls1 P{W6 Poxn-Gal4}13-1/P{W6 Poxn-CD8::GFP}3-3*,

w^{1118}; *P{UAS-CD2}* (Bloomington 1284),

w^{1118}; *P{Gal4}repo* (Bloomington 7415),

w^{1118}; *P{UAS-CD2}*; *P{Gal4}repo, Poxn-CD8::GFP-3-3*,

w^{1118}*; P{GawB}MZ699-6* (from K. Ito),

w^{1118}*; P{GawB}GH146/CyO* (from R. F. Stocker),

w^{1118}; *P{GawB}GH298* (from R.F. Stocker),

y w hs-Flp; UAS>CD2, y^{+}*>CD8::GFP*; $Poxn\text{-}Gal4^{ups1f}$*/TM6B* (from Yanrui Jiang),

w^{1118}; *Poxn-CD8::GFP-15.2*; *P{GawB}MZ699-6*

The *Poxn-CD8::GFP-3-3* transgene expresses, under the direct control of the *Poxn* upstream region that includes the brain enhancer (Figure 11), the fusion protein of the mouse lymphocyte receptor CD8 (alpha chain) with GFP and reveals neuronal

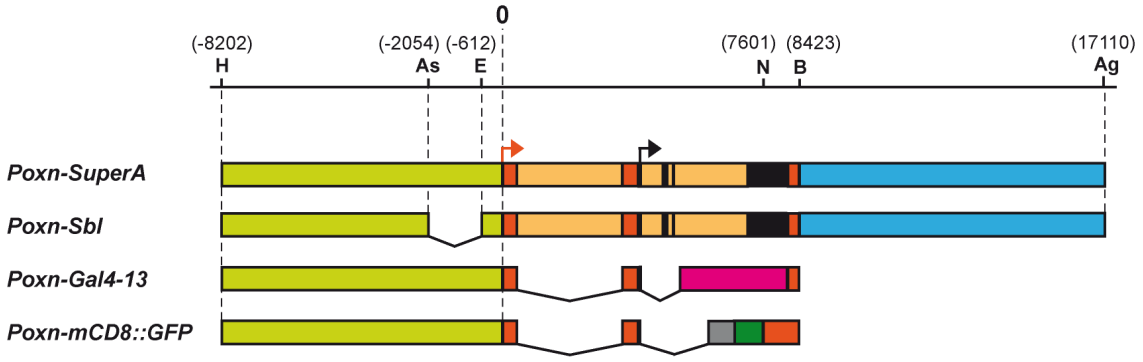

Figure 11. Map of transgenes used for the manipulation of *Poxn* brain functions. Maps of transgenes are shown with regard to a restriction map of the *Poxn* locus. The *Poxn-SuperA* transgene rescues all *Poxn* functions. *Poxn-Sbl* rescues all *Poxn* functions with the exception of the brain function. *Poxn-Gal4-13-1* expresses Gal4 under the control of *Poxn* upstream enhancers. *Poxn-CD8::GFP* expresses the CD8::GFP fusion protein under the direct control of *Poxn* upstream enhancers. Color labeled are the *Poxn* upstream region (olive green), *Poxn* 5'- and 3'-UTR (dark orange), *Poxn* introns (light orange), *Poxn* coding region (black), *Poxn* downstream region (light blue), Gal4 (pink), CD8 (grey), and GFP (green). The orange arrow marks the transcription start, the black arrow the translation start. Positions relative to the transcription start site (0) are in parentheses. Abbreviations of restriction sites: H, *HindIII*; As, *Asc*I; E, *Eco*RI; N, *Not*I; B, *Bam*HI; Ag, *Age*I.

processes (Lee and Luo, 1999). The CD8::GFP-3-3 protein is faithfully expressed, i.e. like Poxn, at various stages of development (Figure 12). It is also expressed in the Poxn domain in the absence of *Poxn* function.

Additional stocks used were w^{1118} (Bloomington stock 5905), Oregon-R (Munich) (from W. McGinnis), *P{UAS-FLP.Exel}1*, *y* w^{1118} (Bloomington stock 8208), w^{1118}; *P{tubP-GAL80*^{ts}*}20*; *TM2/TM6B*, Tb^{1} (Bloomington stock 7019), *P{Act5C>polyA>lacZ.nls1}3*, ry^{506} (Bloomington stock 6355).

2.2. Recording of immunofluorescent patterns in brain specimens and colocalization analysis

Labeled specimens were analyzed with a Leica TCS SP or a Zeiss LSM 710 confocal laser scanning microscope (CLSM). Optical sections ranged from 0.65 µm to 1.0 µm, signals of different fluorochromes were recorded sequentially with a resolution of 1024x1024 pixels. The resulting z-stacks were arranged and processed by the use of Leica 'LCS lite' or 'Zeiss Zen 2009 light edition' and the NIH ImageJ software version 1.41m (http://rsb.info.nih.gov/ij/) (Bearer, 2003; Eliceiri and Rueden, 2005; Carmona *et al*., 2007; Collins, 2007).

Colocalization analysis was performed in ImageJ with the plugins Colocalization Threshold and Colocalization Highlighter (Lachmanovich *et al*., 2003). Colocalization analysis can be graded either as qualitative or quantitative (Lachmanovich *et al*., 2003). In qualitative analysis, the overlapping pixels are highlighted ("quantified percentage overlap"). The two fluorescent channels have particular threshold values (set by the user), and any areas of overlap are regarded as "colocalized". Quantitative analysis, on

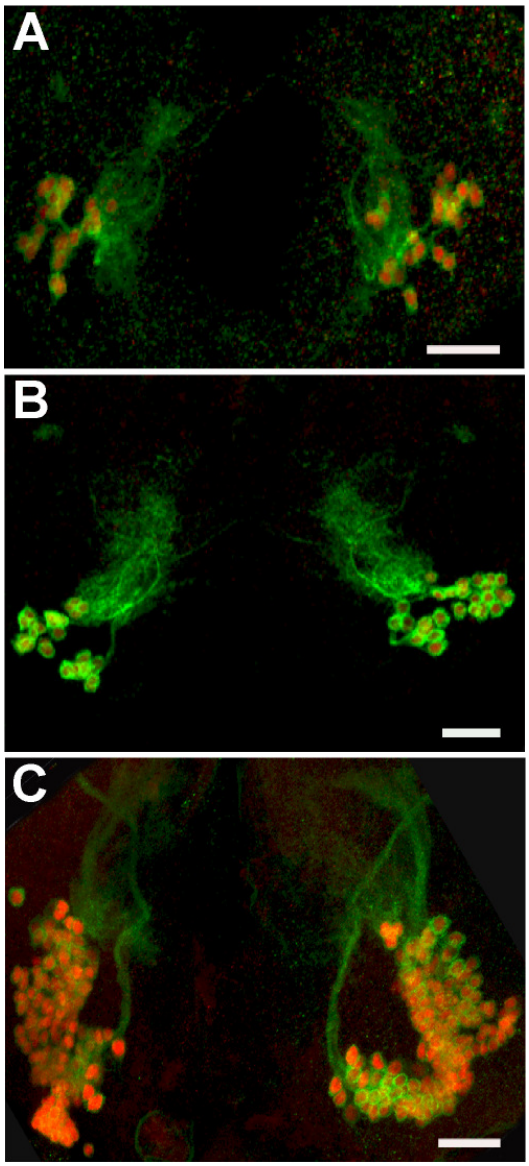

Figure 12. The *Poxn-CD8::GFP-3-3* transgene is faithfully expressed at all stages of larval development. Frontal views of first (A), second (B), and third instar (C) larval brains, immunostained for Poxn (red) and GFP (green), are shown. Maximum projection of z-stacks of CLSM sections at 63x magnification. Size bars: 20 μm.

the other hand, analyzes all the pixels based on their respective intensities. As these intensities do not discriminate against background levels, this method was not used.

The colocalization plugin program generates an image of colocalized pixels and calculates Pearson's correlation coefficient for the channels used (Pearson, 1909; Manders *et al.*, 1992, 1993). Pearson's coefficient for channel 1 is then compared against a number of random channel-2 images.

- Colocalization Threshold Plugin: Orthogonal regression is performed on the image's scatterplot and Pearson's coefficient is calculated. A greyscale image is generated, displaying the colocalized pixels (i.e., wherein both channels have pixel values above their respective threshold values).

- Colocalization Highlighter Plugin: The plugin merges the red and green 8-bit images from the two channels to an RGB image. The image generated from the colocalized pixels is superimposed on the RGB image and colocalized pixels are depicted in white by default (Display value = 255). The threshold of the channels is set at 50 by default.

2.3. Dissection and immunolabeling of larval, pupal, and adult fly brains

Whole-mount preparations of fixed brains were labeled by immuno-fluorescence as described (Wu and Luo, 2006). Brains were dissected in *Drosophila* Ringer's solution (4.7 mM KCl, 130 mM NaCl, 2.0 mM $CaCl_2$, 10 mM HEPES-NaOH, pH 6.9) with Dumont #55 (Dumostar) Tweezers. After dissection, the tissue was collected and fixed for up to 2 h in 4% formaldehyde (Fluka 47629) in PEM buffer (0.1 M PIPES-NaOH, pH

7.0, 2 mM EGTA, 1 mM $MgCl_2$, 0.02% NaN_3), fixed for another 2 h at room temperature, permeabilized for 15 minutes with 1% Triton X-100 (Fluka 93418) in PBS (130 mM NaCl, 7 mM Na_2HPO_4, 3 mM KH_2PO_4, pH 7.0). After blocking the tissue with 3% normal goat serum (NGS, Sigma G6767) in PBST (PBS supplemented with 0.2% Tween-20 (Fluka 93773)), the brains were incubated overnight at 4°C with appropriate dilutions of the preabsorbed primary antiserum in PBST, 3% NGS on a shaking platform. After several washes with PBST, appropriate dilutions of the preabsorbed secondary antiserum in PBST, 3% NGS were added and brains were incubated overnight at 4°C. Brains were then washed and equilibrated in mounting medium (80% Glycerol, 0.1% DABCO (1,4-Diazabicyclo[2.2.2]octane, Fluka 33480), 0.1 M Tris-HCl, pH 7.5). The brain whole-mounts were mounted with the cover slip supported by an appropriate spacer of about 150 μm for subsequent analysis by confocal microscopy.

The following primary and secondary antibodies were used: rabbit anti-Poxn (at a 1:50 dilution; Bopp *et al*., 1989), chicken anti-GFP (1:500; Abcam, Cambridge, UK), rabbit anti-β-galactosidase (1:100; Upstate Biotechnology, Lake Placid, NY), rabbit anti-PH3 (1:1000; Upstate Biotechnology, Lake Placid, NY), mouse anti-CD2 (1:100; Santa Cruz Biotechnology), anti-GABA (1:200; Abcam, Cambridge, UK), mouse anti-Elav-9F8A9 (1:200), mouse anti-BP102 (1:200), mouse anti-BP106 (Neurotactin) (1:200), mouse 1D4 anti-Fasciclin II (1:2.5), mouse 4F3 anti-Discs Large (1:100), mouse anti-Prospero MR1A (1:4), mouse monoclonal antibody NC82 (1:10), mouse anti-G3G4 (anti-BrdU) (1:200), mouse anti-8D12 (anti-Repo) (1:200) and mouse anti-3C11 (anti-SYNORF1) (1:10) (all these monoclonal antibodies are from Developmental Studies Hybridoma Bank, University of Iowa), Alexa Fluor 488-coupled goat anti-mouse IgG, Alexa Fluor 488-coupled goat anti-rabbit IgG, Alexa Fluor 488 goat anti-chicken IgG, Alexa Fluor 594-coupled goat anti-mouse IgG and Alexa Fluor 594-coupled goat anti-

rabbit IgG (all secondary antibodies are from Molecular Probes and were used at a 1:500 dilution). Antisera were routinely preabsorbed with about 10% (V/V) of fixed 0-4 h-old embryos or, where appropriate, 0-16 h-old embryos in PBST, 5% NGS.

2.4. Timing of pupal development

Eggs were collected from 5-6 day-old *D. melanogaster Ore-R* flies at 25°C on standard food containing yeast. After two rounds of one-hour pre-collections, subsequent batches of eggs were harvested at hourly intervals on fresh food with yeast on its surface. The eggs and hatched larvae were allowed to grow at 25°C and the time of white pre-pupa formation was regarded as 0 h APF for the sample. The white pupae were handled with a soft hair brush and grown for different lengths of time at 25°C and 65% relative humidity (RH) in petri dishes containing a piece of wet tissue paper to provide humidity. The developmental stage of selected pupae was assessed according to a detailed description (Bainbridge and Bownes, 1981).

2.5. Analysis of mitotic activity in Poxn-expressing cells by incorporation of 5-bromo-2-deoxyuridine (BrdU)

The thymidine analog BrdU gets incorporated into the newly synthesized DNA of replicating cells during S-phase (Bodmer *et al*., 1989; Ito and Hotta, 1992). BrdU (Sigma, B9285) was dissolved in 40% ethanol at a concentration of 10 mg/ml and mixed with fly medium. Larvae were feeding on substrate containing 0.2 mg/ml BrdU (Truman and Bate, 1988) from the time of hatching till wandering third instar. Feeding was monitored by the uptake of the vital dye phenol red, which was added in trace amounts to

the food. Non-feeding larvae were discarded. The brains were dissected and fixed immediately in 4% formaldehyde, PEM buffer. After fixation, the brains were washed 3×15 min in PBST, incubated in 2 M HCl for 45 min to denature the BrdU-labeled DNA, washed 3 times for 15 min in PBST, and immunostaining was carried out according to the procedure described above.

2.6. Lineage Analysis

Lineage analysis was based on flipase-mediated recombination, which was spatially controlled by Gal4 and temporally controlled by temperature-sensitive $Gal80^{ts}$ (McGuire *et al*., 2003; 2004). Embryos of the genotype w^{1118} *UAS-Flp*; *tub-*$Gal80^{ts}$/+; *Act5C>polyA>lacZ.nls1 P{W6 Poxn-Gal4}13-1/P{W6 Poxn-CD8::GFP}3-3* were collected and kept at 18°C and 65% RH until third larval instar. At early third instar, larvae were heat-shocked at 32°C for 6 h and allowed to develop to adulthood at 18°C and 65% RH. Flipase is expressed under the indirect control of the *Poxn* enhancer and hence can mediate flip-out only in these cells and only at the time of heat shock when the $Gal80^{ts}$ repressor is inactive. Cells in which flip-out has occurred and their offspring then express nuclear β-galactosidase.

The brains of about 5-day old adult flies were dissected and fixed as described above, and β-galactosidase and GFP patterns were analyzed in brain whole-mounts by immunofluorescent labeling and confocal laser scanning microscopy.

2.7. Labeling a sub-population of Poxn-expressing neurons

Flies with genotype *y w hs-Flp*; *UAS>CD2, y*$^{+}$*>CD8::GFP*; *Poxn-Gal4*^{ups1f}*/TM6B* were used for the single-neuron labeling experiments. They carry three transgenes: the yeast flipase (*flp*) gene whose expression is under the control of the *hsp70* promoter, the reporter *UAS>CD2 y*$^{+}$*>CD8::GFP*, and the *Poxn-Gal4*^{ups1f} driver. In the *Poxn-Gal4*^{ups1f} driver, a derivative of the *Poxn-Gal4-13-1* (Boll and Noll, 2002), the Gal4 expression is under control of the *Poxn* promoter and upstream control region, which includes the enhancer region driving the brain expression throughout development.

In order to generate clones in the clusters of cells expressing *Poxn* in the brain, we combined spatial control by the Gal4/UAS system with temporal control by the Flp/FRT recombination system (Figure 13). The optimal conditions were determined by varying temperature and duration of the heat shock to control the levels of Flipase and therefore the number of recombination events in the brain. Flp-mediated recombination between the two FRT sites leads to the excision of the *CD2, y*$^{+}$ cassette from the reporter *UAS>CD2, y*$^{+}$*>CD8::GFP* and the expression of *CD8::GFP* under control of the *Poxn-Gal4*^{ups1f} driver, which resulted in the differential GFP-labeling of few Poxn-expressing neurons. The recombination events were analyzed by immunofluorescent labeling and confocal microscopy in adult brain whole mounts.

Late pupae were heat-shocked after allowing flies to lay eggs and develop until late pupal stages in plastic bottles that were directly submerged in a pre-heated 37°C water bath for 1 h.

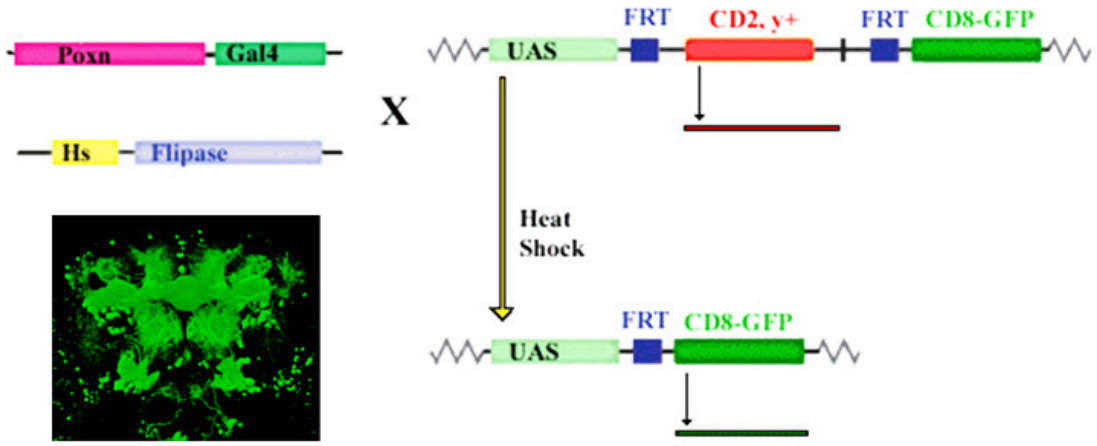

Figure 13. Schematic diagram showing the methodology to generate a differentially labeled sub-population of *Poxn*-neurons. *y w hs-flp*; *UAS>CD2, y*$^{+}$*>CD8::GFP*; *Poxn-Gal4*^{ups1f}*/TM6B* flies were heat-shocked at different developmental stages. The heat-shock-induced activation of flipase leads to infrequent recombination events that remove the CD2-cassette and hence force these cells to express CD8::GFP under the indirect control of the *Poxn*^{ups1f} enhancer. In cells that express *Poxn* under control of the *Poxn*^{ups1f} enhancer region but did not undergo Flp-mediated recombination continue to express CD2. This technique makes it possible to differentially label and analyze small cell populations or single cells in the Poxn domain.

3. Results

3.1. Patterns of Poxn-expression in the developing brain

The Poxn protein is first detected in the brain of stage 12 embryos and continues to be expressed in discrete domains of the brain throughout development (Table 1). In stage 16 embryos, two groups including about 28 to 30 cells per brain hemisphere express Poxn with bilateral symmetry (Table 1). After hatching, Poxn is expressed in approximately 40 to 43 cells in each brain hemisphere, a number that increases markedly by the end of the second instar (Figure 14 and Table 1). By early third instar, the number of Poxn-expressing neurons - for simplicity, these neurons are also called *Poxn*-neurons, also in *Poxn* mutants - almost triples to about 163 to 168 cells per brain hemisphere and does not appear to change significantly by late third instar (Figure 14 and Table 1). In the pupal brain, the Poxn-expressing cells appear to increase further since their numbers have been underestimated (Table 1). The two closely grouped Poxn-expressing clusters of cells observed at the end of larval development form two distinct clusters with bilateral symmetry by 30 h APF. In 5-day old adult flies, the dorsal cluster consists of 148 to 162 cells and the ventral cluster of 75 to 78 cells (Table 1).

It appears that a large fraction of the cells that acquire a *Poxn* fate during larval brain development are already present in the embryonic brain, as there is little BrdU-incorporation in the Poxn-expression domain of third instar wandering larvae that have been kept on BrdU-containing food throughout larval development. Only 30±5 Poxn-expressing cells in each brain hemisphere of late third instar larvae have incorporated BrdU and hence gone through S-phase during larval development (Figure 15A-C).

Developmental Stage	Wild-type Brain	*Poxn* Mutant Brain
embryonic stage 12	11 to 13	12 to 14
embryonic stage 14	18 to 20	17 to 19
embryonic stage 16	28 to 30 AC: 12-13 PC: 16-17	25 to 28
end of first larval instar	40 to 43	40 to 42
end of second larval instar	58 to 63	55 to 60
early third larval instar	163 to 168	n.d.
late third larval instar	162 to 176	138 to 143
20 h APF	152 to 166	124 to 132
40 h APF	DC: 110-123 VC: 65-68	DC: 109-117 VC: 67-70
60 h APF	DC: 110-120 VC: 65-74	DC: 86-97 VC: 51-58
80 h APF	DC: 107-118 VC: 56-64	DC: 92-98 VC: 52-63
adult	DC: 148-162 VC: 75-78	DC: 123-137 VC: 62-70

Table 1. The total number of Poxn-expressing cells per brain hemisphere from embryonic stage 12 to the adult stage is indicated in both wild-type *Oregon R* and *Poxn* mutants (*Poxn*$^{\Delta M22\text{-}B5}$; *P{W6 Poxn-CD::GFP}3-3*). Each study includes at least three brains. Note that the numbers of Poxn-expressing cells at pupal stages are probably underestimates because of a relatively low signal to noise ratio produced by histochemical staining with the anti-Poxn antiserum available at the time. Abbreviations: AC, anterior cluster; PC, posterior cluster; DC, dorsal cluster; VC, ventral cluster; APF, after puparium formation; n.d., not determined.

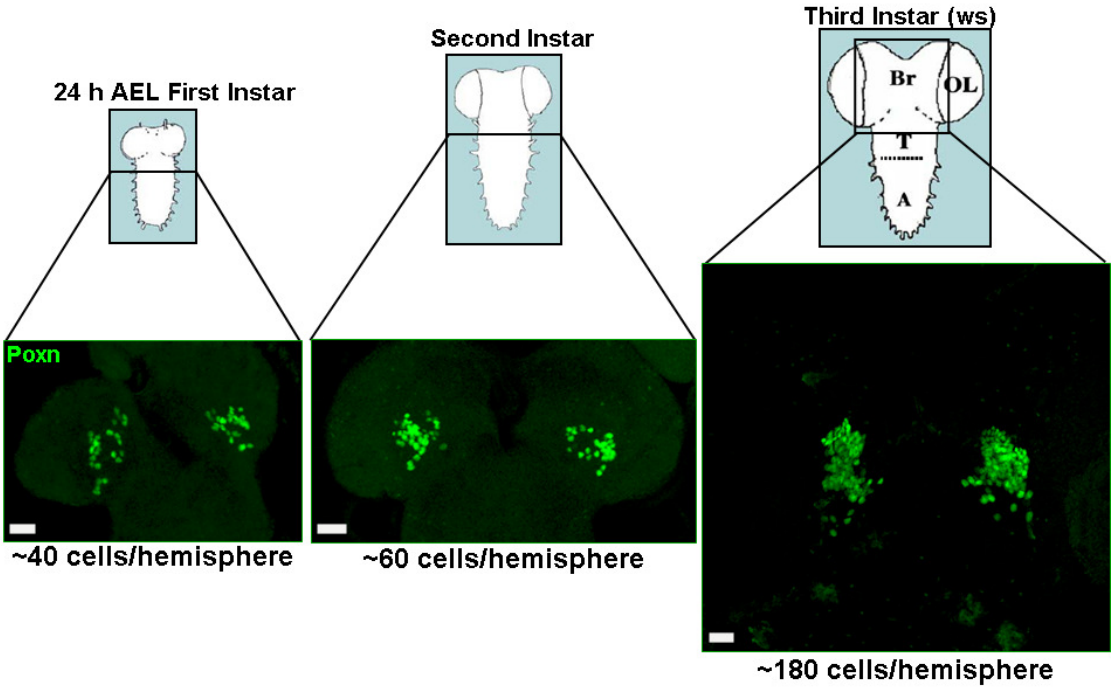

Figure 14. Poxn expression in developing larval brain. Bilaterally symmetrical Poxn-expression, visualized with rabbit anti-Poxn, in the brain of early first instar larvae, second instar larvae and wandering third instar larvae. There is a marked increase in Poxn-expressing cells between the second and late third instar larval brain. Maximum projection of z-stack of CLSM sections at 20x magnification. Size bar: 20 µm.

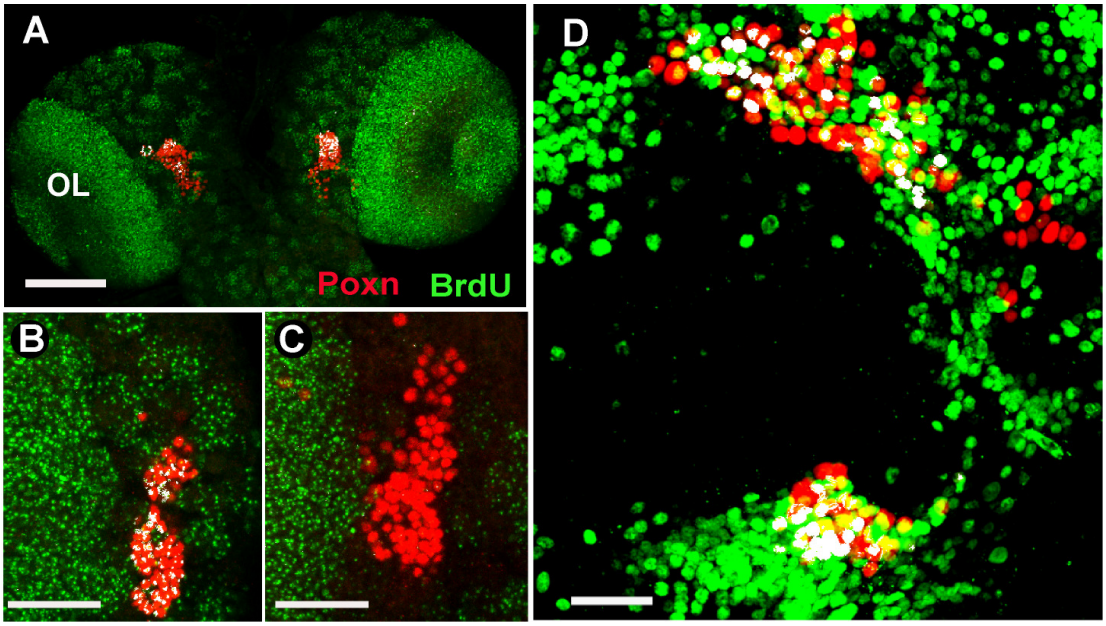

Figure 15. In each hemisphere, 50±5 cells of the Poxn domain undergo mitosis during brain development. Nuclei of cells expressing Poxn (red) and revealing incorporation of BrdU (green) are labeled in the brain of late third instar larvae reared on BrdU-containing food throughout larval development. Colocalized signals are shown in white. (**A**) Frontal view of late third instar larval brain at 20x magnification and maximum projection of z-stack of optical CLSM sections. OL, larval optic lobe. (**B**, **C**) Detailed views (of panel A) of cluster in left brain hemisphere of third instar larva at 63x magnification and maximum projections of sections 1-11 µm and 12-27 µm of the z-stack. (**D**) Frontal view of right hemisphere of adult brain at 40x magnification and maximum projection of z-stack of CLSM sections. Colocalization of Poxn and BrdU are shown in white. Note that the number of Poxn-expressing neurons stained for BrdU incorporation in larval brains is probably underestimated because the anti-BrdU antiserum used was of lower quality than that used for adult brains. Size bars: 50 µm (A) and 20 µm (B-D).

This number is probably an underestimate, as the quality of the anti-BrdU antiserum was not optimal (Figure 15). However, in adults raised on BrdU-containing food since larval hatching, only 28-30 cells of the DC and 23-28 cells of the VC in each brain hemisphere have incorporated BrdU during larval and pupal development (Figure 15D). If we assume that, after BrdU-incorporation during S-phase, cells have undergone mitosis, these results imply that approximately a quarter (55 cells) of the adult Poxn domain of 230±10 neurons (Table 1) have divided during larval and pupal development.

3.2. All Poxn-expressing cells in the brain are post-mitotic neurons

Elav, an RNA-binding protein, is one of the earliest markers of neuronal differentiation and is expressed exclusively in all post-mitotic neurons (Campos *et al*., 1987; Robinow and White, 1988). All cells in the Poxn domains of the developing brain express Elav, from embryonic stage 12 to late third larval instar and adulthood, which suggests that these cells are post-mitotic neurons (Figure 16A-D). Some of these *Poxn*-neurons extend neurites from late stage 12 of embryogenesis (Figure 17). In a complementary experiment, none of the Poxn-expressing cells colocalized with Repo (Figure 18), a marker for differentiating glia (Xiong *et al*., 1994; Halter *et al*., 1995). On the other hand, Prospero (Pros), which acts as binary switch regulating the transition from neural stem cell fate to terminally differentiated neuronal fate (Chu-Lagraff *et al*., 1991; Choksi *et al*., 2006; Li and Vaessin, 2000), is expressed in longitudinal glia as well as in immature neurons (Doe *et al*., 1991; Xiong *et al*., 1994). Approximately, 70% of Poxn-expressing cells in late third instar larval brains express Pros (Figure 19A-C).

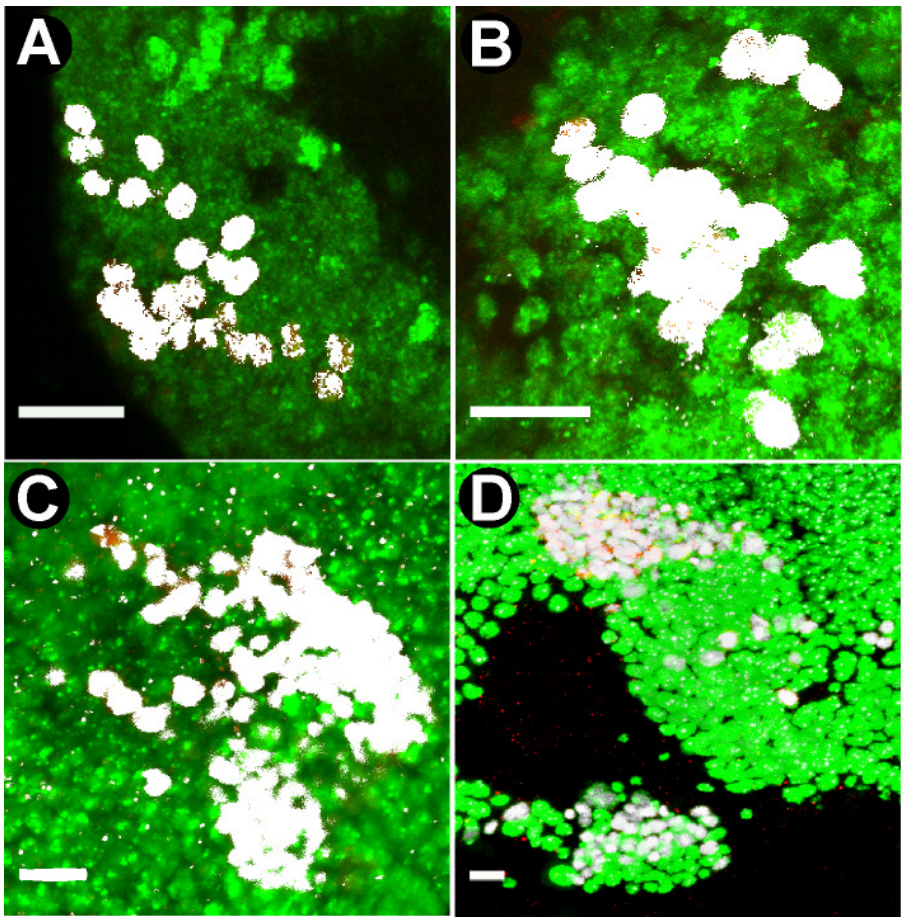

Figure 16. All Poxn-expressing cells in larval and adult *Oregon-R* brains are post-mitotic neurons. Expression of Poxn (red) and Elav (green) is visualized by immunohistochemical staining, and their colocalization is shown as white pixels in frontal views of right brain hemispheres of first (**A**), second (**B**), and late third instar larvae (**C**), and of the left adult brain hemisphere (**D**). Pictures were taken at 63x (A-C) and 40x magnification (D) and maximum projections of z-stacks of CLSM sections. Size bar: 10 µm.

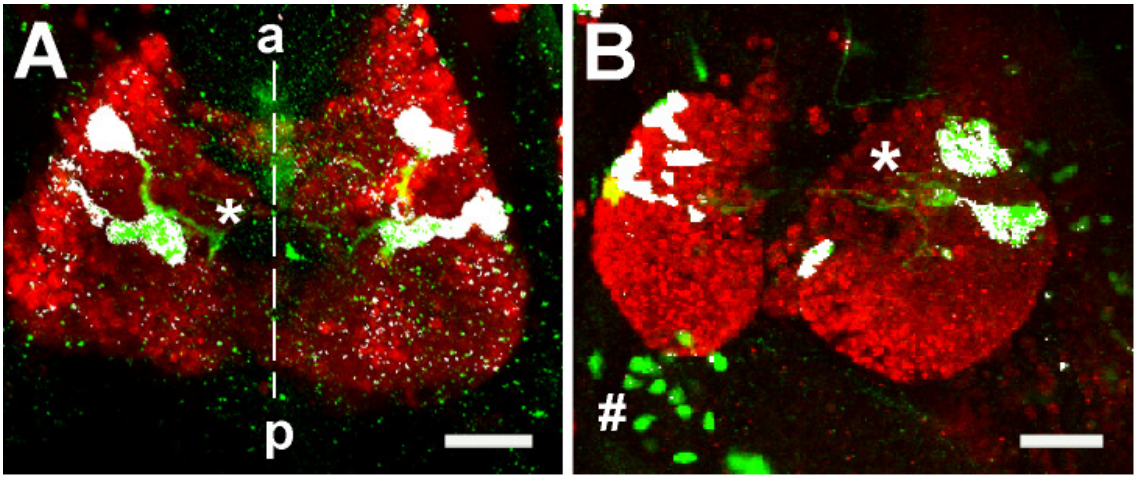

Figure 17. Poxn-expressing cells possess neurites from embryonic stage 12. Expression of the pan-neuronal marker Elav (red) and of GFP (green), representing Poxn-expressing cells, is shown in dorsal views of the brain of a stage 12 (**A**) and a stage 14 (**B**) w^{1118}; *P{W6 Poxn-Gal4}13-1 P{y*$^{+}$*UAS-GFP}* embryo (63x magnification, maximum projections of z-stacks of CLSM sections). The neurites marked by asterisks can be seen at this early stage of development in both brain hemispheres. Some Poxn-expressing cells, marked by hash, can also be seen in the developing larval PNS. Colocalization of Elav and GFP is indicated by white pixels, the midline extending from anterior (a) to posterior (p) in (A) by a dashed line. Size bar: 25 µm.

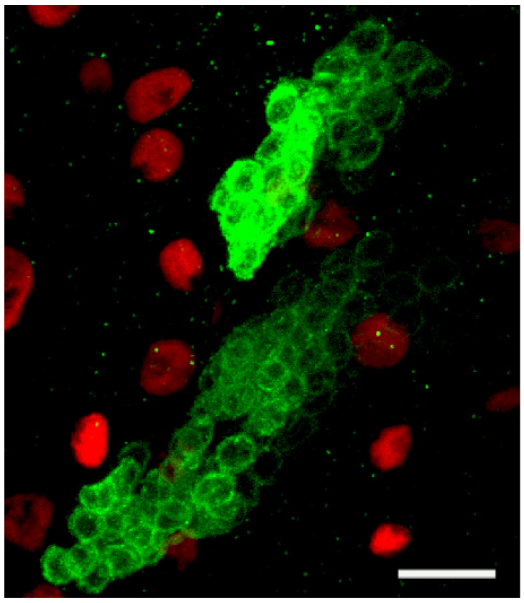

Figure 18. None of the Poxn-expressing cells are glia. Colocalization of GFP, representing Poxn-expressing cells (green), with Repo (red) in brains of w^{1118}; *P{W6 Poxn-CD8::GFP}3-3* late third instar larvae (frontal view at 63x magnification, maximum projection of z-stack of CLSM sections). No colocalization is observed, which would be marked as white pixels. Size bar: 10 μm.

Neurons expressing Pros and Poxn do not possess any apparent neurites, whereas the *Poxn*-neurons with neurites do not express Pros (Figure 19D-F). In each late third instar larval brain hemisphere 162 to 176 neurons express Poxn, of which 120±5 acquired their Poxn-expression fate during larval development and coexpress Prospero and Elav and hence appear to represent immature neurons.

3.3. *Poxn*-neurons in the brain survive metamorphosis

In each brain hemisphere, the number of *Poxn*-neurons increases by 35% during metamorphosis. Since little is known about the remodeling of neuronal circuits during metamorphosis (Levine *et al*., 1995; Consoulas *et al*., 2000; 2002), we permanently labeled the larval *Poxn*-neurons to examine whether they survive metamorphosis and keep their Poxn-expression fate in the adult brain. In *UAS-Flp*; *tub-Gal80^{ts}*/+; *Act5C>polyA>lacZ.nls1 Poxn-Gal4-13-1/Poxn-CD8::GFP* females, *Poxn*-neurons were permanently labeled with β-Gal by bringing *lacZ* under control of the actin promoter through Flipase-mediated recombination at the FRT sites. In these flies, the expression of Flipase was spatially controlled by the *Poxn-Gal4-13-1* driver. Activation of *flp* transcription by Gal4 was temporally controlled by the inactivation of the temperature-sensitive repressor Gal80^{ts} (McGuire *et al*., 2003; 2004) during heat shock at the non-permissive temperature of 32°C. The *Poxn-CD8::GFP* transgene was introduced to label all cells of the Poxn-expression domain at all stages of brain development.

When *flp* transcription was activated for 6 h in Poxn-expressing brain cells of early third instar larvae to avoid their labeling with β-Gal during pupal stages (Table 1) because of a possible perdurance of Flipase, about 80% of the GFP-positive cells express

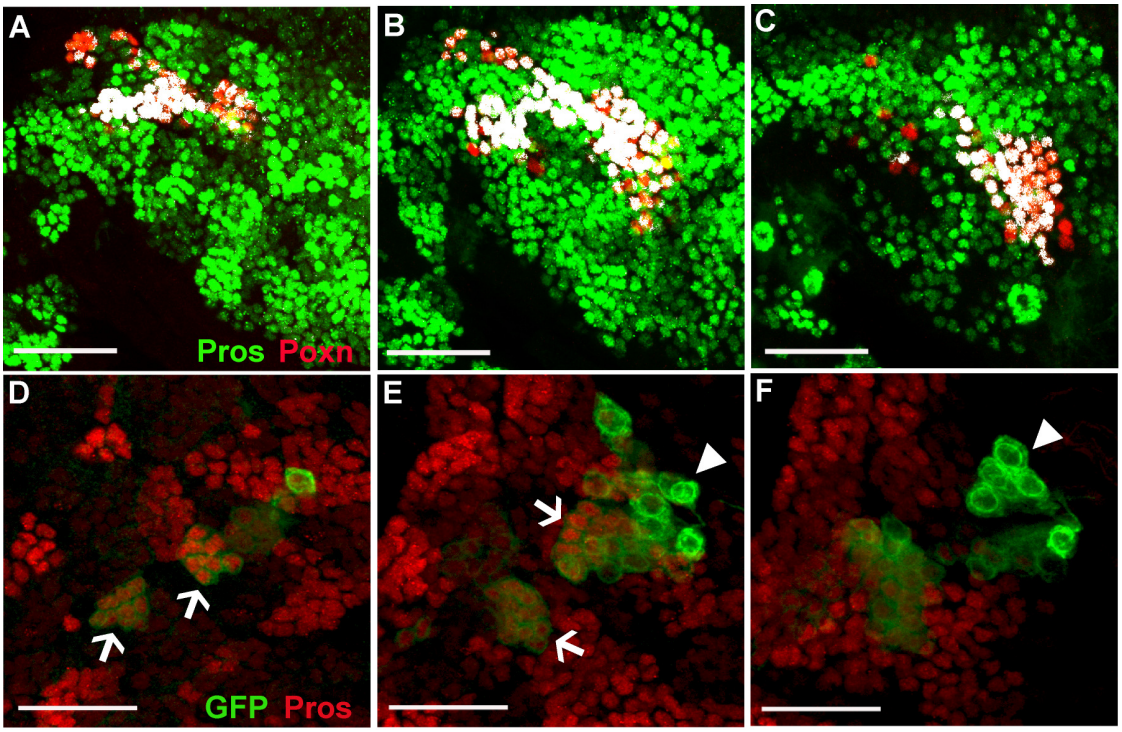

Figure 19. Most Poxn-expressing cells in the brain of late third instar larvae are immature neurons. (**A**, **B**, **C**) Expression of Poxn (red) and Pros (green) shown as frontal view of a brain hemisphere of a late third instar larva. Colocalization of the two nuclear proteins is indicated in white. Maximum projections of CLSM sections 1-12 µm, 13-20 µm, and 21-29 µm of the z-stack. (**D**, **E**, **F**) Expression of GFP and Prospero shown as frontal view of a brain hemisphere of a *Poxn-CD8::GFP3-3* late third instar larva. Maximum projections of confocal z-substacks at 1-8 µm, 9-15 µm, and 16-21 µm. Note that the CD8::GFP pattern of the Poxn-expressing cells reveals neurites only in cells that do not co-express Pros (arrowheads) but not in those that express Pros (arrows). All images were taken at 63x magnification. Size bar: 20 µm.

β-Gal in the adult brain, which implies that most, if not all, neurons that express Poxn in the third instar larval brain are preserved throughout metamorphosis (Figure 20 and Table 1). In addition, up to 10 cells were observed that were labeled only with β-Gal, which indicates that these neurons expressed Poxn in third instar larvae but have lost Poxn-expression during metamorphosis. Finally, a small population of 8-10 neurons did not express β-Gal but only CD8::GFP, which indicates that they are part of the Poxn domain in the adult brain and acquired Poxn-expression after larval stages, i.e. during metamorphosis or early adulthood. That not more neurons of this type were observed, as would be expected from Table 1, may result from labeling with β-Gal during pupal stages due to perdurance of Flipase.

3.4. Analysis of neuronal projection patterns in wild-type and *Poxn* mutant brains

3.4.1. The developing brain in larvae

The *Poxn-CD8::GFP-3-3* transgenic line was used to analyze the morphology of *Poxn*-neurons in the developing brain. This transgene expresses the membrane-associated CD8::GFP fusion protein in all cells of the Poxn domain throughout brain development, as determined by immunostaining with Poxn- and GFP-antiserum at all stages of larval development. In addition, this line expresses CD8::GFP ectopically in a few cells close to, but distinct from, the ventral cluster of Poxn-expressing cells (see, for example, the strongly labeled cells closest to the midline in Figure 21C).

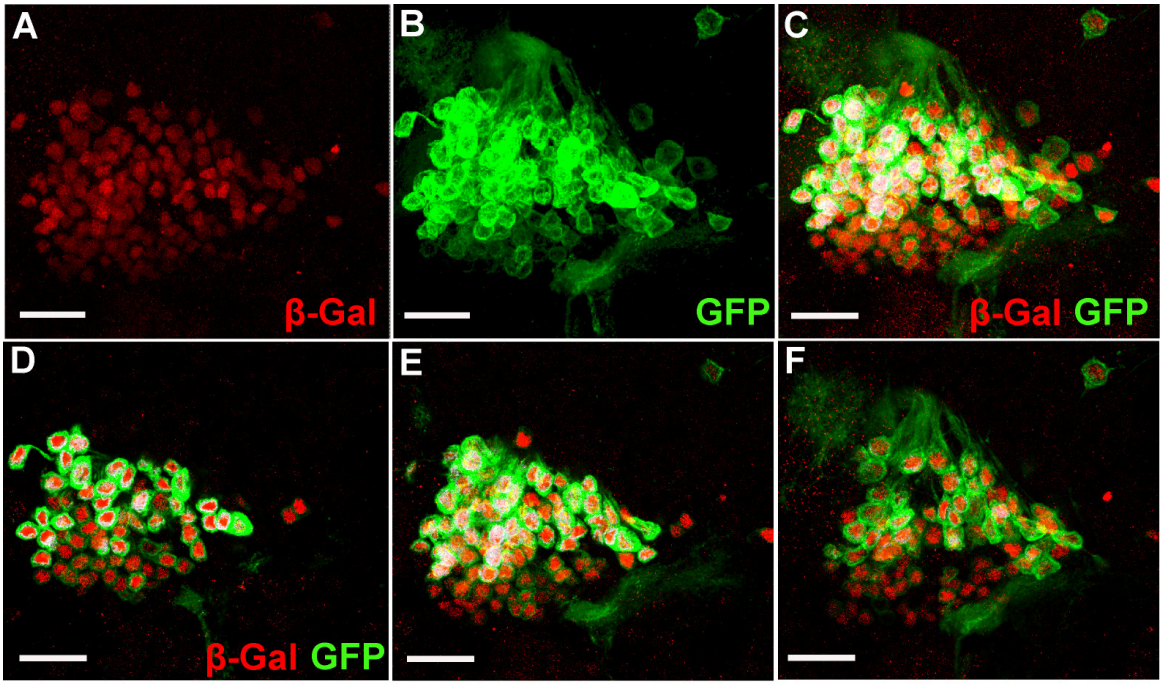

Figure 20. Most *Poxn*-neurons of late third instar larvae survive metamorphosis. (**A**) Dorsal cluster of Poxn-expressing cells in the adult brain stained with anti-β-Gal. β-Gal-positive nuclei belong to cells that expressed Poxn in a third instar larva at the time of heat shock. (**B**) The identical cluster labeled with GFP. The membrane-associated CD8::GFP represents the dorsal Poxn-expressing cells in the adult brain at the time of fixation. (**C**) Maximum projection of the entire z-stack combining both labels. (**D**-**F**) Maximum projections of substacks at 1-5 µm (D), 6-10 µm (E), and 11-31 µm (F) of the z-stack shown in (C). All images show frontal views at 63x magnification. Similar results were obtained for the ventral cluster (not shown). Size bar: 20 µm.

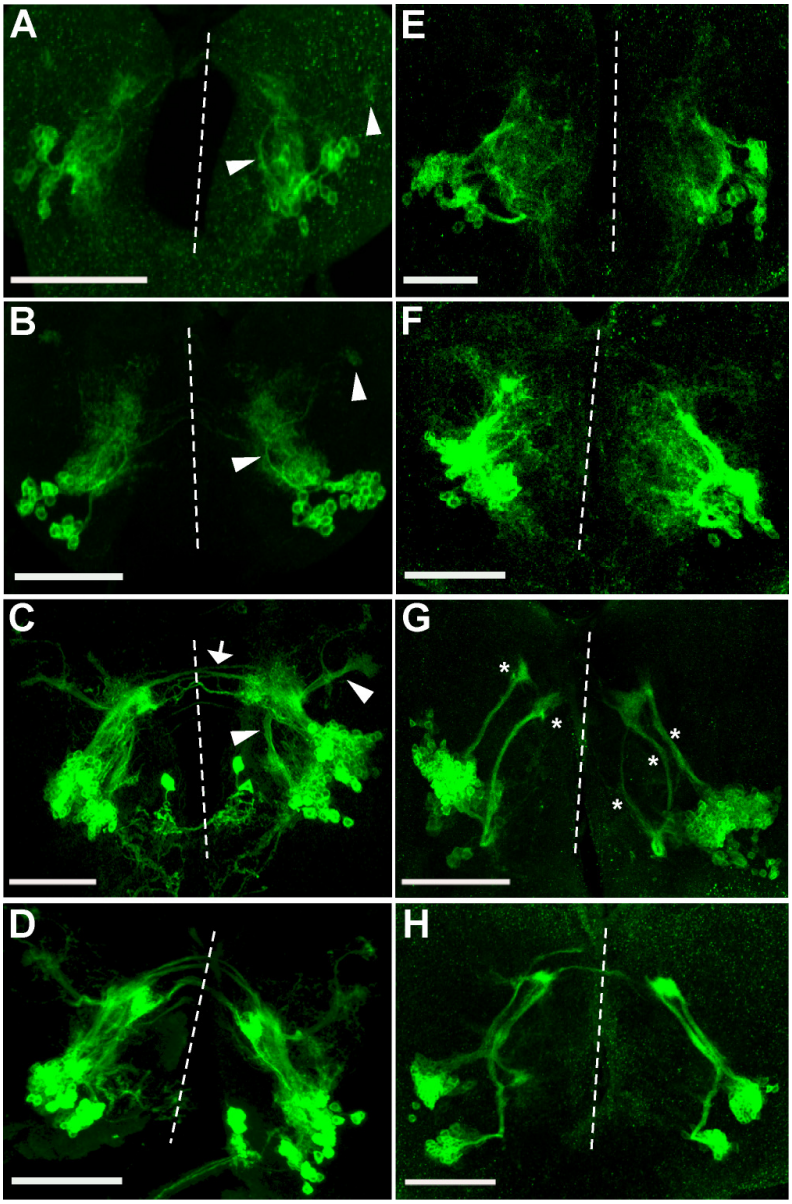

Figure 21. Projections of *Poxn*-neurons in wild-type and *Poxn* mutant larval brains, as revealed by expression of *Poxn-CD8::GFP3-3*. Brains of first (**A**), second (**B**), and late third instar (**C**) larvae labeled with GFP and corresponding images of *Poxn* mutant larval brains (**E-G**). (**D** and **H**) Projection patterns of *Poxn-CD8::GFP* expressing neurons in late third instar larval brains of *Poxn* mutants, rescued by *PoxnSuperA* (D) and *PoxnSbl* (H), resemble those of wild-type (C) and *Poxn* mutant brains (G), respectively. All panels show frontal views. Dashed lines indicate midlines, anterior is to the top. Arrowheads in A, B, and C point to arc-like projections of posterior cluster, and arrow in C indicates projections in the commissure from the anterior Poxn-expression domain in the wild type. Asterisks in G indicate aberrant morphologies of projections from both neuronal clusters in the *Poxn* mutant. All immunofluorescent images are at 63x magnification, maximum projections of z-stacks of CLSM sections. Scale bar: 50 µm.

The developing brain in first and second instar larvae

Only a minority of Poxn-expressing cells extend neurites during larval stages of brain development. In first and second instar larval brains, the somewhat diffuse neuronal projections from the anterior-most cells of the Poxn domain are oriented anteriorly and towards the midline, whereas the projections of the posterior-most cells of the Poxn domain exhibit an arc-like morphology and are oriented towards the anterior-lateral brain regions (Figure 21A, B). It is evident from the two distinct projection patterns that the Poxn-expressing cells observed at these early stages of larval development are already divided into two separate populations of neurons, a dorsal and a ventral cluster.

The Gal4 enhancer trap line *MZ699* labels vPNs, which project through the mACT, at all larval stages and thus can be used to identify larval vPNs (Ito *et al*., 1997). In first instar larval brains, the mACT formed by *MZ699*-expressing fibers clearly colocalized with the projections of the ventral *Poxn*-neurons (Figure 22A). Four Poxn-expressing cells colocalized with *MZ699*-positive cells (Figure 22B-D). Similarly, in second instar larval brains, six to seven Poxn-expressing cells colocalized with the *MZ699* vPN marker **(**Figure 23B–D**),** and the mACT formed by the *MZ699*-expressing neurons clearly colocalized with the projections of the ventral *Poxn*-neurons (Figure 23A) and exhibited the same morphology as observed during the first instar. Projections in the mACT appeared to be tightly bundled with no apparent arborizations except in the lateral protocerebral region (Figure 23A).

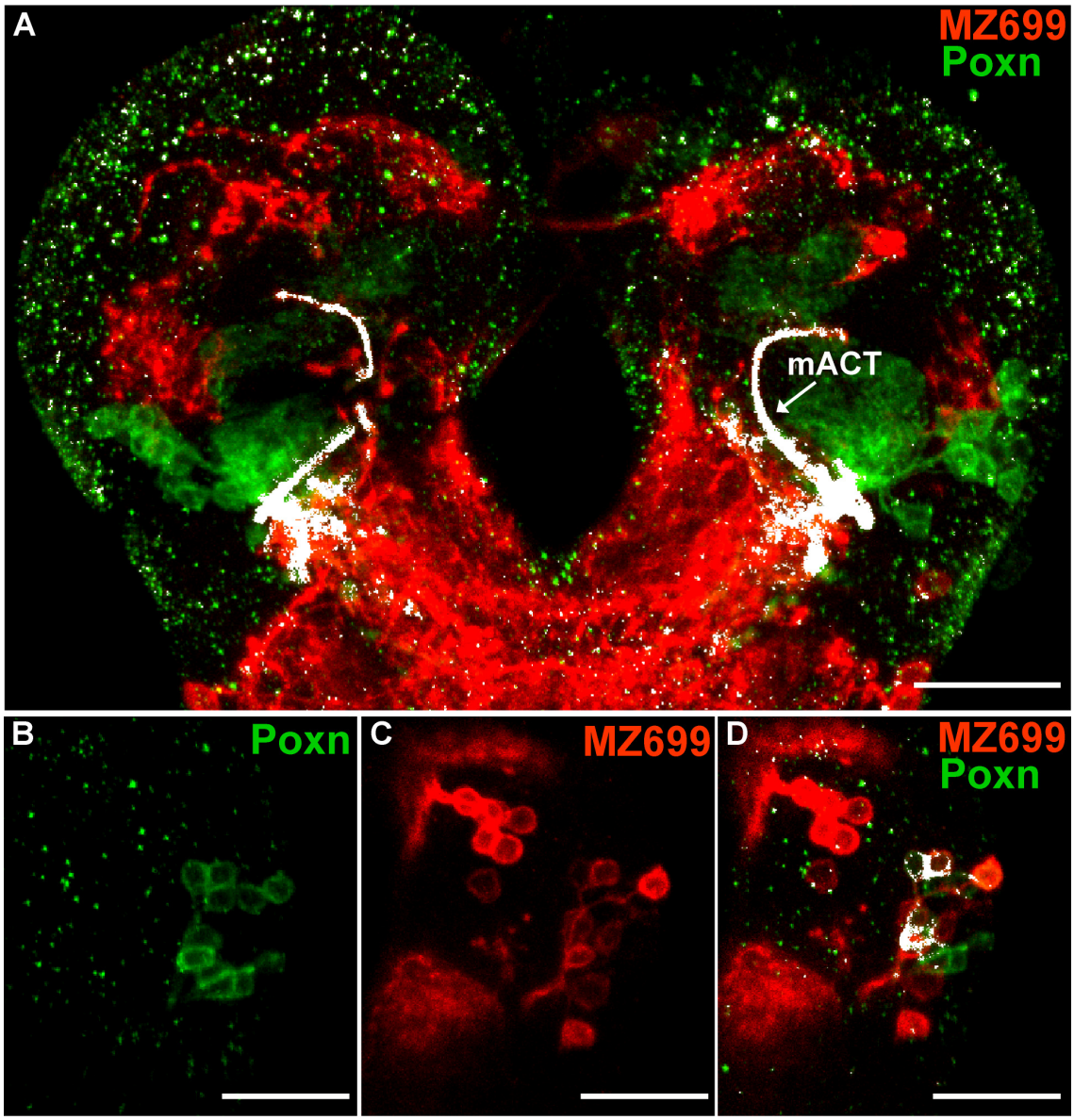

Figure 22. Colocalization of *Poxn*-neurons with the marker for ventral projection neurons, *MZ699-Gal4*, in first instar larval brain. (**A**) Frontal view of w^{1118}; *Poxn-CD8::GFP15.2/UAS-CD2*; *P{GawB}MZ699* first instar larval brain, stained for CD2 (red) in the *MZ699* expression domain and GFP (green) in the Poxn expression domain. Colocalization of CD2 and GFP, indicated by white pixels, is clearly visible in the mACT. (**B-D**) Frontal view of first instar larval brain, displaying GFP-stained (B) and CD2-stained (C) cell bodies and their merge (D). In (D), 4 cells are visible that express both CD2 (*MZ699-Gal4*) and GFP (*Poxn-CD8::GFP*). 40x magnification, maximum projection of confocal z-stacks. mACT, middle antennocerebral tract. Size bar: 20 µm.

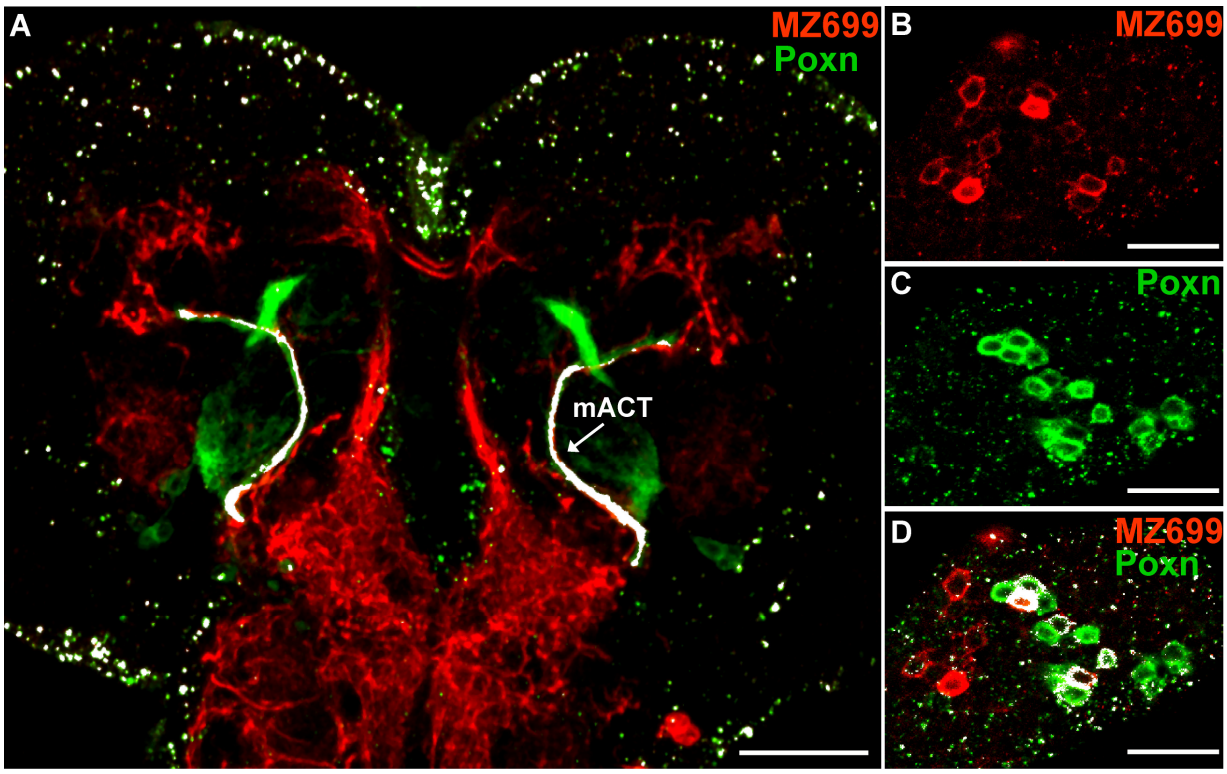

Figure 23. Colocalization of *Poxn*-neurons with the marker for ventral projection neurons, *MZ699-Gal4*, in second instar larval brains. (**A**) Frontal view of w^{1118}; *Poxn-CD8::GFP15.2/UAS-CD2*; *P{GawB}MZ699* second instar larval brain, stained for CD2 (red) in the *MZ699* expression domain and GFP (green) in the Poxn expression domain. Colocalization of CD2 and GFP, indicated by white pixels, is clearly visible in the mACT. (**B-D**) Frontal view of second instar larval brain, displaying CD2-stained (B) and GFP-stained (C) cell bodies and their merge (D). In (D), 6-7 cells are visible that express CD2 (*MZ699-Gal4*) and GFP (*Poxn-CD8::GFP*). 40x magnification, maximum projection of confocal z-stacks. mACT, middle antennocerebral tract. Size bar: 20 μm.

The developing brain in third instar larvae

In third instar larval brains, the density of neurites grows considerably. The neuronal projections appear to follow the pathways established during the first and second instar (Figure 21A, B). The Poxn domain now consists of two clearly distinguishable but closely spaced clusters of neurons (Figure 21C). Most of the neuronal processes of the dorsal cluster, DC, project towards the dorsomedial part of the brain, and some of them extend into several tracts of the supraesophageal commissure. The projections of the ventral cluster, VC, exhibit an arc-like morphology and target the lateral regions of the brain (Figure 21C).

To further map the projection patterns observed in third instar larval brains, the pan-neuronal synaptic marker Dlg (Woods and Bryant, 1991; Zito *et al*., 1997; Menon *et al*., 2004) and the long axon tract marker Fasciclin-II (Grenningloh *et al*., 1991; Nassif *et al*., 2003) were used. The synaptic neuropil region, especially the mushroom body lobes and larval antennal lobes (LAL), are distinctly labeled with Dlg. Staining for Dlg and Poxn revealed that some of the neuronal projections emanating from the dorsal Poxn cluster colocalize with the medial lobes of the larval mushroom bodies (Figure 24A). In addition, *Poxn*-neurons form a relatively thick bundle and up to three fine projections of neurites at the midline in the supraesophageal commissure (Figure 24A).

Some projections of the VC target the larval AL, as revealed by colocalization of GFP with Dlg (Figure 24A). The neurites of the *Poxn*-neurons seem to pass through only few lateral glomeruli in the LAL (Figure 24A'). The projections then follow an arc-like path and target the lateral protocerebral region (Figure 24A), the larval equivalent of the adult lateral horn (Stocker *et al*., 1997). It is evident that the projections use the middle branch of the antennocerebral tract. While the majority of the projection neuron fibers

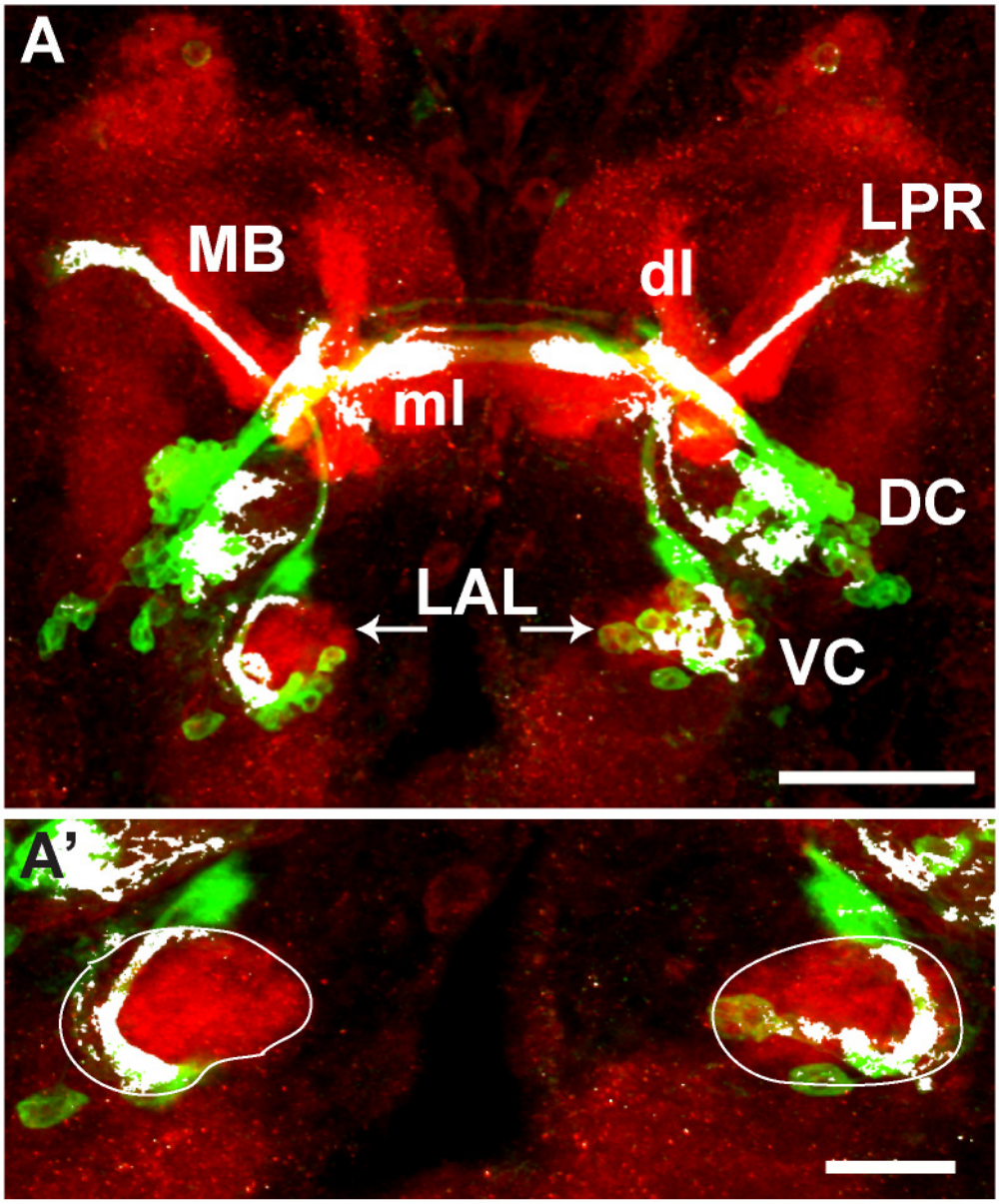

Figure 24. Projection patterns of *Poxn*-neurons in late third instar larval brains stained for the synaptic marker Dlg. Frontal views of a *Poxn-CD8::GFP3-3* late third instar larval brain, stained for GFP (green) and Dlg (red), at 40x **(A)** and an enlarged view of the LALs (encircled) at 63x magnification **(A')** and maximum projection of z-stacks. Note that axons of *Poxn*-neurons passing through the mACT contact a small subset of specific LAL glomeruli. MB, larval mushroom bodies; dl, dorsal lobe of MB; ml, medial lobe of MB; LAL, larval antennal lobes; LPR, lateral protocerebral region; DC, dorsal cluster; VC, ventral cluster. Size bars: 50 µm (A) and 20 µm (A').

target the higher olfactory centers, the mushroom bodies and lateral protocerebral region, via the inner antennocerebral tract, only few projection neuron fibers, projecting from lateral glomeruli, use the middle antennocerebral tract, the mACT (Stocker *et al*., 1997). This tract branches off the inner antennocerebral tract posterior to the LAL, passes just ventral to the mushroom body, and then directly extends towards the lateral protocerebral region (Stocker *et al*., 1990; 1997). The tract does not show many arborizations between the cell bodies and the terminals but appears as tight bundle with few arborizations, visible only in the lateral protocerebral region (Figure 24A). The morphology of the mACT formed by the projections of the *Poxn*-neurons remains the same at all larval stages.

We compared the positions, shapes, and neurites of major Fasciclin-II (FasII)-immunopositive long axon tracts with those of the Poxn-expressing neurons. The cell bodies of the *Poxn*-neurons are located between the ventral larval optic commissural tract (LOCTv) and the ABTp (posterior branch of basoanterior tract), near the junction of the brain hemisphere and the ventral nerve cord (Figure 25A). The *Poxn*-neurons project towards the LOCTv as well as the dorsal larval optic commissural tract (LOCTd). Due to the appearance of a large number of axons during late larval stages, the supraesophageal or dorsal commissure increases in size. As a result, a number of fibers of *Poxn*-neurons of the DC, along with many other fibers, pass the commissure between the anterior and posterior component (DPCa and DPCp) of the dorsoposterior commissure (labeled 1 in Figure 25A). Some projections of *Poxn*-neurons of the DC pass the commissure posterior to the DPCp (labeled 2, 7, and 8 in Figure 25A). Many projections of *Poxn*-neurons of the VC populate the anterior hub area (AH in Figure 25A).

Figure 25. **Position of *Poxn*-neurons with respect to axonal tracts marked by Fas-II in wild-type and *Poxn* mutant late third instar larval brains.** (**A**) Frontal view of *P{W6 Poxn-CD8::GFP}3-3* late third instar larval brain, displaying the major long axon tracts stained for Fas-II (numbered 1 to 10; Nassif *et al*., 2003) and the neurites of *Poxn*-neurons. (**B, C**) Frontal views of $Poxn^{\Delta M22\text{-}B5}$ *P{W6 PoxnSbl107}*; *P{W6 Poxn-CD::GFP}3-3* late third instar mutant larval brains, displaying the two different types of neuronal projection patterns commonly observed in *Poxn* mutants. In (B), the projections from the ventral cluster seem to follow the iACT, whereas in (C) they adopt a completely different path. All brains are stained for GFP (green) and FasII (red). Pictures are maximum projections of z-stacks of CLSM sections, taken at 40x magnification. ABTp, posterior branch of basoanterior tract; AH, anterior hub; dlb, dorsal lobe of mushroom body; DPCa, anterior limb of dorsoposterior commissure; DPCp, posterior limb of dorsoposterior commissure; iACT, inner antennocerebral tract; LOCTd, dorsal larval optic commissural tract; LOCTv, ventral larval optic commissural tract; mACT, middle antennocerebral tract; mlb, medial lobe of mushroom body; PH, posterior hub. Colocalized pixels are shown in white. Size bar: 50 μm.

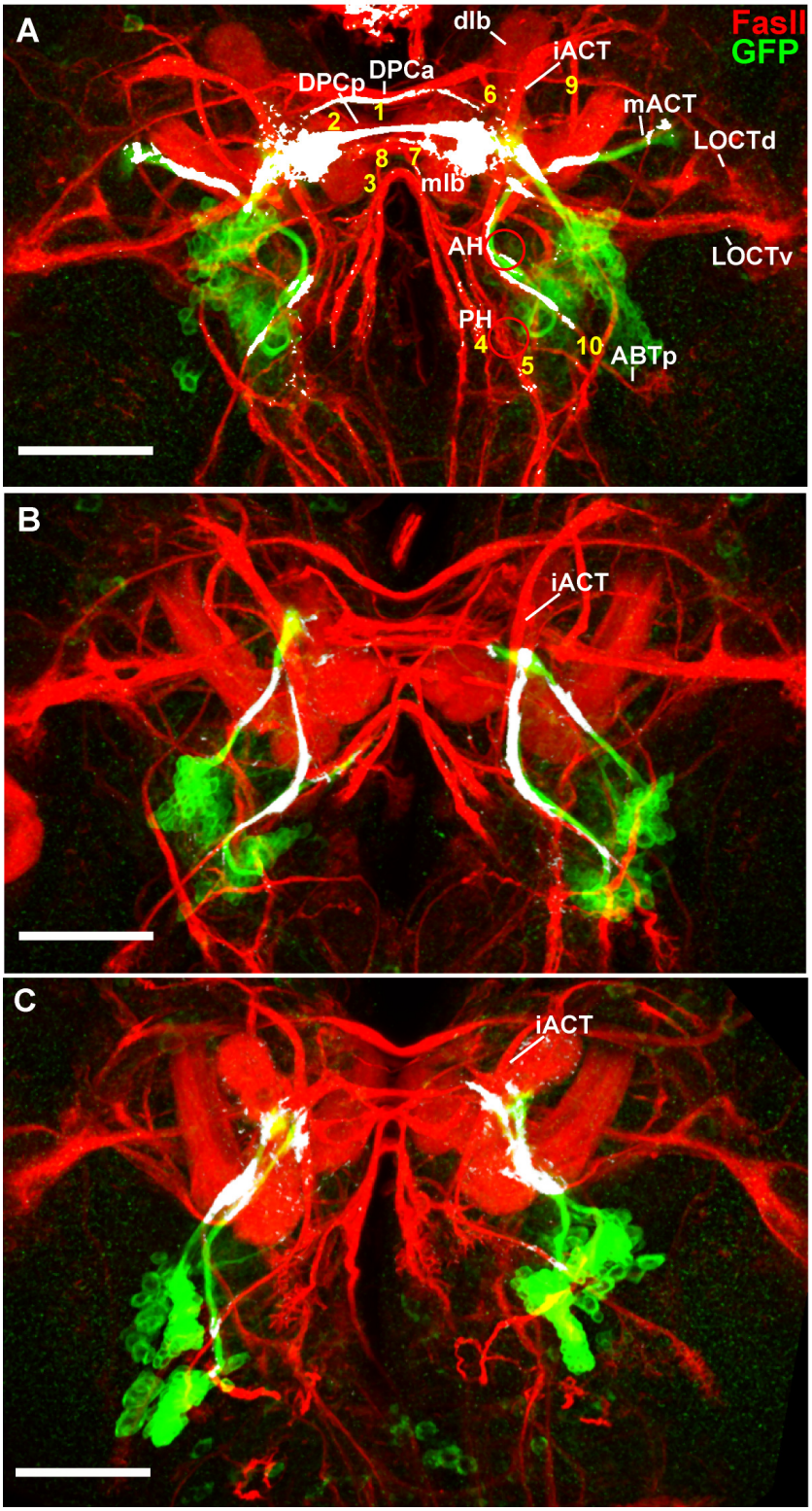
A
FasII
GFP
dlb
iACT
DPCp
DPCa
6
9
2
1
mACT
LOCTd
8
7
3
mlb
AH
LOCTv
PH
4
10
ABTp
5
B
iACT
C
iACT

As described above, the *Poxn*-neurons of the VC send their neurites through the mACT to target the lateral protocerebral region (LPR), a higher olfactory center (Figure 26). The mACT is formed by a subset of projection neurons in the larva (Figure 26). Certain Gal4-enhancer trap lines label distinct sets of neurons processing olfactory input in the larval brain. For example, *GH146* labels anterodorsal, lateral, and ventral projection neurons in third instar larvae (Stocker *et al*., 1997). Most neurons marked by this enhancer trap line send processes through the inner antennocerebral tract and target higher olfactory centers, but a very small fraction of PN fibers project through the mACT (Stocker *et al*., 1997). Colocalization of Poxn and GFP-expression driven by *GH146* was analyzed in late third instar larval brains. No Poxn-expressing cells were found to colocalize with projection neurons labeled by *GH146* at this stage of development (Figure 27B). This result is not very surprising in view of the fact that most of the projection fibers labeled with *GH146* in the larval brain pass through the iACT whereas only a very small number of these fibers passes through the mACT used by the *Poxn*-neurons. In the adult brain, however, 4 Poxn-expressing vPNs colocalize with *GH146*-positive vPNs, of which there are six in the adult brain (Werner Boll, personal communication).

The *MZ699*-labeled neurons and the *Poxn*-neurons of the VC send projections along the mACT in third instar larvae (Figure 28A), as observed in first and second instar larvae (Figures 22 and 23). The projections of the *Poxn*-neurons of the VC are much thicker and denser than in second instar larvae (Figure 23A). In addition, they have substantially increased their density relative to the projections of the *MZ699*-expressing neurons (cf. Figure 28A with Figure 23A). The *Poxn*-neurons colocalizing with *MZ699*-positive neurons roughly doubled since the second instar to 10-12 neurons observed by the end of larval development (Figure 28B, C). Along with the increased thickness of

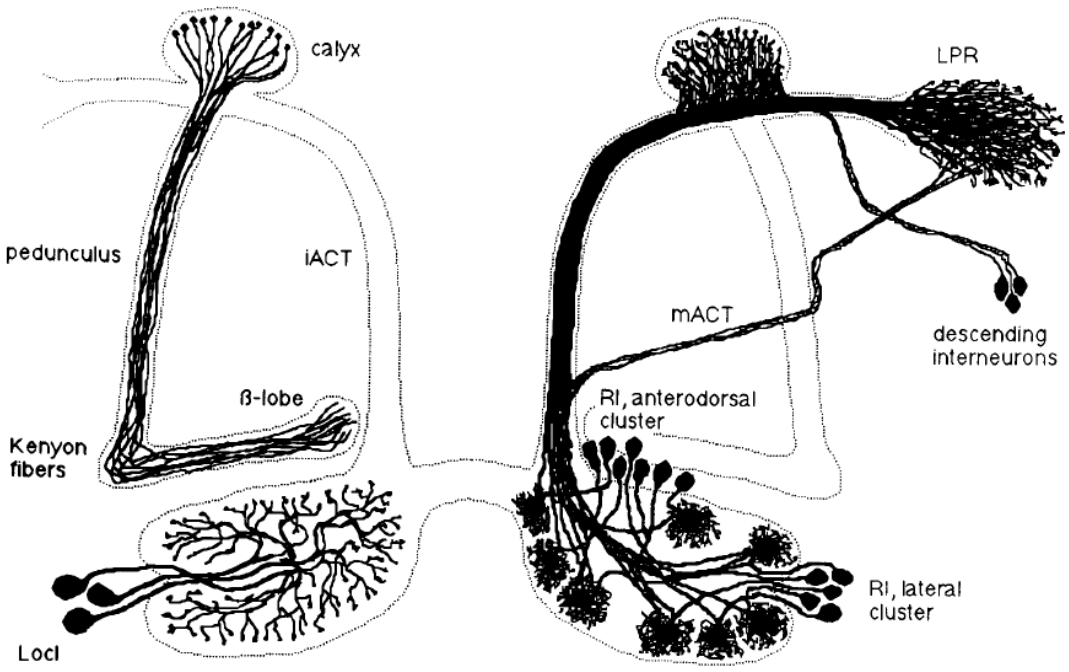

Figure 26. Schematic diagram displaying the different types of projection neurons in third instar larval brain. Three distinct neuronal clusters, anterodorsal, lateral, and ventral (not shown here), contribute to the formation of the three antennocerebral tracts i.e., the outer antennocerebral tract (oACT) (not shown), middle antennocerebral tract (mACT), and inner antennocerebral tract (iACT). The mACT branches off from the iACT behind the larval antennal lobe and passes below the pedunculus of the mushroom body (MB) to target the lateral protocerebral region (LPR) directly. The iACT first targets the MB calyx and then establishes profuse arborizations in the LPR. Like the mACT, the oACT targets the LPR directly but exits from the iACT more ventrally and turns laterally to continue in a tract to the LPR directly (not shown here). LocI, local interneurons. Modified from Stocker *et al*., 1997.

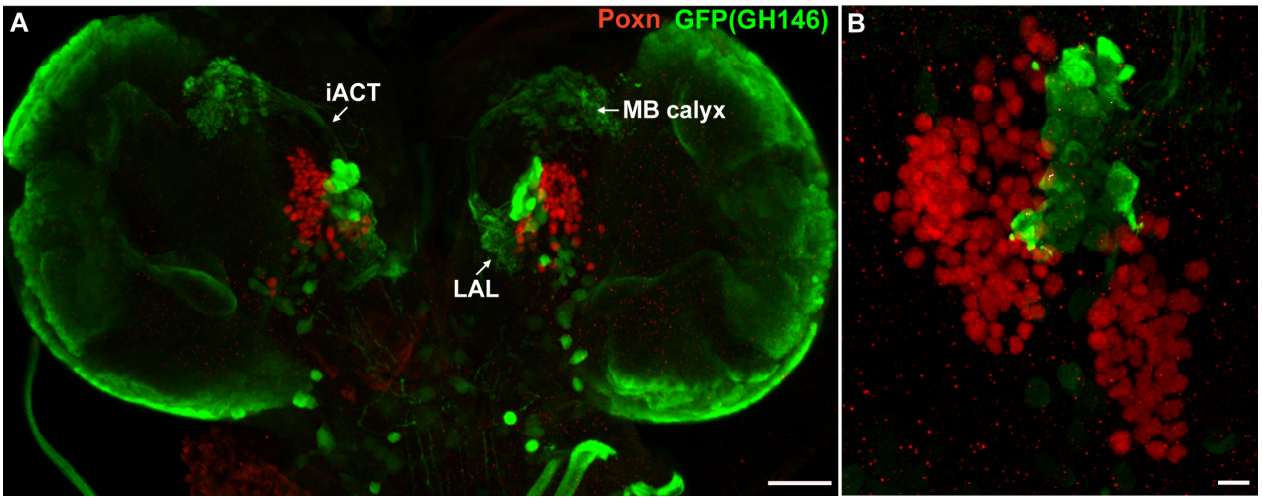

Figure 27. Colocalization of Poxn-expressing cells with the expression of the projection-neuron marker *GH146* in the brain of late third instar larvae. (**A**) Frontal view of a w^{1118}; *P{GawB}GH146*; *UAS-GFP* late third instar larval brain, stained for Poxn (red) and GFP (green). The iACT is clearly visible, whereas the mACT is not seen since it is not marked very strongly by GFP. 20x magnification, maximum projection of confocal z-stacks. (**B**) Late third instar brain stained for Poxn and GFP. No colocalization with GFP is evident in the Poxn expression domain. 63x magnification, maximum projection of confocal z-stacks. iACT, inner antennocerebral tract; LAL, larval antennal lobe; MB, mushroom body. Size bars: 100 μm (A) and 20 μm (B).

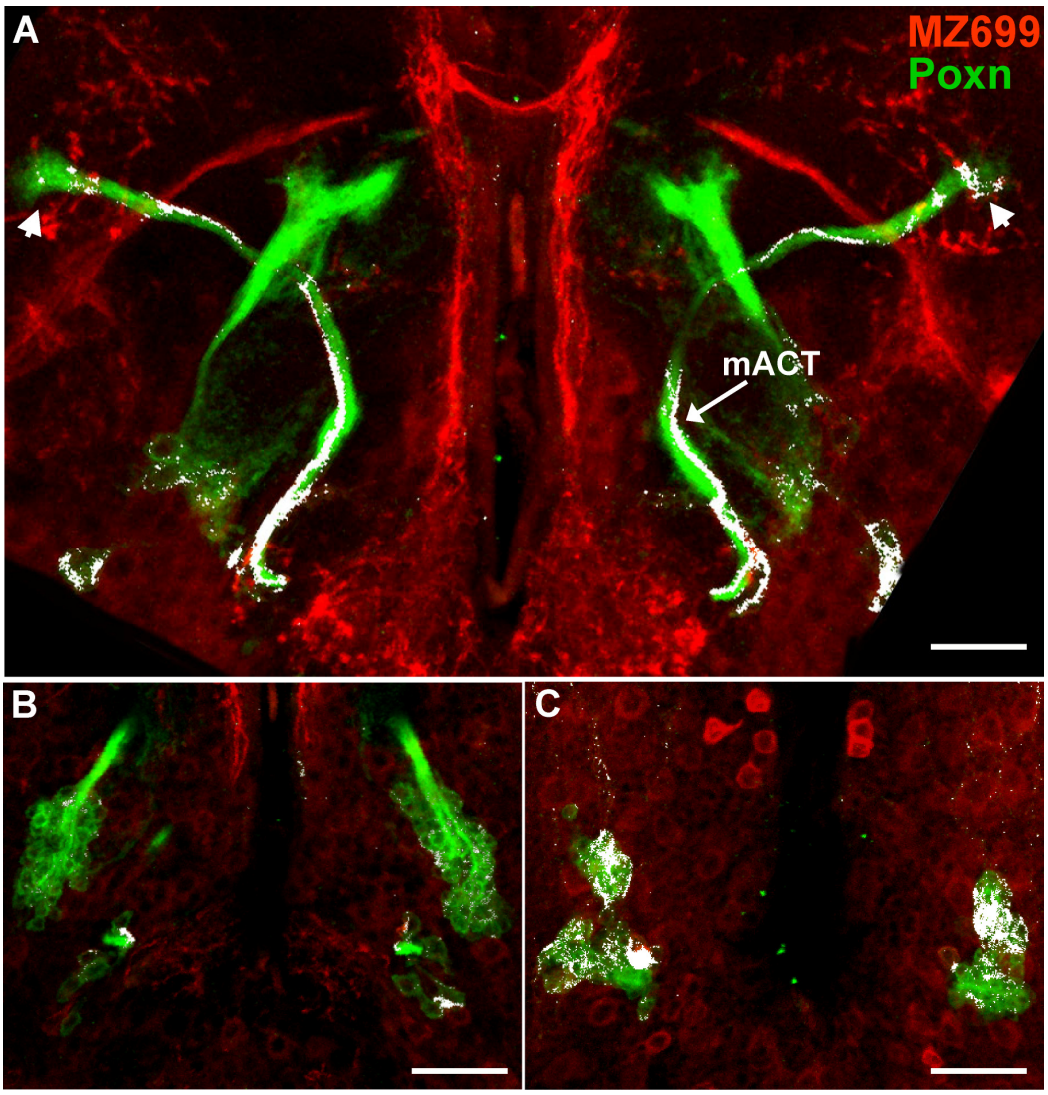

Figure 28. Colocalization of *Poxn*-neurons with *MZ699* in late third instar larvae. Frontal views of w^{1118}; *Poxn-CD8::GFP15.2/UAS-CD2*; *P{GawB}MZ699* late third instar larval brains, stained for GFP (green) and CD2 (red), labeling the Poxn- and *MZ699*-expressing neurons, respectively. Colocalization of the two signals (white pixels) is observed in the mACT in maximum projections of confocal z-stacks **(A)** and in individual cell bodies in deeper sections (29 to 48 µm) of the cell cluster **(C)**, whereas no colocalization is seen in cell bodies in sections from 1 to 28 µm **(B)**. Approximately 10-12 cells co-express CD2 and GFP. Arrowheads in (A) point to the increased volume of arborizations at the lateral protocerebral region. All pictures are taken at 40x magnification. Middle antennocerebral tract, mACT. Size bar: 20 µm.

their projections through the mACT, the arborizations of the *Poxn*-neurons in the LPR appear to have increased in volume (arrowheads in Figure 28A) as compared to earlier larval stages (Figure 22A and 23 A).

The adult antennal lobe begins to develop adjacent and dorsal to the LAL and can be recognized near the LAL as separate entity in late third instar larvae (Figure 9). The developing adult antennal lobe is targeted by newly developing dendrites of embryonic- and larval-born projection neurons. It is not labeled by the presynaptic marker, NC82 (Wagh *et al*., 2006), but can be clearly seen with the glial cell membrane marker, *repo-Gal4* driving *UAS-CD2* expression (Jefferis *et al*., 2004). The larval antennal lobe begins to degenerate at the onset of pupariation and has completely degenerated by 18 h APF. Neurites of *Poxn*-neurons were visualized together with glial membranes, marked by *repo-Gal4* driving *UAS-CD2* expression, in w^{1118}; *UAS-CD2*; *repo-Gal4 Poxn-CD8::GFP-3-3* third instar larvae (Figure 29). The developing adult antennal lobe is recognized by the absence of glial cells and their profuse filopodial processes present in the surrounding area (Jefferis *et al*., 2004; Figure 29). Glial invasion into the developing adult antennal lobes is observed only around 50 h APF (Jefferis *et al*., 2004). The *Poxn*-neurons of the ventral cluster send processes through the lateral region of the LAL that pass through the developing adult antennal lobe and the mACT to target the lateral protocerebral region (Figure 29). They do not have any distinct arborizations in the LAL, but a fuzzy swelling of the projection is observed in the developing adult antennal lobe, while in the mACT the neurites are again tightly bundled. Because the ventral *Poxn*-neurons show traces of dendritic arborizations in the developing adult antennal lobe but no dendritic invasion in the larval antennal lobe, most probably they have no function in larvae, but are developing to perform a function in the olfactory network of the adult brain.

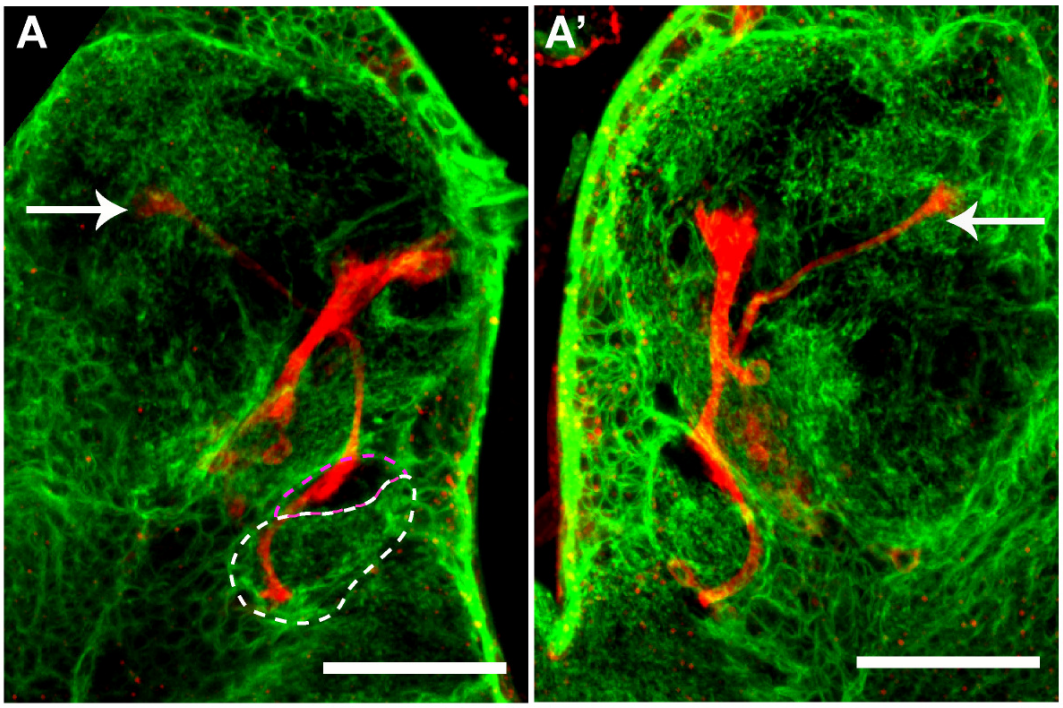

Figure 29. **Projection pattern of *Poxn*-neurons with respect to a glial cell membrane marker in late third instar larval brain.** Left (**A**) and right (**A'**) hemisphere of *w*; *UAS-CD2*; *repo-Gal4 Poxn-CD8::GFP3-3* late third instar larval brain, stained for GFP (red), labeling *Poxn*-neurons, and CD2 (green), marking glial membranes. The axons of the *Poxn*-neurons pass through the lateral region of the LAL (encircled by white dashed line in panel A), form dendritic arbors in the developing adult antennal lobe (encircled with purple dashed line) and follow the mACT to target the lateral protocerebral region (marked by arrows). Both images are maximum projections of z-stacks of CLSM sections at 40x magnification. Size bar: 50 µm.

3.4.2 The developing brain in *Poxn* mutant larvae

In the transgenic line *Poxn-CD8::GFP-3-3*, expression of CD8::GFP in the Poxn domain of the developing brain not only coincides with cells that express Poxn protein (Figure 12), but is also observable in a *Poxn* null mutant background and hence serves as marker for these neurons in the developing brain of *Poxn* mutants. The number and positions of the neurons expressing *Poxn-CD8::GFP*, i.e. of *Poxn*-neurons, in *Poxn* mutant larvae are comparable to those observed in wild-type larvae. In *Poxn* mutants and in mutants including the *PoxnSbl* transgene, which rescues *Poxn* expression everywhere except in the brain, a reduced symmetry of the neuronal projection patterns is revealed by *Poxn-CD8::GFP* in both brain hemispheres during all larval stages (Figure 21E-H). As a control, a projection pattern similar to that in a wild-type larval brain was observed in *Poxn* mutant larvae harboring the *PoxnSuperA* transgene that rescues all *Poxn* functions (Figure 21D). In the mutant, the projections are aberrant at all larval stages (Figure 21E-G). The typical arc-like morphology of neurites from the posterior-most cells of the CD8::GFP-expressing cluster in the wild type (Figure 21A-C, arrowhead) is missing in the *Poxn* mutant, and the projections lack specific orientation but are diffusely directed towards the midline in first and second instar larvae (Figure 21E, F). During the third instar, the neurons form two discernable clusters, and their neurites fasciculate, generating two, sometimes three, bundles that emanate in the dorsomedial direction (Figure 21G). In the region where in the wild type these neurites turn towards their target regions (arrowheads and arrow in Figure 21C), they seem to stall in the mutant and form small arbors at their distal ends (asterisks in Figure 21G). Consequently, very few neurites appear at the supraesophageal commissure and none in the LPR (Figure 21G, H).

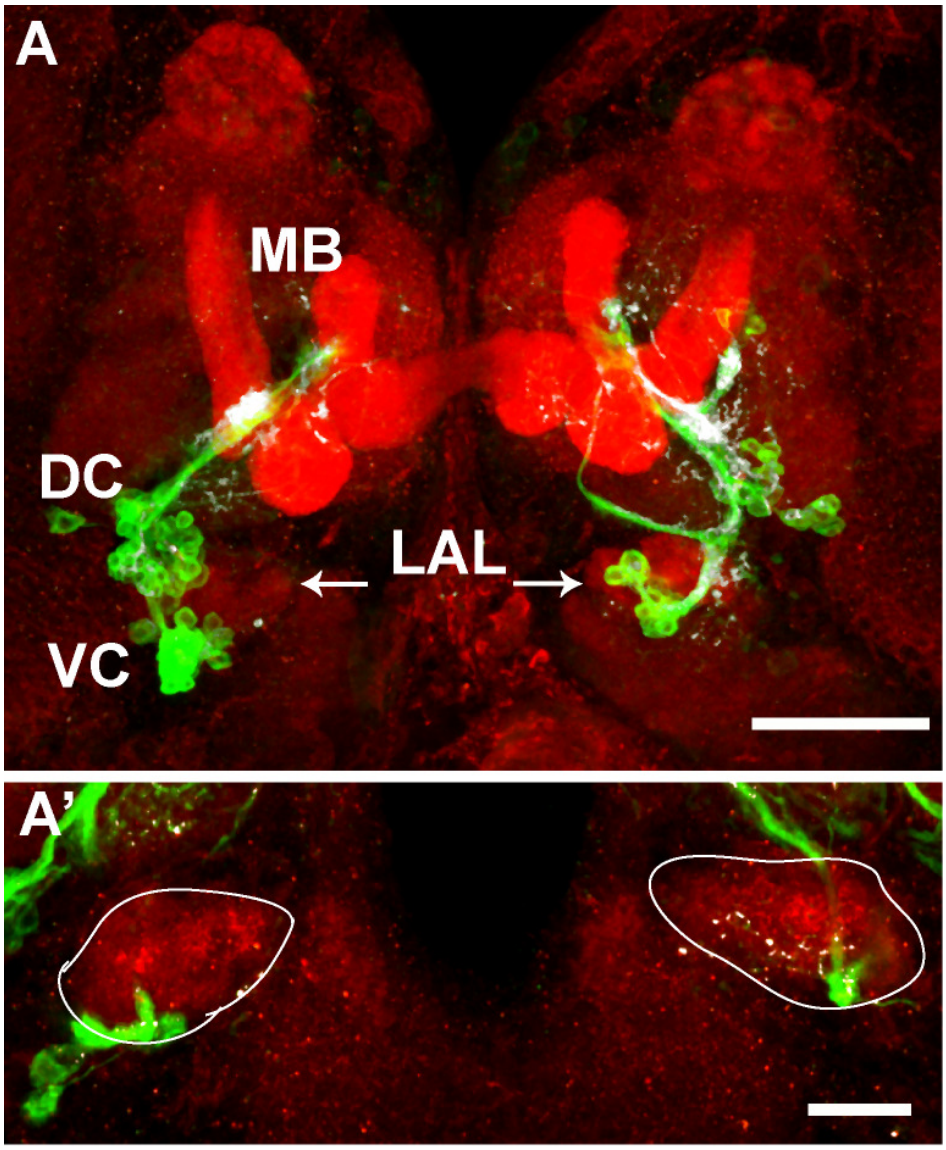

Figure 30. Projection pattern of *Poxn*-neurons in *Poxn* mutant late third instar larval brains stained for the synaptic marker Dlg. Frontal views of a $Poxn^{\Delta M22\text{-}B5}$ *P{W6 PoxnSbl107}*; *P{W6 Poxn-CD::GFP}3-3* late third instar larval brains, stained for GFP (green) and Dlg (red), at 40x **(A)** and an enlarged view of the LALs (encircled) at 63x magnification (**A'**) and maximum projection of confocal z-stacks. The axons of the *Poxn*-neurons do not pass through the LAL, as evident from the absence of colocalization of Dlg with GFP. Note also in (A) that the processes from the *Poxn*-neurons of the right and left ventral clusters follow the two different types of paths illustrated in Figure 25B and C, respectively. MB, larval mushroom bodies; LAL, larval antennal lobes; DC, dorsal cluster; VC, ventral cluster. Size bars: 50 µm (A) and 20 µm (A').

Similar results were obtained after labeling with the synaptic marker Dlg (Figure 30) or the long axon marker FasII (Figure 25B, C). In the brain of wild-type late third instar larvae, staining for Dlg and CD8::GFP indicates that projections from the *Poxn*-neurons pass through few lateral glomeruli of the larval antennal lobes (LAL) and through the medial lobes of the mushroom bodies to target via the mACT the LPR (Figure 24). By contrast, in the *Poxn* mutant the invasion of the LALs is absent, and the medial lobes of the mushroom bodies as well as the LPRs are not targeted (Figure 30). In *Poxn* mutant brains, the neurites from the ventral cluster of *Poxn*-neurons begin to follow the inner antennocerebral tract (Figure 25B) or run parallel to the processes emanating from the dorsal cluster of *Poxn*-neurons and stall near the midline (Figure 25C). In the latter case, they bypass the LAL, turn laterally behind it, and extend towards the dorsal regions of the brain.

3.4.3. The developing brain in wild-type pupae

At late third instar and the onset of pupariaton, few neurons of the dorsal *Poxn*-cluster extend their neurites into the supraesophageal commissure (Figure 21C and 31A). By 10 h APF their number has markedly increased (Figure 31B). The neurons now extend their neurites along the specific pathways predefined by persistent larval projections of the pioneering *Poxn*-neurons. Around 15 hours APF, two swellings (arrow heads) flanking the developing ellipsoid body neuropil begin to appear (Figure 31C). By 20 hours APF, the neurites at the commissure expand considerably and a kidney-like structure begins to appear (Figure 31D). The two *Poxn*-clusters separate and can be easily distinguished by 30 hours APF (Figure 31E). The relatively dense kidney-shaped

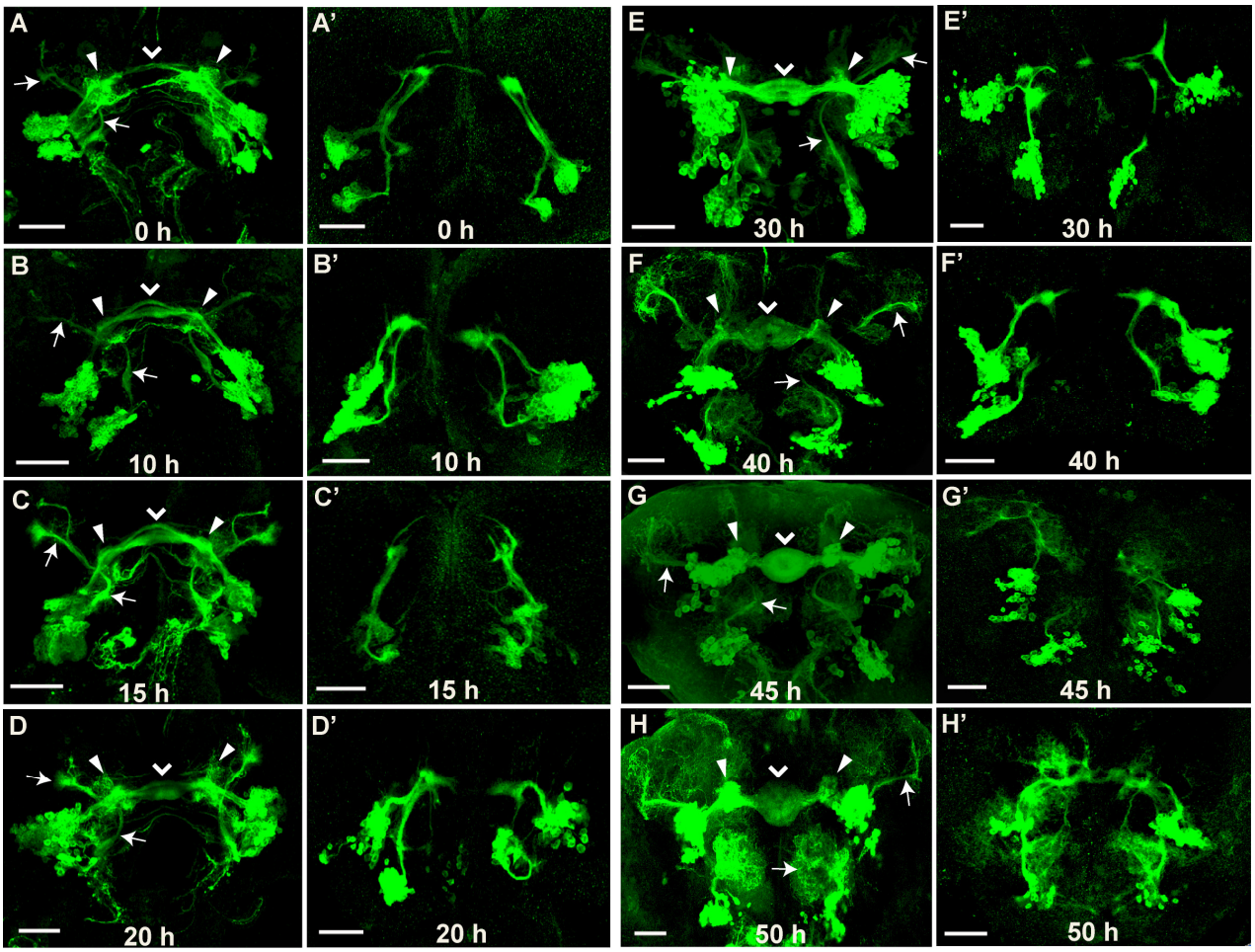

Figure 31. *Poxn*-neurons form the ellipsoid body by 45 h APF, whereas it is missing in *Poxn* mutants. (A-H) Brains of *P{W6 Poxn-CD8::GFP}3-3* pupae, immunostained for GFP at 0 h APF (A), 10 h APF (B), 15 h APF (C), 20 h APF (D), 30 h APF (E), 40 h APF (F), 45 h APF (G), and 50 h APF (H). **(A'-H')** Brains of $Poxn^{\Delta M22\text{-}B5}$ *P{W6 PoxnSbl107}*; *P{W6 Poxn-CD::GFP}3-3* pupae immunostained for GFP at 0 h APF (A'), 10 h APF (B'), 15 h APF (C'), 20 h APF (D'), 30 h APF (E'), 40 h APF (F'), 45 h APF (G'), and 50 h APF (H'). Arrows point to the arc-like morphology of the mACT visible at all pupal stages. Closed arrowheads point to the arborizations at the region of the lateral triangle, while open arrowheads point to the midline neuropil structure that gives rise to the ellipsoid body. All images are maximum projections of confocal z-stacks at 20x magnification. Size bar: 50 μm.

structure is now obvious. By 40 h APF, the kidney-shaped neuropil is transformed into the final doughnut-shaped structure of the ellipsoid body, which at this stage is still open on the ventral side (Figure 31F). By 45 h APF, the axonal arborizations of the DC *Poxn*-neurons clearly outline the doughnut-like structure (Figure 31G) and assume by 50 h APF the typical shape of the adult ellipsoid body (Figure 31H). Consistent with previous observations of large-field neurons of the ellipsoid body (Hanesch *et al.*, 1989), the DC neurons form compact dendritic arborizations in the lateral triangles (ltr) (Figure 31H). The excessive gain in volume and density of arborizations from DC neurons during pupal development result from the expansion of processes of the neurons that already exist at the end of larval development since their number in the DC do not increase significantly during pupal development.

The *Poxn*-neurons of the VC send their processes through the mACT at all pupal stages. During pupariation, the typical arc-like morphology or the mACT, already observed in the larval brain (Figure 21C), is maintained by the fibers of the *Poxn*-neurons of the VC. The targeted regions, the pupal antennal lobe and lateral horn region, are equivalents of the larval structures (LAL and LPR) throughout pupal development (Figure 31A-H). The VCs appear to target mainly the developing adult antennal lobes (ALs), visualized by the glial ensheathment of this structure labeled by *repo-Gal4*-directed CD2 expression in third instar larvae (Figure 29). During larval stages, not many arborizations between cell bodies and terminals are visible. This changes during early pupal stages when small arborizations appear. This appearance correlates in time with the formation of glomeruli in the adult antennal lobe. The arborizations of VC neurons increase in density by 20 h APF (Figure 31D) and are clearly recognized by 30 h APF (Figure 31E). The developing adult ALs harbor profuse arborizations of the VC neurons by 50 h APF, which correlates perfectly with the timing of the acquisition of

mature glomerular structures by the antennal lobes (Jeferris *et al*., 2004). The axonal arborizations in the lateral horn region also increase during late pupal stages (Figure 31F-H) and might correlate temporally with the development of the lateral horn region (Ito *et al*., 1997).

The *Poxn*-neurons of the VC were related to the *MZ699*-positive vPN clusters in the late pupal brain at 80 h APF by double-labeling. The mACT formed by the *MZ699* fibers clearly colocalized with the projections of the ventral *Poxn*-neurons. The tract displays many arborizations between cell bodies and terminals, particularly in the region of the developing adult antennal lobe. Almost 80% Poxn-expressing cells of the VC colocalize with *MZ699* positive vPNs (Figure 32) and hence are ventral projection neurons. None of the dorsal *Poxn*-neurons colocalize with *MZ699* expression.

3.4.4. The developing brain in *Poxn* mutant pupae

The number and positions of the neurons expressing *Poxn-CD8::GFP* in *Poxn* mutant pupae is comparable to those of wild-type pupal brains. In *Poxn* mutant brains of early pupal stages, the *Poxn*-neurons of the DC display a similar phenotype as observed in mutant larvae. The arborization pattern visualized by *Poxn-CD8::GFP* is symmetric till 40 h APF, with most of the neuronal processes of the DC neurons stalled before turning towards the midline (Figure 31A'-F'). Although the number of *Poxn* neurites increases, those that cross the midline do not. The projections through different commissural tracts, apparent in early wild-type pupae (Figure 31A-C), and the kidney-shaped structure, formed in wild-type pupal brains between 20 and 40 h APF (Figure 31D-F), are not observed in mutant pupal brains (Figure 31A'-F'). The neurites appear to fasciculate and

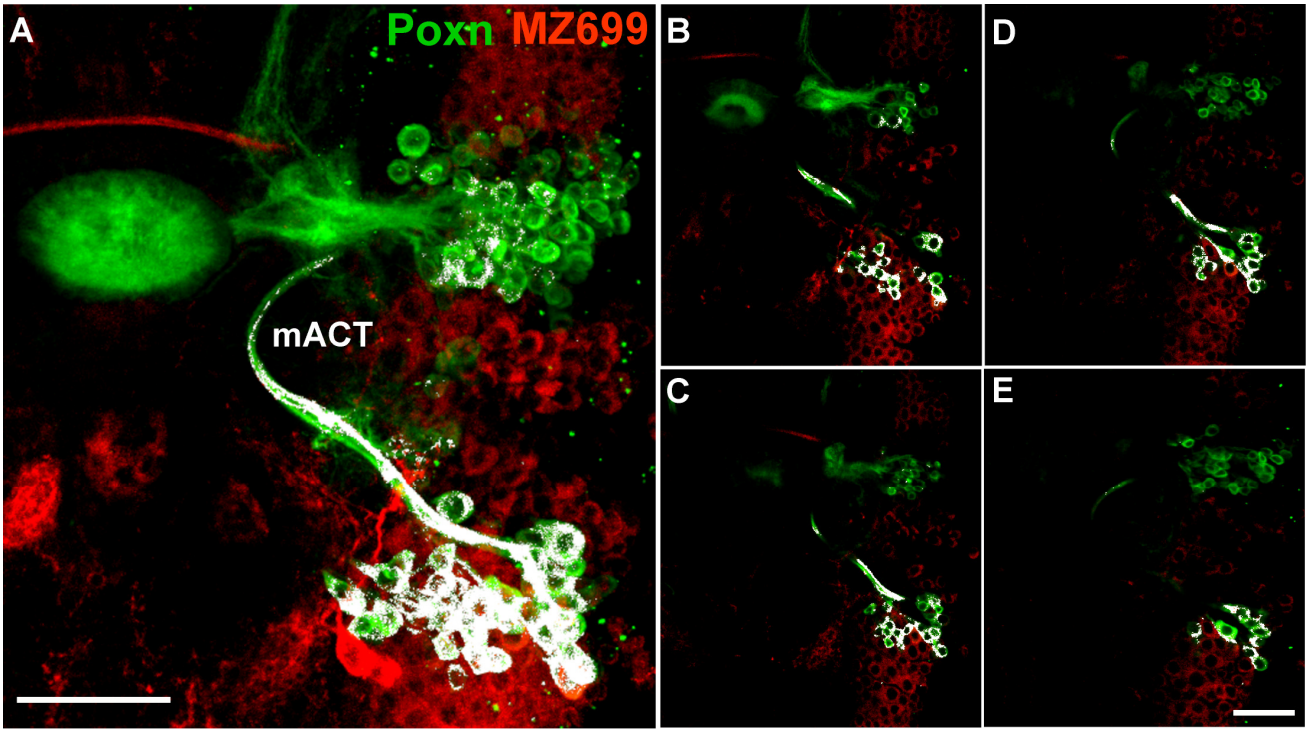

Figure 32. Colocalization of *Poxn*-neurons with ventral projection neurons marked by *MZ699* in pupal brains. (**A**) Brain of w^{1118}; *Poxn-CD8::GFP-15.2*; *P{GawB}MZ699/UAS-CD2* pupa (80 h APF), immunostained for CD2 (red), labeling the *MZ699* expression domain, and GFP (green), labeling the Poxn expression domain. The colocalization of the two signals in the mACT is evident. Almost 90% of ventral *Poxn*-neurons also express CD2 under control of the *MZ699* enhancer. Maximum projection of z-stack of optical CLSM sections. (**B-E**) Single optical sections of the pupal brain shown in (A). Most ventral Poxn-expressing cells co-express CD2 (*MZ699-Gal4*) and GFP (*Poxn-CD8::GFP*). No colocalization of the *MZ699* marker with the dorsal Poxn domain (only right brain hemisphere is shown) is observed. All pictures are taken at 40x magnification. mACT, middle antennocerebral tract. Size bar: 20 µm.

form thicker bundles than in wild-type brains. Furthermore, the projection pattern after 40 h APF is more asymmetric in *Poxn* mutants (Figure 31G', H'). During late pupal stages, the GFP-labeled neuronal processes form a neuropil structure at the midline with an irregular morphology and no resemblance to the ellipsoid body (Figure 31H') formed by the projections of the same neurons in the wild type (Figure 31H).

The neuronal projections of the VC project in a direction similar to that of the DC neurons and display irregular orientations during all pupal stages (Figure 31A'-H'). In early pupae, these projections form thick bundles that stall in the same region as the projections of the DC neurons (Figure 31A'-F'). During pupal stages after 40 h APF, however, the projections appear diffuser and less symmetric than during earlier pupal stages. The innervations of the developing adult ALs are far less prominent (Figure 31G', H') than those observed in wild-type pupal brains (Figure 31G, H). As in mutant larvae, the region of the lateral horn, the structure analogous to the LPR in the larval brain, is not targeted (Figure 31A'-H') and hence the *Poxn*-neurons of the VC do not contribute to the mACT at any stage of pupal brain development in the *Poxn* mutant.

3.4.5. The wild-type adult brain

In a previous report from our lab we have shown the projection pattern of *Poxn*-neurons in *Poxn-Gal4-13-1 UAS-GFP* adult brains (Boll and Noll, 2002; Figure 10D). Werner Boll in our lab noticed that this pattern is altered in heterozygous *Poxn* mutant flies, which could be attributed to the presence of the Gal4 driver. In addition, the projection patterns revealed by *CD8::GFP* driven by *Poxn-Gal4-13-1* and that observed with the *Poxn-CD8::GFP* transgene, in which the expression of *CD8::GFP* is under the direct control of the *Poxn* promoter and enhancer, are quite different in *Poxn* mutant

brains although they look very similar in a wild-type brain. It has also been shown in another study that Gal4 can cause developmental defects (Kramer and Staveley, 2003). Therefore, to avoid possible problems caused by the expression of Gal4 transgenes, we used the *Poxn-CD8::GFP* transgene to investigate the fate of *Poxn*-neurons and their projection patterns in wild-type and *Poxn* mutant adult brains.

Most of the adult *Poxn*-neurons of the DC are R neurons, as judged by position and morphology, forming ring-shaped arbors in the ellipsoid body (Hanesch *et al.*, 1989), as evident from colocalization of Poxn in the DC with the expression of enhancer trap lines specific for various subpopulations (R1 to R4) of R neurons (Renn *et al.*, 1999; Schmid, 2005). The major target of the DC is the ellipsoid body neuropil and the lateral triangles (Figure 33A, B, E, F). The projections at the ellipsoid body and lateral triangles appear to be more pronounced than in the brain at 50 h APF. There are no apparent projections to any other parts of the central complex, and the mushroom body lobes are not targeted either (Figure 33). The neurons do not seem to exhibit any obvious sexual dimorphism (not shown). The projection pattern in brains of *Poxn* mutants rescued by a *Poxn* transgene (Figure 33B) that carries all *Poxn* functions, *SuperA* (Boll and Noll, 2002; Figure 11), is very similar to that in wild-type brains (Figure 33A). This last observation is consistent with previous studies from our lab, in which paraffin sections (Jäger and Fischbach, 1987) of adult brains have been analyzed (Mariotta, 2007). In these sections, the ellipsoid body is clearly visible and similar in wild-type (Figure 34A, C) and *Poxn* mutant brains rescued by *Poxn-SuperA158* (Figure 34B, D).

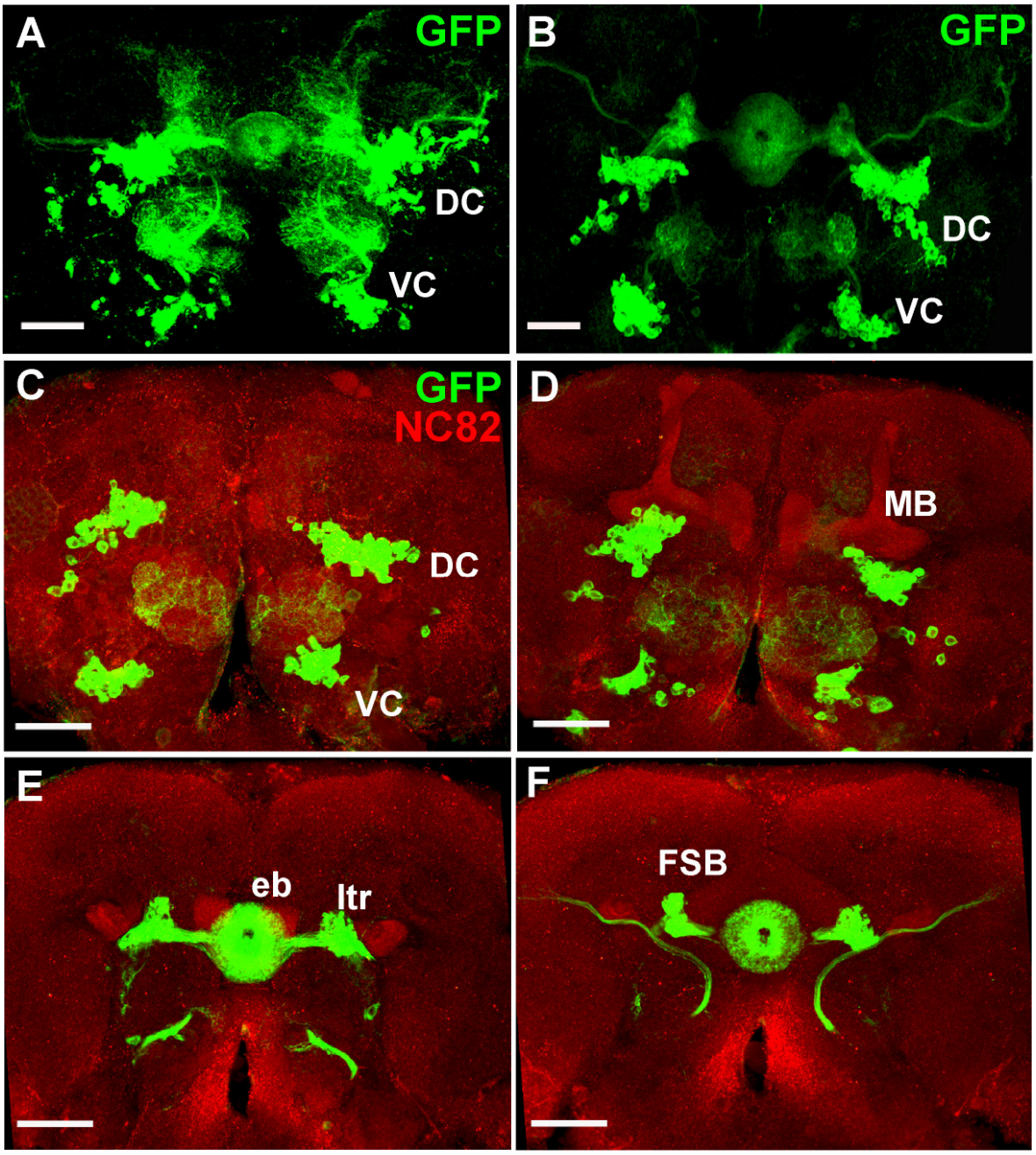

Figure 33. Projection pattern of *Poxn*-neurons in adult brains. (**A, B**) Neuronal projection patterns of w^{1118}; *P{W6 Poxn-CD8::GFP}3-3* (A) and w^{1118}; $Poxn^{\Delta M22\text{-}B5}$ *SuperA-158*; *Poxn-CD8::GFP-3-3* (B) adult brains (frontal views), immunolabeled for GFP and shown as maximum projection of CLSM z-stacks at 20x magnification. The projection pattern of the *Poxn* mutant brain rescued by the *Poxn* transgene *SuperA-158* (B) is similar to that of the wild-type brain (A). (**C-F**) Brain of w^{1118} adult, shown as maximum projections of confocal z-substacks of 7-14 µm (C), 15-25 µm (D), 35-43 µm (E), and 44-66 µm (F) at 40x magnification. AL, antennal lobe; DC, dorsal cluster; eb, ellipsoid body; FSB, fan-shaped body; LH, lateral horn; ltr, lateral triangle; MB, mushroom body; VC, ventral cluster. Size bar: 50 µm.

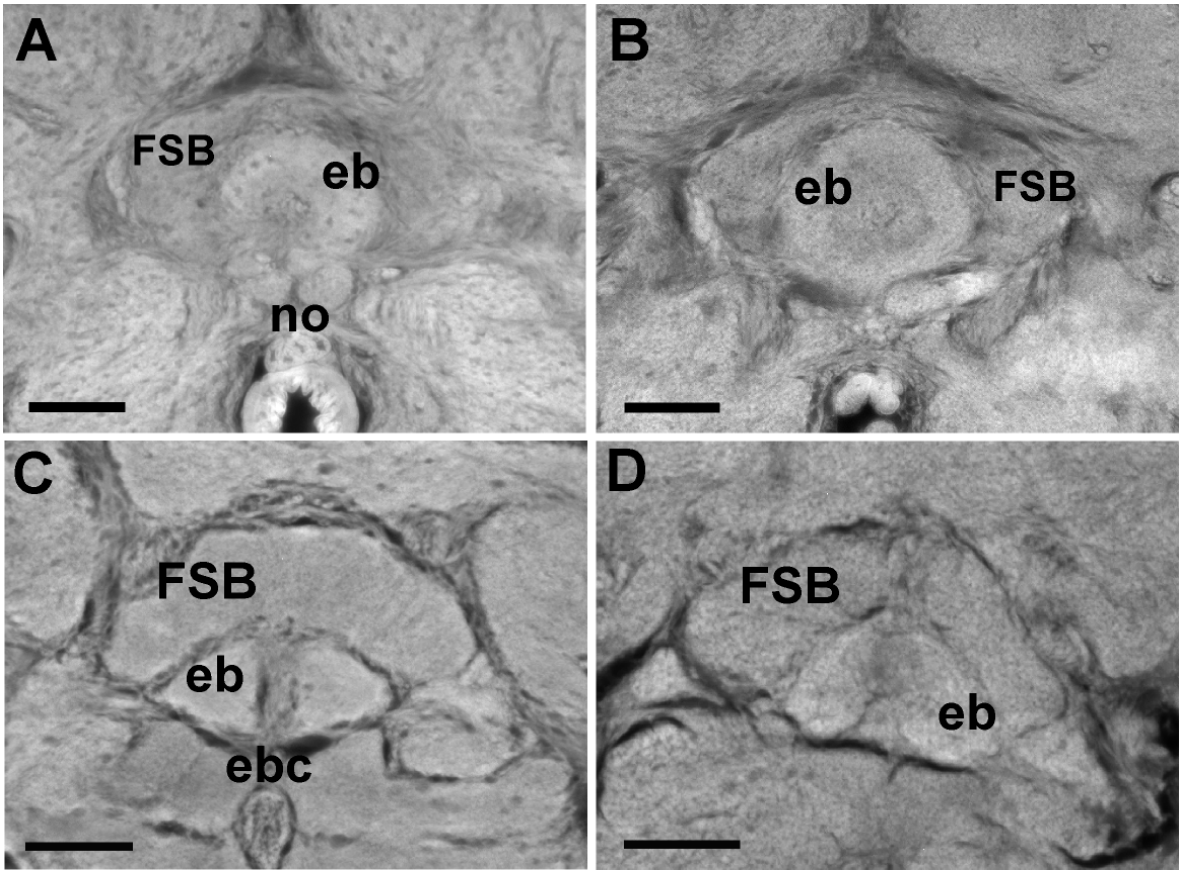

Figure 34. Ellipsoid body and central complex of wild-type adult brains. Frontal (A, B) and horizontal (C, D) paraffin sections of w^{1118} (A, C) and w^{1118}; $Poxn^{\Delta M22\text{-}B5}$ *P{W6 PoxnSuperA}158* adult brains are shown as wide-field autofluorescence images at 25x (A-C) and 40x magnification (D). The ellipsoid body (eb) and the fan-shaped body (FSB) of the *Poxn* mutant brain rescued by the *PoxnSuperA* transgene (B, D) are similar to those of the wild-type brain (A, C). In (C), the ellipsoid body canal (ebc) is clearly visible as well as the FSB posterior to the eb. no, noduli. Size Bar: 25 µm. From Werner Boll, except panel A, which is from Luca Mariotta (Master thesis, 2007).

Like in third instar larvae and pupae, most VC neurons in the adult brain project to the antennal lobe and lateral horn (Figure 35). The projections at the antennal lobe and lateral horn are more pronounced compared to those at 50 h APF. The *Poxn*-neurons target many glomeruli in the adult antennal lobe, as judged by their colocalization with the glomeruli labeled by the synaptic marker NC82 (Figure 35A). The arc-like morphology of the major long axon tract, the mACT, seen in both larvae and pupae is maintained. The dendritic projections of *Poxn*-neurons invade the glomeruli of the antennal lobe, while the axonal projections pass through the mACT to target the lateral horn (Figure 35A). Many glomeruli are targeted by *Poxn*- neurons (Figure 36). Most of the anterior glomeruli are targeted, but many ventral and most posterior glomeruli are not targeted (Figure 36). Of the three sexually dimorphic glomeruli, VA1m+1, VL2a and DA1 (Kondoh *et al*., 2003; Vosshall and Stocker, 2007; Laissue and Vosshall, 2008), VA1m+1 and VL2a are targeted extensively, whereas DA1 is not targeted to the same extent (Figure 37). Similar results were obtained by visualizing *Poxn*-neurons in a background of marked glial cells by the use of *repo-Gal4* driving *UAS-CD2*, which labels the entire adult brain and marks all the salient neuropil structures that are ensheathed by glia (Figure 38). All glomeruli of the antennal lobe are clearly visible, as well as the major neuropil regions, such as the lobes of the mushroom body, the central complex regions, and the antennal lobes. The colocalizations of the neurites of *Poxn* neurons with the glomeruli of the antennal lobes (Figure 38) confirmed those observed with the synaptic marker, NC82 (Figure 37). Most of the anterior glomeruli are targeted, such as VA1m+1, VA2, DM5, and DM6, but many ventral glomeruli, like VL1, V, VM6, VM4, VC3l, and posterior glomeruli, like DM1, DM4, VL2p, are not targeted. No colocalization was observed at the mushroom body lobes and the neuropils of the

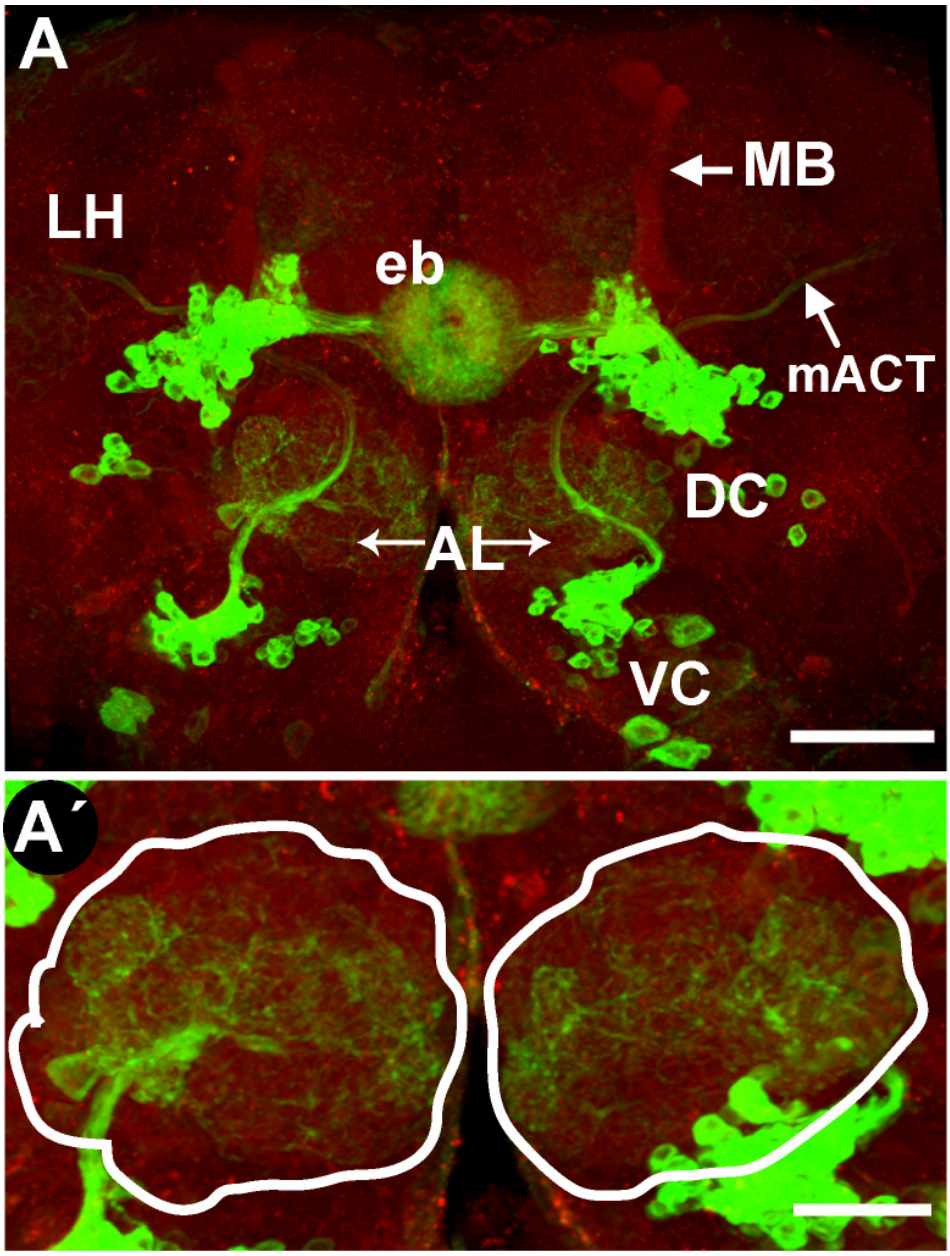

Figure 35. Projection pattern of *Poxn*-neurons of the ventral cluster in adult brains. **(A)** Frontal view of a w^{1118}; *Poxn-CD8::GFP-3-3* adult brain, immunostained for GFP (green) and the synaptic marker NC82 (red). The neurites from the ventral Poxn-cluster, VC, target the adult antennal lobe, AL, and pass through the mACT to target the region of the lateral horn, LH. (**A'**) Magnified frontal view of confocal sections that include the antennal lobes (encircled) of the adult brain shown in (A). Both images were taken at 40x magnification and (A') as maximum projections of z-stacks. DC, dorsal cluster; eb, ellipsoid body; mACT, middle antennocerebral tract; MB, mushroom bodies; VC, ventral cluster. Size bars: 50 µm (A) and 25 µm (A').

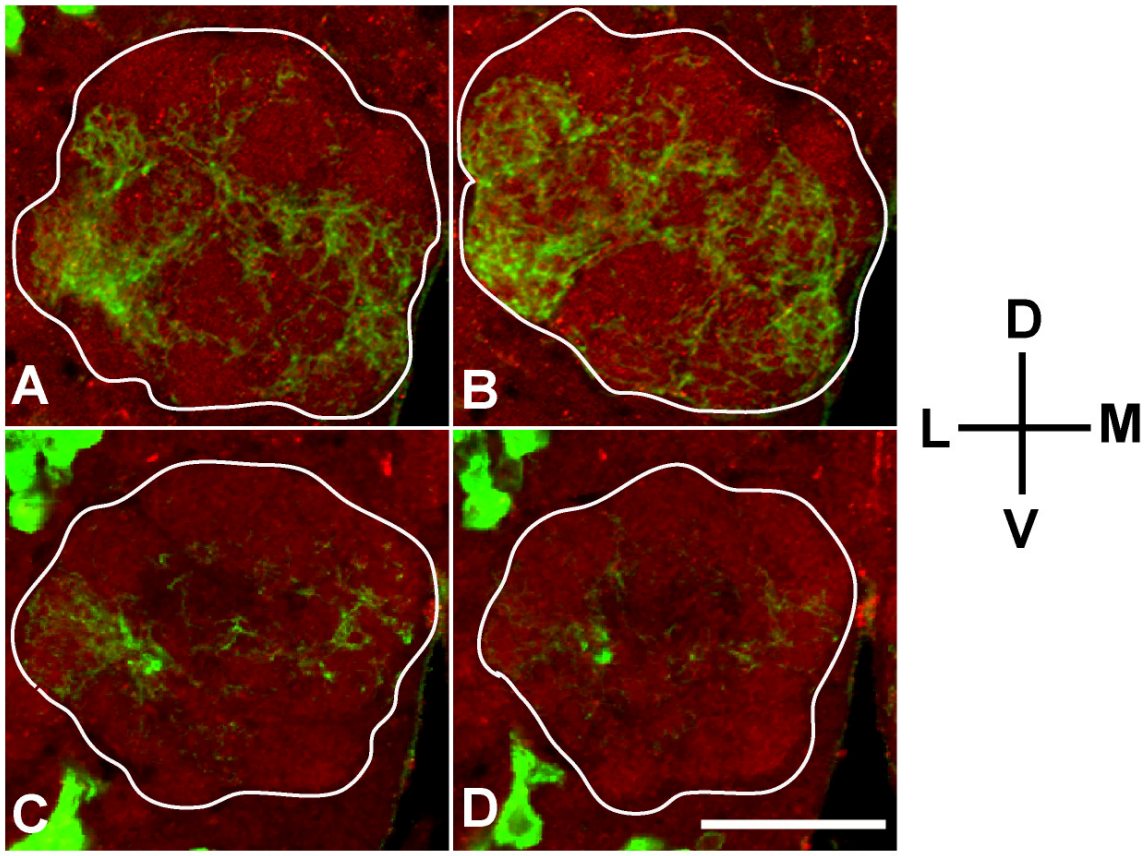

Figure 36. Differential targeting of antennal lobe glomeruli by *Poxn*-neurons of the VC in wild-type adult brains. Single frontal confocal sections, from anterior to posterior **(A to D)**, through the antennal lobe (encircled in white) of a w^{1118}; *P{W6 Poxn-CD8::GFP}3-3* adult brain, immunostained for GFP (green) and the synaptic marker NC82 (red). The anterior glomeruli are targeted by neurites of *Poxn*-neurons of the VC, whereas most of the posterior glomeruli are not targeted. Many of the anterior ventral glomeruli are also not targeted. All pictures were taken at 40x magnification. D, dorsal; L, lateral; M, medial; V, ventral. Size bar: 50 μm.

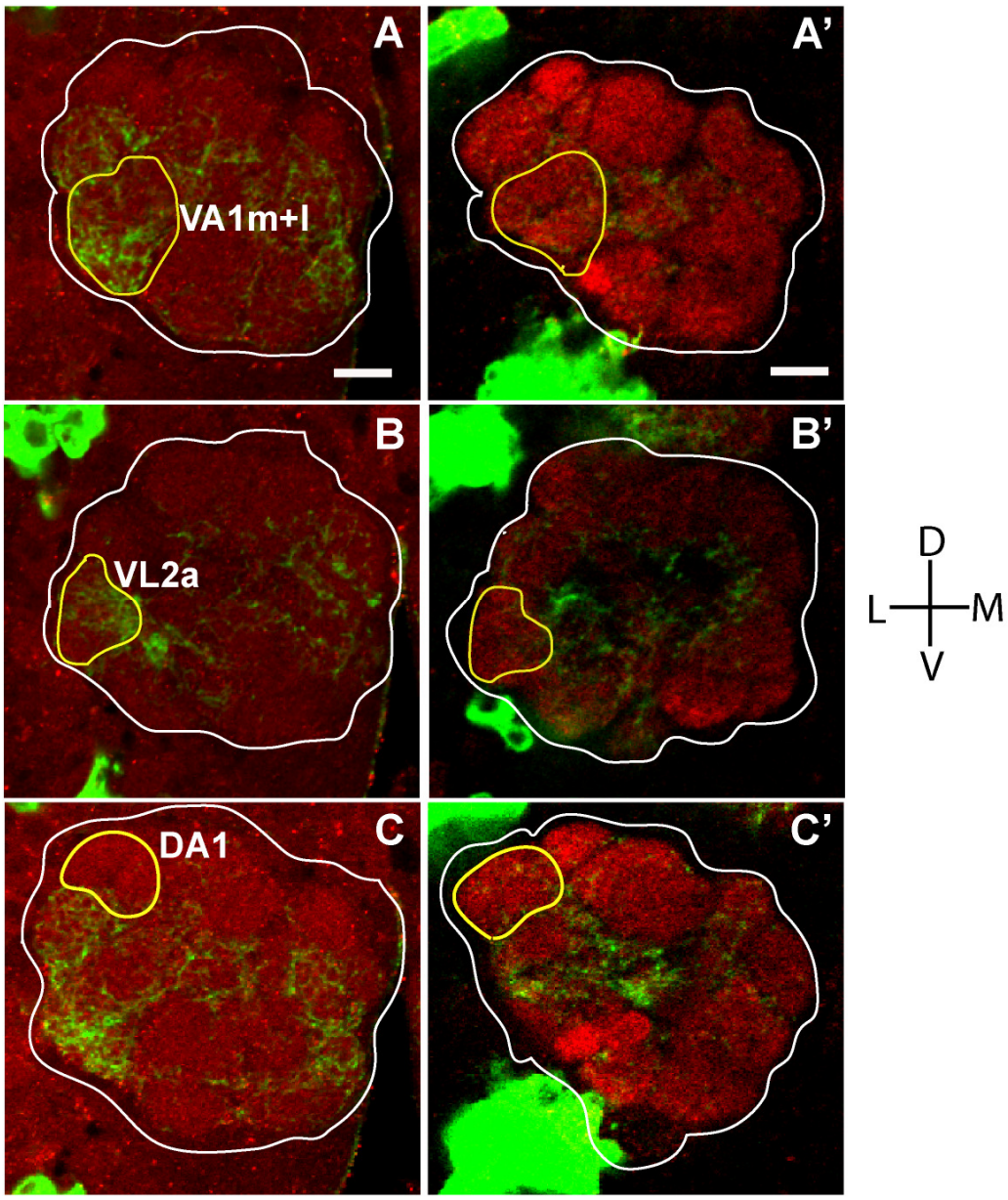

Figure 37. Differential targeting of sexually dimorphic glomeruli in antennal lobe by ventral Poxn-expressing cells in wild-type and *Poxn* mutant adult brains. Frontal confocal sections through the antennal lobes of a w^{1118}; *P{W6 Poxn-CD8::GFP}3-3* (**A-C**) and a w^{1118}; $Poxn^{\Delta M22\text{-}B5}$ *P{W6 Poxn-Sbl107}*; *P{W6 Poxn-CD8::GFP}3-3* (**A'-C'**) adult brain, immunostained for GFP (green) and NC82 (red). The antennal lobe and the sexually dimorphic glomeruli are encircled. The targeting of the anterior glomerulus VA1m+l (Or47b) by neurites of ventral *Poxn*-neurons is extensive in the wild type (A), but drastically reduced in the *Poxn* mutant (A'). Similarly, the VL2a glomerulus is extensively targeted in the wild-type brain (B), while targeting is completely missing in the *Poxn* mutant brain (B'). The DA1 glomerulus is not targeted to the same extent as other glomeruli in wild-type brains (C), while only few faint neurites are visible in *Poxn* mutant brains (C'). All images are at 40x magnification. D, dorsal; L, lateral; M, medial; V, ventral. Size bar: 20 μm.

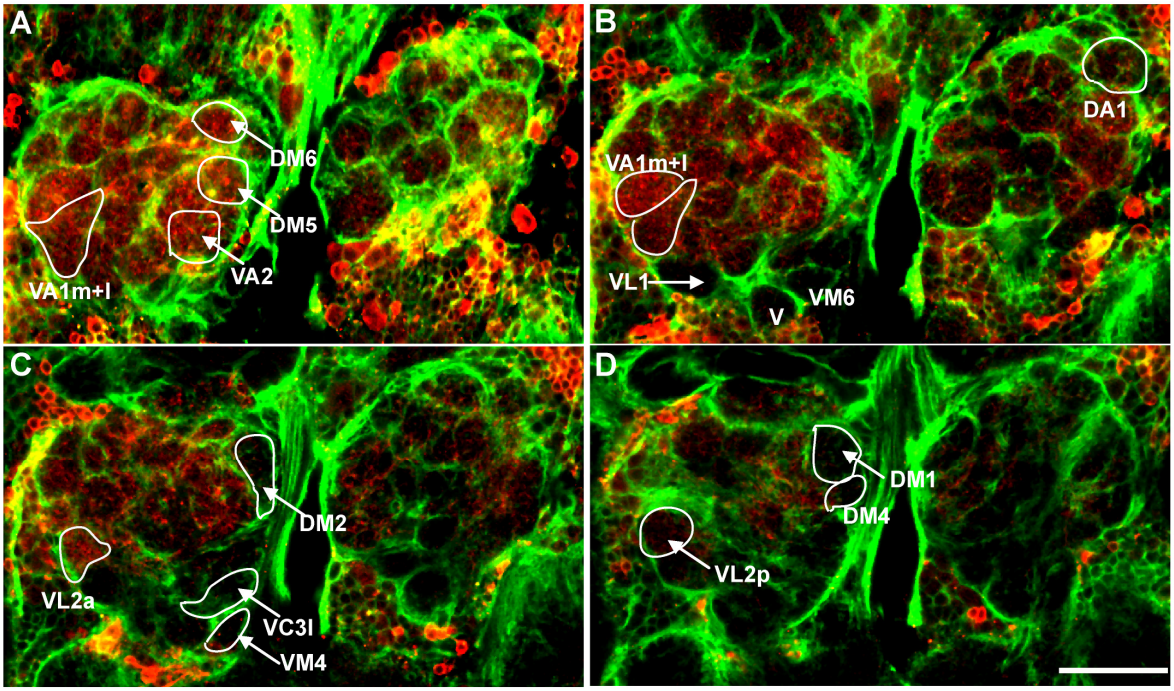

Figure 38. Projection pattern of *Poxn*-neurons in the antennal lobes of a wild-type adult brain marked for glial membranes. Frontal confocal sections, from anterior to posterior **(A to D)**, through the antennal lobes of a w^{1118}; *P{UAS-CD2}*; *P{Gal4}repo Poxn-CD8::GFP-3-3* adult brain, immunostained for GFP (red), labeling *Poxn*-neurons, and CD2 (green), labeling glial membranes, at 40x magnification. The neurites of *Poxn*-neurons target many anterior glomeruli of the antennal lobe, a few of which are encircled and labeled (A-D), including the sexually dimorphic glomerulus VA1m+l (A, B). Many of the ventral glomeruli are not targeted by *Poxn*-neurons, such as glomerulus V, VM6, VL1, while the sexually dimorphic glomerulus DA1 is not targeted as much as the other two sexually dimorphic glomeruli, VA1m+l and VL2a (B). Many posterior glomeruli, like VM4, VC3l, DM2 are not targeted (C), while most posterior-most glomeruli are not targeted (D). Size bar: 50 µm.

central complex, with the exception of the ellipsoid body and the adjacent region of the lateral triangle (Figure 39). The *Poxn*-neurons of the adult brain were also mapped with respect to the expression domain of *MZ699* by Werner Boll in our lab. He found that about 80% of the *Poxn*-neurons of the VC colocalized with the *MZ699* expression domain (Figure 40), as has also been observed in the late pupal brain (Figure 32).

The larval and adult *Poxn*-neurons were further tested for the production of γ-aminobutyric acid (GABA), a major neurotransmitter at inhibitory synapses (Witten and Truman, 1998; Homberg, 2002; Küppers *et al.*, 2003). The concentration of γ-aminobutyric acid (GABA) in the larval brain has been documented to be twice that in the whole larva (Neckameyer and Cooper, 1998), and GABA is detected in many neurons, especially local interneurons, of the larval antennal lobe (Python and Stocker, 2002). In the adult brain, GABA is found in the local interneurons and in the projection neurons, which relay information from the antennal lobe via mACT to higher olfactory centers (Wilson and Laurent, 2005; Okada *et al*., 2009). Approximately, 10-12 larval *Poxn*-neurons were found to harbor immunostained GABA, which suggests that these neurons produce the inhibitory neurotransmitter GABA in third instar larval brains (Figure 41A). In the adult brain, 10-11 neurons of the Poxn domain of the DC and 20-22 cells of the VC express GABA (Figure 41B, B').

To investigate the connectivity of individual *Poxn*-neurons in the adult brain, we labeled a subpopulation of them by the induction of flip-outs in single or a few cells (Figure 13). Random recombination events between FRT-sites were induced in *y w hs-flp*; *UAS>CD2, y+>CD8::GFP*; *Poxn-Gal4*^{ups1f}*/TM6B* late pupae by the expression of Flipase, activated by heat shock in the *hs-flp* transgene. As a result, CD2 expression, driven by the *Poxn-Gal4* transgene in the Poxn domain, is replaced by CD8::GFP

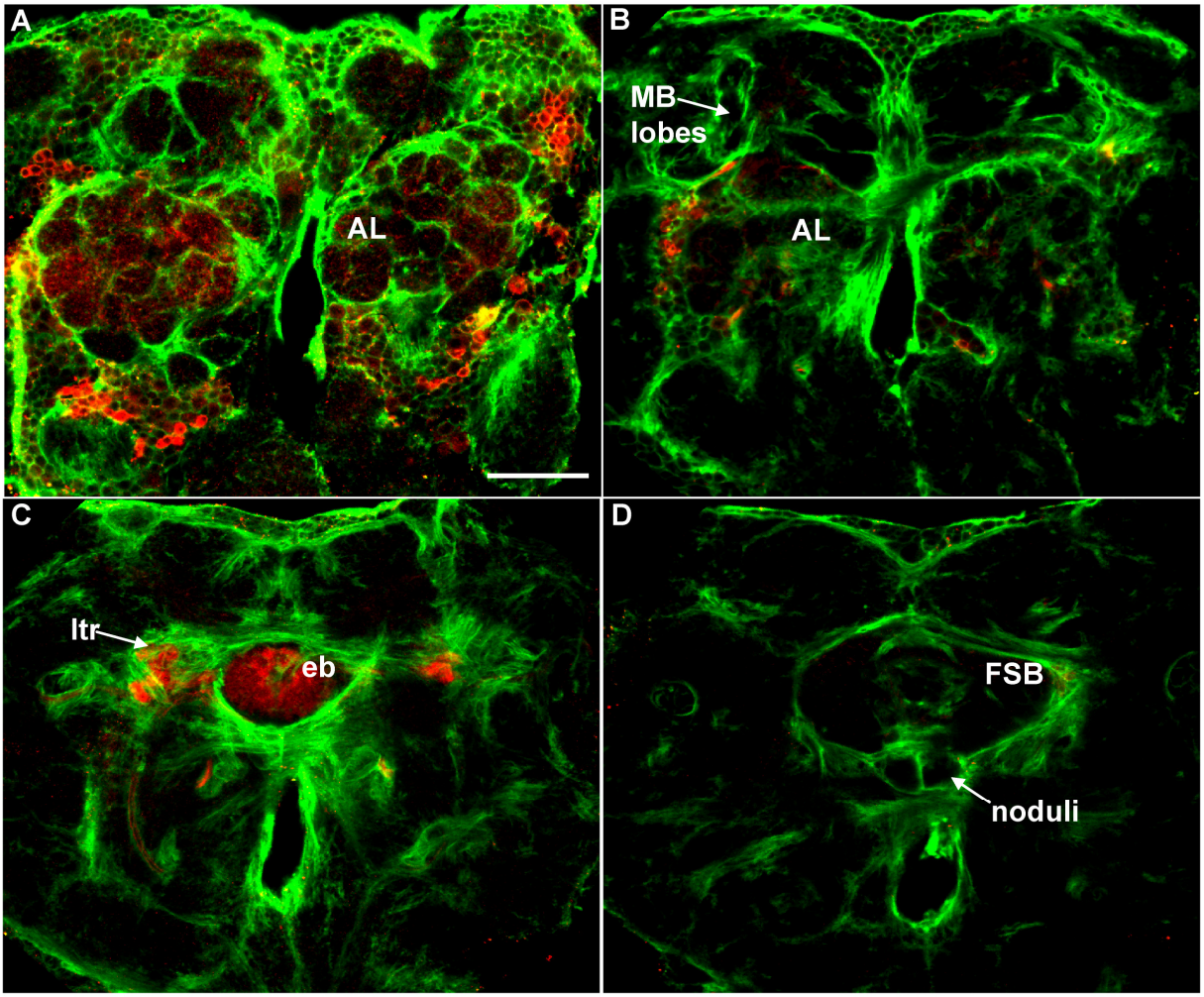

Figure 39. Projection pattern of *Poxn*-neurons in a wild-type adult brain marked for glial membranes. Frontal confocal sections, from anterior to posterior **(A to D)**, of a w^{1118}; *P{UAS-CD2}*; *P{Gal4}repo Poxn-CD8::GFP-3-3* adult brain, immunolabeled for GFP (red), labeling *Poxn*-neurons, and CD2 (green), labeling glial membranes, at 40x magnification. The *Poxn*-neurons of the VC target many glomeruli of the antennal lobe (AL) (A), but many ventral and posterior glomeruli are not targeted (A, B). The mushroom body (MB) lobes are not targeted by *Poxn*-neurites of the DC (B), which target the lateral triangles (ltr) and contribute to the formation of the ellipsoid body neuropil (eb) (C). The fan-shaped body (FSB) and paired noduli are not targeted by *Poxn*-neurites (D). Size bar: 50 μm.

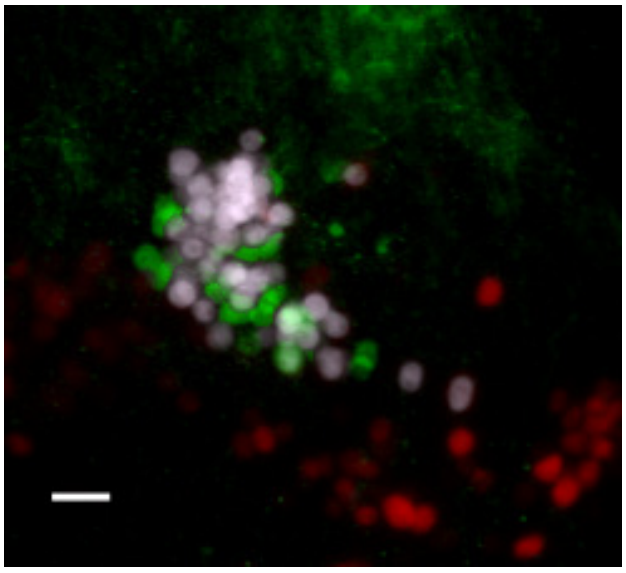

Figure 40. Colocalization of *Poxn*-neurons of the VC with a marker for ventral projection neurons. Whole mount of a w^{1118}; *P{GawB}MZ699/UAS-LacZ(nls)* 5-day old adult male brain, immunostained for β-galactosidase (red), labeling the expression domain of *MZ699*, and for Poxn (green). Almost 80% of the Poxn-positive nuclei colocalize with β-gal-positive nuclei (colocalization in gray). The image shows a maximum projection of confocal z-stacks at 40x magnification. Size bar: 5 µm. From Werner Boll.

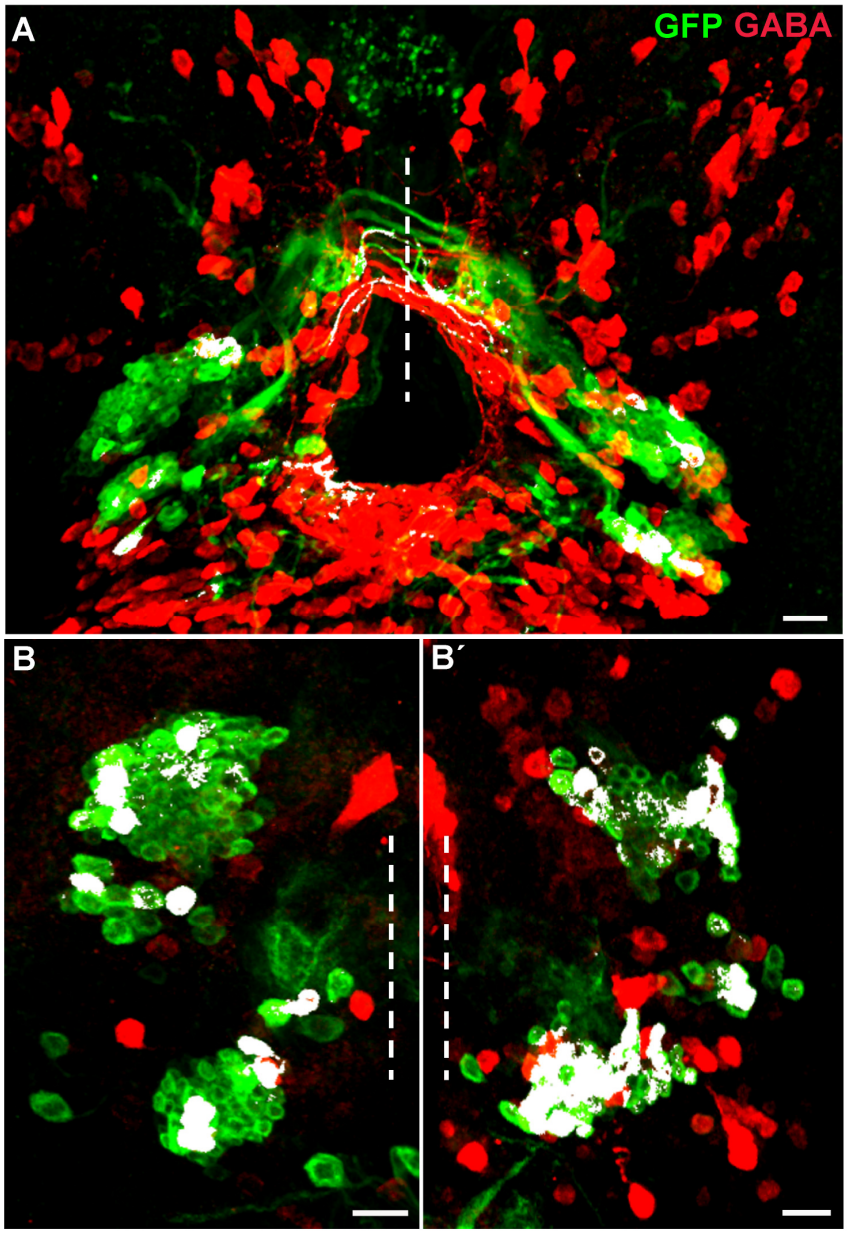

Figure 41. Few *Poxn*-neurons of the developing and adult brain express the neurotransmitter GABA. Frontal views of w^{1118}; *P{W6 Poxn-CD8::GFP}3-3* third instar larval brain (**A**), and of left (**B**) and right (**B'**) hemispheres of adult brain of the same genotype, immunostained for GFP (green), labeling the *Poxn*-neurons, and for GABA (red). 10-12 larval *Poxn*-neurons express GABA, of which about 7 belong to the DC and 5 to the VC (A), while 10-11 *Poxn*-neurons of the DC and about 20-22 *Poxn*-neurons of the VC express GABA in the adult brain (B, B'). The dashed lines indicate the midline. The images are maximum projections of confocal z-stacks at 20x magnification. Size bar: 50 µm.

expression in one or a few *Poxn*-neurons, which are analyzed in the adult brain. Flip-outs in the dorsal Poxn domain labeled a small population of neurons whose projections contributed to the formation of a partial ellipsoid body-like structure (Figures 42-44). Distinct targeting of the lateral triangle region by compact fibers could also be seen (Figures 43 and 44), as has been documented earlier for R-neurons (Hanesch *et al.*, 1989). Most flip-outs in the VC were multi-glomerular projection neurons since they targeted many glomeruli of the antennal lobe and passed through the mACT to target the lateral horn region (Figures 43). In some of the flip-outs, only few of the many glomeruli targeted by *Poxn*-neurons in the adult antennal lobe were distinctly labeled (Figures 42 and 44). With this technique, we did not observe any neurons that exhibited pan-glomerular arborization patterns (Figures 42-44).

3.4.6. The *Poxn* mutant adult brain

In adult brains of *Poxn* mutants (Figure 45B) or *Poxn* mutants rescued for all but the brain functions by *Poxn-Sbl107* (Figure 45A), the projection pattern of the *Poxn*-neurons, visualized by the expression of the *Poxn-CD8::GFP* transgene, deviates from bilateral symmetry, is highly aberrant, and fails to make the connections detected by expression of the same transgene in wild-type adults. Many neuronal projections of the DC fail to properly target the lateral triangles and the ellipsoid body (Figure 45C-F). The projections do not shape the ellipsoid body but form a degenerate structure (Figure 45E, F), exhibiting a globular arborization pattern at the midline (Figure 46B) that is also evident from paraffin sections of such brains (Figure 47A'-D'; Mariotta, 2007).

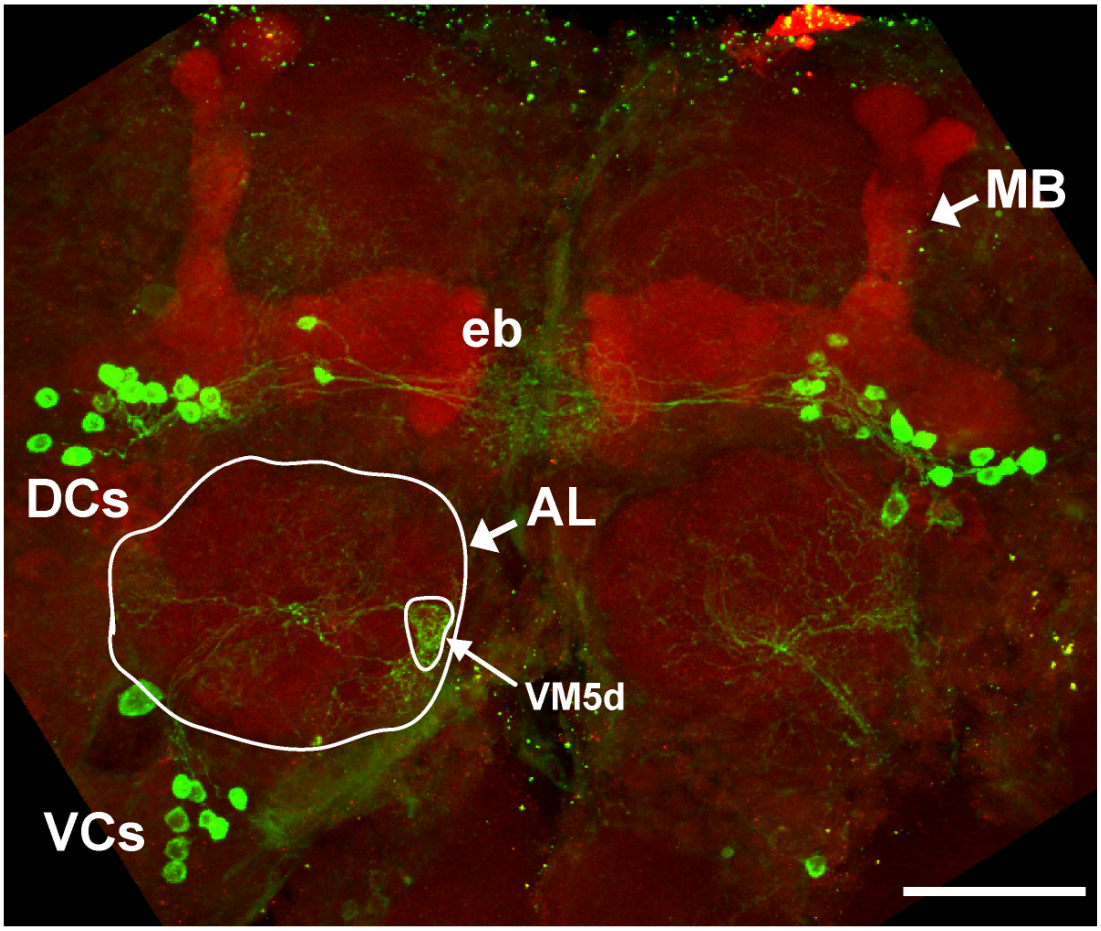

Figure 42. Labeled subpopulation of *Poxn*-neurons in the adult brain. Frontal view of a *y w hs-Flp; UAS>CD2, y*$^{+}$*>CD8::GFP*; *Poxn-Gal4*^{ups1f}*/TM6B* adult brain, in which a subpopulation of *Poxn*-neurons was labeled by flip-out during a 1-h heat shock at 37°C at a late pupal stage. A few *Poxn*-neurons of the VC with projections in the antennal lobe (AL) are labeled in both brain hemispheres. They have dendritic arborizations in many glomeruli, one of which, VM5d, in the left antennal lobe was sufficiently distinct to be identified. A few marked *Poxn*-neurons of the DC label a partial ellipsoid body (eb). DCs, subpopulation of labeled *Poxn*-neurons in the dorsal cluster; MB, mushroom body; VCs, subpopulation of labeled *Poxn*-neurons in the ventral cluster. The confocal image is a maximum projection of z-stacks at 40x magnification. Size bar: 50 µm.

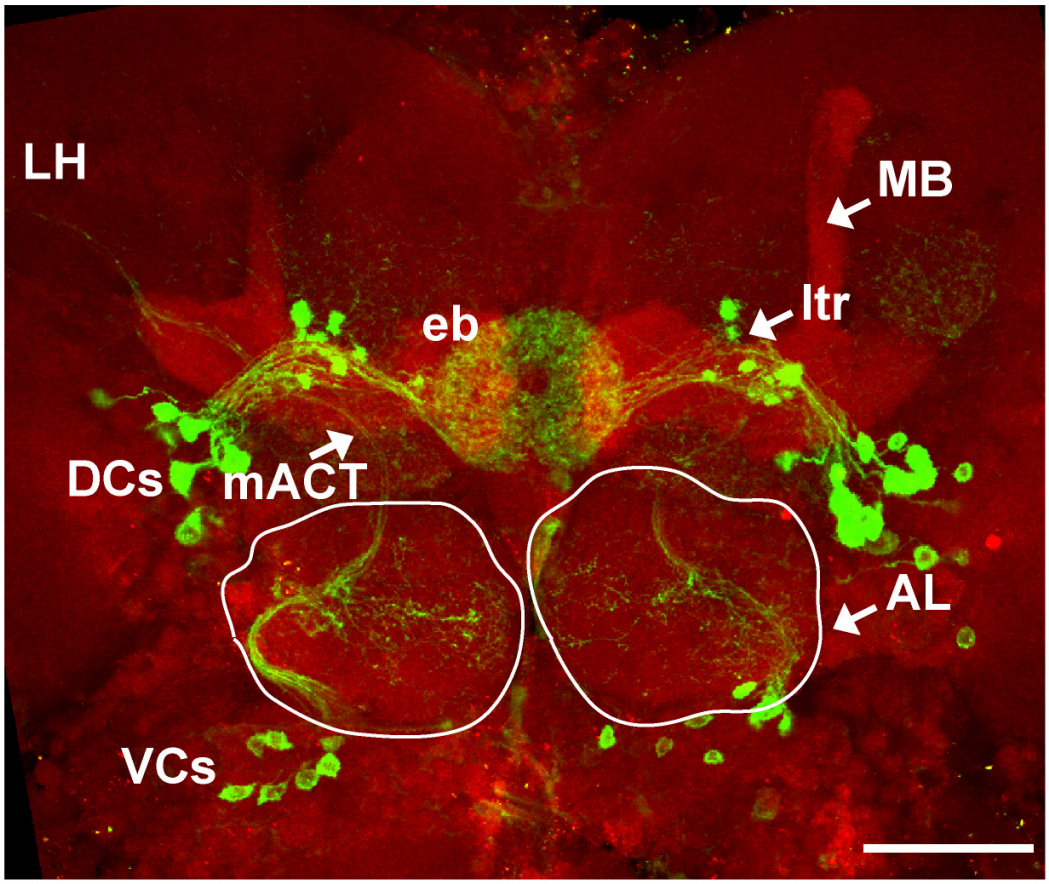

Figure 43. Labeled subpopulation of *Poxn*-neurons in the adult brain. Frontal view of a *y w hs-Flp; UAS>CD2, y*$^{+}$*>CD8::GFP*; *Poxn-Gal4*^{ups1f}*/TM6B* adult brain, in which a subpopulation of *Poxn*-neurons was labeled by flip-out during a 1-h heat shock at 37°C at a late pupal stage. A few *Poxn*-neurons of the VC are labeled, which show projections and dendritic arborizations in many glomeruli of the antennal lobe (AL) in both brain hemispheres. The mACT marked by these *Poxn*-neurons is also clearly visible in both brain hemispheres. Several marked *Poxn*-neurons of the DC form a partial ellipsoid body (eb) and display distinct compact arborizations, visible as blobs, at the lateral triangle (ltr). DCs, subpopulation of labeled *Poxn*-neurons in the dorsal cluster; LH, lateral horn; mACT, middle antennocerebral tract; MB, mushroom body; VCs, subpopulation of labeled *Poxn*-neurons in the ventral cluster. The confocal image is a maximum projection of z-stacks at 40x magnification. Size bar: 50 µm.

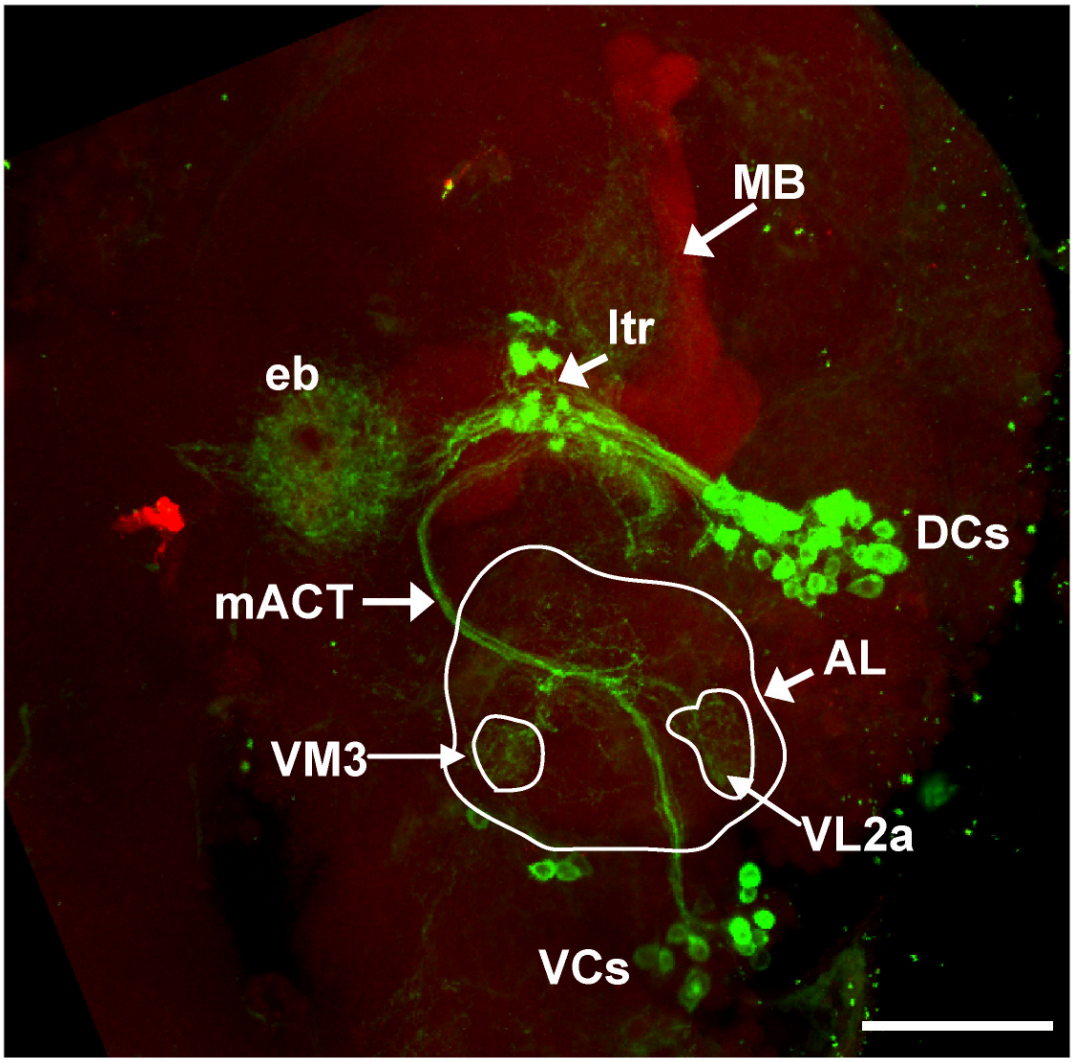

Figure 44. Labeled subpopulation of *Poxn*-neurons in the adult brain. Frontal view of a *y w hs-Flp; UAS>CD2, y*$^{+}$*>CD8::GFP*; *Poxn-Gal4*^{ups1f}*/TM6B* adult brain, in which a subpopulation of *Poxn*-neurons was labeled by flip-out during a 1-h heat shock at 37°C at a late pupal stage. A few labeled *Poxn*-neurons of the left VC are visible, which show projections and dendritic arborizations in many glomeruli of the left antennal lobe (AL) two of which, VM3 and the sexually dimorphic glomerulus VL2a, are sufficiently distinct to be identified. The mACT marked by these *Poxn*-neurons is also clearly visible. Several marked *Poxn*-neurons of the DC form a partial ellipsoid body (eb) and display distinct compact arborizations, visible as blobs, at the lateral triangle (ltr). DCs, subpopulation of labeled *Poxn*-neurons in the dorsal cluster; mACT, middle antennocerebral tract; MB, mushroom body; VCs, subpopulation of labeled *Poxn*-neurons in the ventral cluster. The confocal image is a maximum projection of z-stacks at 40x magnification. Size bar: 50 μm.

Frontal and horizontal paraffin sections of the mutant brain indicate that the prominent ellipsoid body structure is formed neither in *Poxn* mutants (Figure 47A', C') nor in *Poxn* mutants rescued in all but the brain functions by *Poxn-Sbl107* (Figure 47B', D'), yet is replaced by several smaller globular structures. Some projections seem also to aberrantly target the fan-shaped body (Figure 45F). Such invasions by *Poxn*-neurons of the FSB are not observed in the wild-type brain (Figure 33F). Since the numbers of *Poxn*-neurons in the wild-type and *Poxn* mutant brain are very similar, if not identical, it follows that the *Poxn* function is not important for the survival of most, if not all, of these cells, but is crucial for their correct neuronal projection patterns.

The dendritic projections of the VC to the ALs are dramatically reduced (Figure 48) as compared to the wild-type brain (Figure 35). The projections through the mACT cannot be observed, and the LH is not targeted (Figure 48A). It is evident that the phenotype visualized in the adult *Poxn* mutant is similar to that observed in earlier phases of development, i.e., in mutant larvae and pupae (Figure 21E-H and Figure 31A'-H'). The processes seem to fasciculate and stall just before turning towards the lateral horn region where they are very close to the projections of the dorsal *Poxn*-neurons (Figure 48A), and their pattern with respect to the two brain hemispheres is asymmetrical.

The arborizations in the antennal lobe are not only decreased in number, but no longer invade and innervate the glomeruli and end at the ensheathment boundaries of the glia (Figure 49). None of the anterior or posterior glomeruli are targeted to the same extent as in wild-type brains (cf. Figure 49 with Figures 36 and 38). Consequently, none of the two extensively targeted sexually dimorphic glomeruli, VA1m+l and VL2a, are targeted in the *Poxn* mutant brain while some projections can be still seen at DA1 (Figure 37).

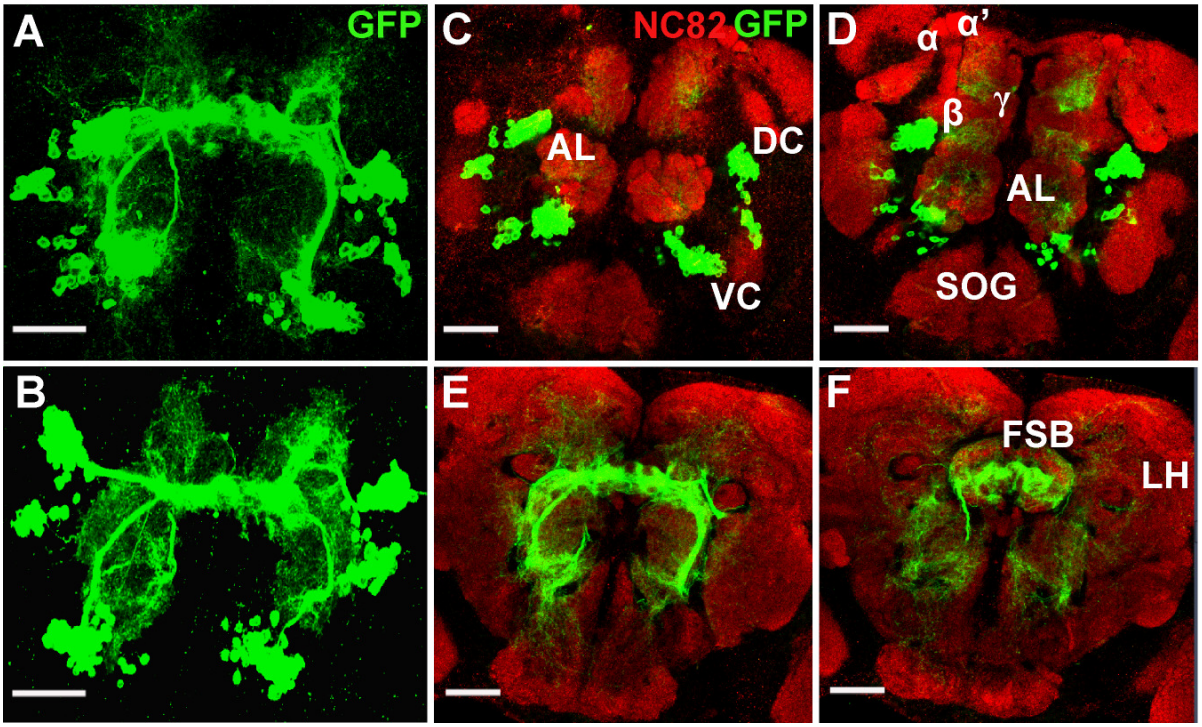

Figure 45. Projection patterns of *Poxn*-neurons in *Poxn* mutant adult brains. **(A, B**) Frontal views of w^{1118}; $Poxn^{\Delta M22\text{-}B5}$ *P{W6 Poxn-Sbl107}*; *P{W6 Poxn-CD8::GFP}3-3* (A), and w^{1118}; $Poxn^{\Delta M22\text{-}B5}$; *P{W6 Poxn-CD8::GFP}3-3* (B) brains, immunostained for GFP (green), show similar projections patterns of the *Poxn*-neurons in maximum projection of z-stacks. (**C**-**F**) Frontal views of w^{1118}; $Poxn^{\Delta M22\text{-}B5}$ *P{W6 Poxn-Sbl107}*; *P{W6 Poxn-CD8::GFP}3-3* adult brains, immunostained for GFP (green) and NC82 (red), illustrate maximum projections of z-substacks at 1-11 µm (C), 12-24 µm (D), 36-42 (E), and 51-57 µm (F). AL, antennal lobe; DC, dorsal cluster; FSB, fan-shaped body; LH, lateral horn; SOG, subesophageal ganglion; VC, ventral cluster; α, α', β, γ, lobes of mushroom bodies. All images are at 40x magnification. Size bar: 50 µm.

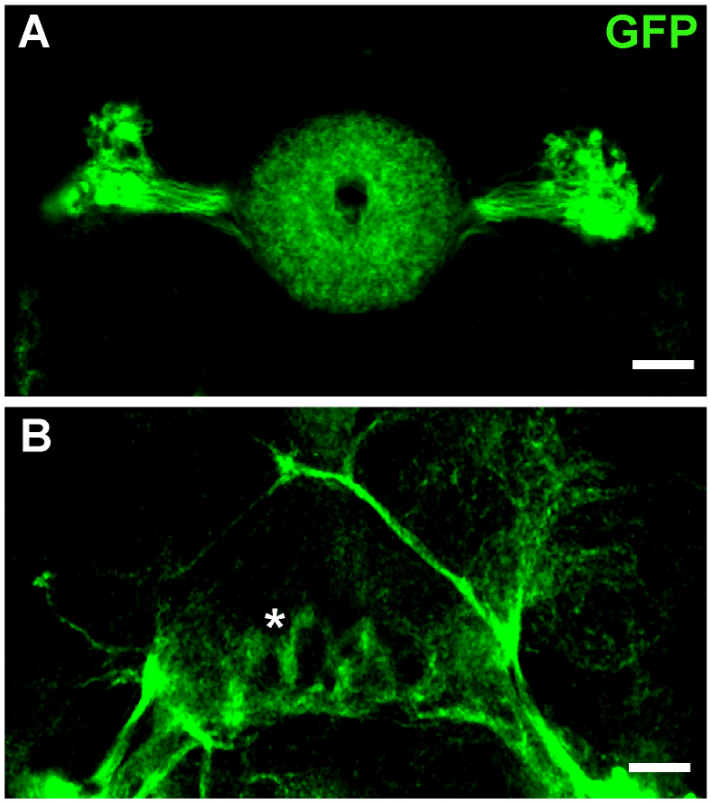

Figure 46. Projections of ellipsoid body large field neurons in wild-type and Poxn mutant adult brains. Frontal views of w^{1118}; *P{W6 Poxn-CD8::GFP}3-3* **(A)** and w^{1118}; $Poxn^{\Delta M22\text{-}B5}$ *P{W6 Poxn-Sbl107}*; *P{W6 Poxn-CD8::GFP}3-3* **(B)** adult brains, immunostained for GFP (green). In the wild-type brain, the doughnut-shaped ellipsoid body is formed by axonal projections from the DC of *Poxn*-neurons (A). In the *Poxn* mutant brain, projections of the same neurons are aberrant and hence produce a degenerate ellipsoid body structure visible at the midline (marked by an asterisk in B). Both images are maximum projections of confocal z-stacks at 40x magnification. Size bar: 20 µm.

Figure 47. Degenerate structure of ellipsoid body neuropil in adult brain of *Poxn* mutants. Frontal (A, B, A', B') and horizontal (C, D, C', D') paraffin sections of w^{1118} **(A, C)** and w^{1118}; $Poxn^{\Delta M22\text{-}B5}$ *P{W6 Poxn-SuperA}158* **(B, D)** 'wild-type' adult brains, and of w^{1118}; $Poxn^{\Delta M22\text{-}B5}$ **(A')**, w^{1118}; $Poxn^{\Delta M22\text{-}B5}$ *P{W6 Poxn-Sbl107}* **(B')**, w^{1118}; $Poxn^{\Delta M22\text{-}B5}$ *P{W6 Poxn-Sbl107}* **(C')**, and w^{1118}; $Poxn^{\Delta M22\text{-}B5}$ *P{W6 Poxn-Sbl44}* **(D')** *Poxn* mutant adult brains. The ellipsoid body (eb) and fan-shaped body (FSB) of mutant brains rescued by the *Poxn-SuperA* transgene (B, D) appear like the corresponding neuropils of wild-type brains (A, C). By contrast, the ellipsoid body of *Poxn* mutants rescued by the *Poxn-Sbl* transgene (B'-D') resembles that of *Poxn* mutants (A'), which is degenerate, exhibiting a few globular structures in its place (arrowheads in A'-D'), while the fan-shaped body appears normal (A'-D') as in wild-type brains (A-D). All panels show autofluorescence images recorded by wide-field microscopy at 25x magnification, except panel B' which is at 40x magnification. ebc, ellipsoid body canal; no, noduli. Size bar: 25 µm (A, A', B, B') and 50 µm (C, C', D, D'). From Luca Mariotta (Master thesis, 2007).

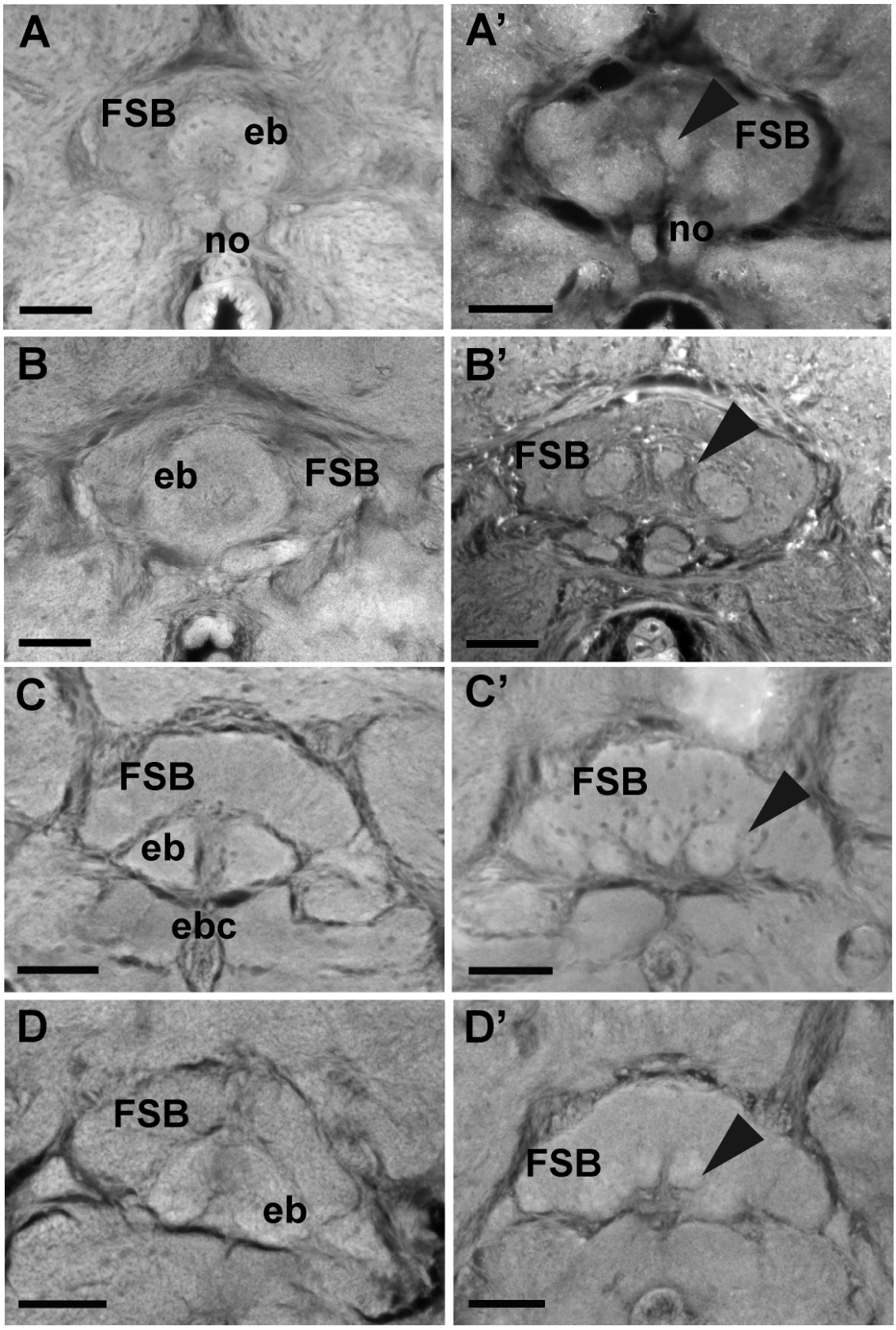
A
FSB
eb
no
A'
FSB
no
B
eb
FSB
B'
FSB
C
FSB
eb
ebc
C'
FSB
D
FSB
eb
D'
FSB

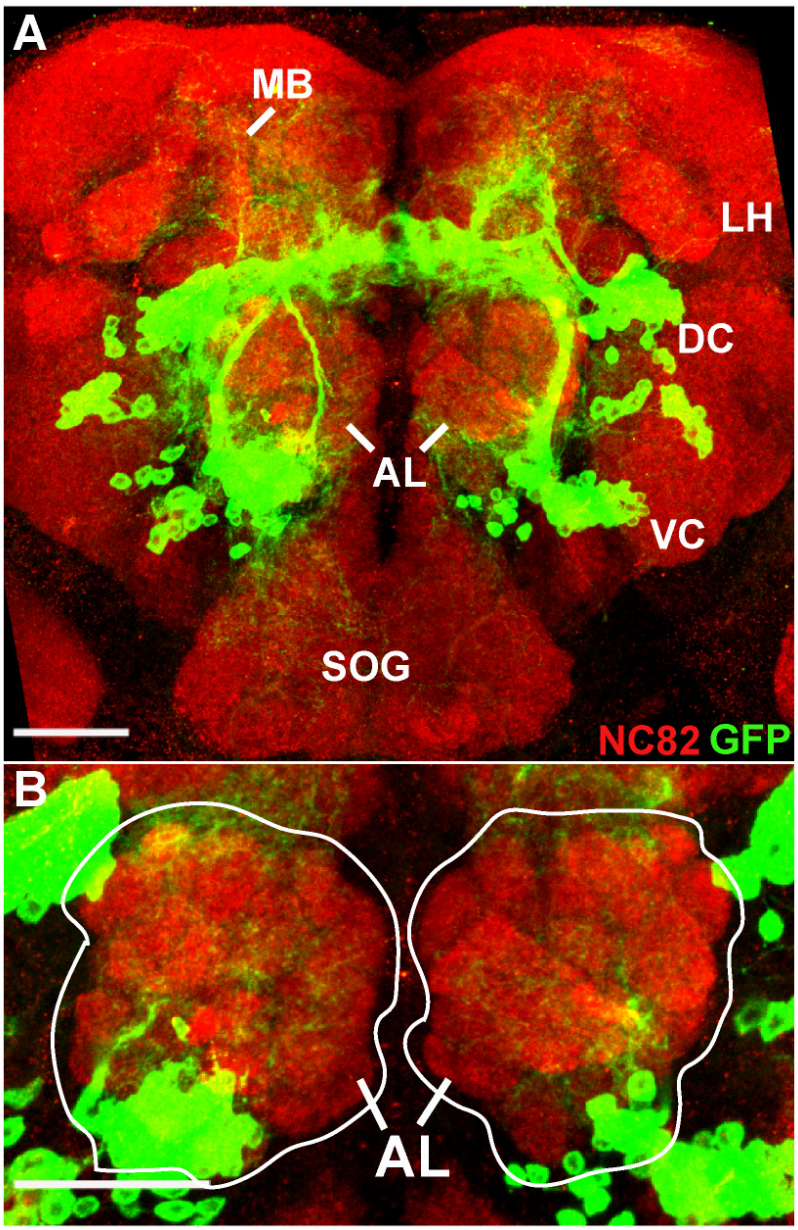

Figure 48. Projection pattern of *Poxn*-neurons of the ventral cluster in *Poxn* mutant adult brains. (**A**) Frontal view of a w^{1118}; $Poxn^{\Delta M22\text{-}B5}$ *P{W6 Poxn-Sbl107}*; *P{W6 Poxn-CD8::GFP}3-3* mutant adult brain, immunostained for GFP (green), labeling the *Poxn*-neurons, and the synaptic marker NC82 (red). The ellipsoid body displays a degenerate structure. Colocalization of projections from *Poxn*-neurons of the ventral cluster (VC) with glomeruli of the antennal lobes (AL) is drastically reduced, and the neurites emanating from the VC do not pass through the mACT. The lateral horn (LH) region is not targeted at all. The projection pattern is highly disorganized and asymmetrical. (**B**) Magnified frontal view of confocal sections that include the antennal lobes (AL, encircled) of the *Poxn* mutant brain shown in (A). The targeting of the AL by neurites of *Poxn*-neurons is drastically reduced. Both images were taken at 40x magnification and (A) as maximum projection of z-stacks. MB, mushroom bodies; DC, dorsal cluster of *Poxn*-neurons; LH, lateral horn; SOG, subesophageal ganglion. Size bar: 50 µm.

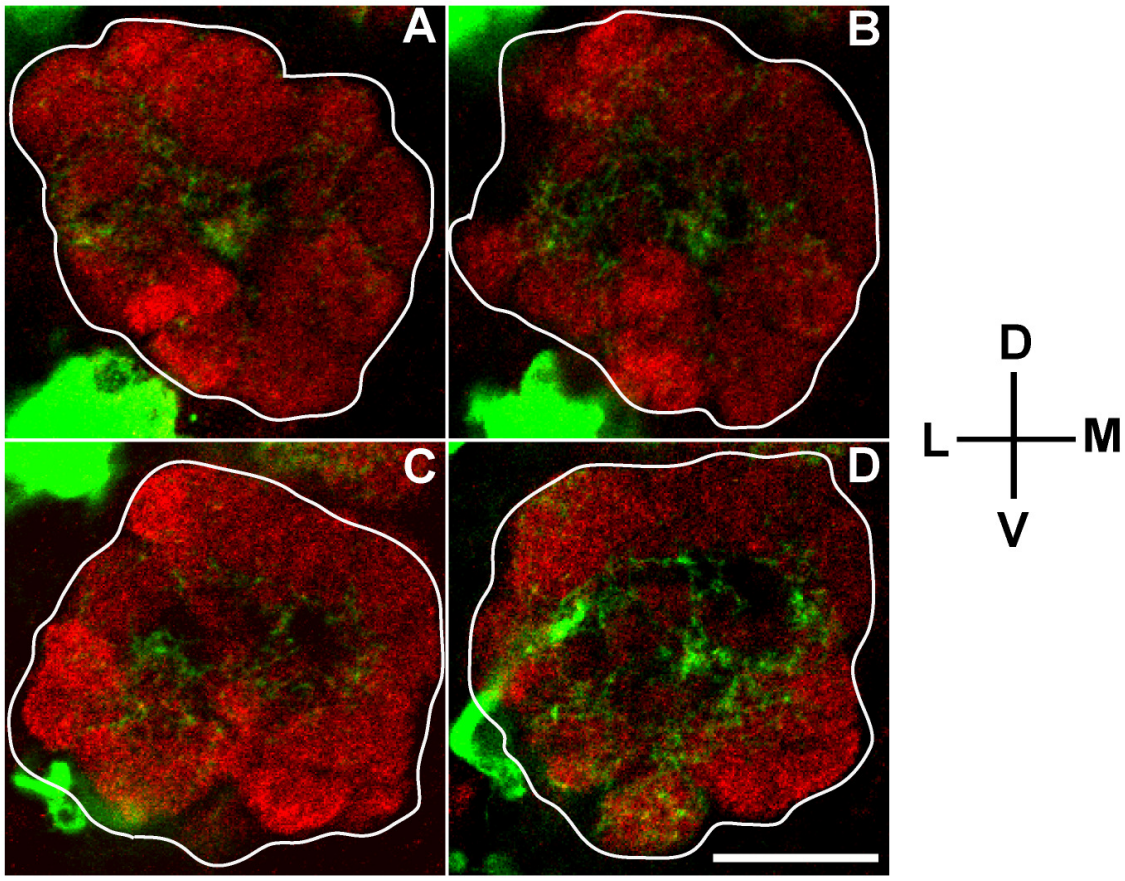

Figure 49. Differential targeting of glomeruli in the antennal lobe by *Poxn*-neurons of the ventral cluster in *Poxn* mutant adult brains. Single frontal confocal sections, from anterior to posterior **(A to D)**, through the right antennal lobe (encircled in white) of a w^{1118}; $Poxn^{\Delta M22\text{-}B5}$ *P{W6 Poxn-Sbl107}*; *P{W6 Poxn-CD8::GFP}3-3* adult brain, immunostained for GFP (green), labeling the *Poxn*-neurons, and the synaptic marker NC82 (red). The number of GFP labeled neurites of *Poxn*-neurons that target the antennal lobe and invade glomeruli is drastically reduced. None of the glomeruli are targeted specifically, and the neurites seem to be located in the space between glomeruli. All pictures were taken at 40x magnification. D, dorsal; L, lateral; M, medial; V, ventral. Size bar: 50 µm.

4. Discussion

4.1. *Poxn*-neurons act like pioneer neurons in early stages of development

In contrast to the developing PNS, all Poxn-expressing cells in the developing brain are postmitotic neurons, as they express the pan-neuronal marker Elav at all stages. Therefore, no Poxn-expressing neuroblasts or ganglion mother cells (GMC) were observed. In this context, it is interesting to note that during embryogenesis *Poxn* is not expressed either in NBs of the developing brain although expression in GMCs was not excluded (Urbach, 2007). Furthermore, most *Poxn*-neurons already display neuronal outgrowths during embryonic and larval stages but appear to form a functional network only in late pupae and adult, which suggests that during early development *Poxn*-neurons act as pioneer neurons for some parts of the adult brain. This is consistent with the observation that soon after the initial Poxn expression in the developing brain of stage 12 embryos, neurites of these *Poxn*-neurons, like those of other pioneer neurons in the embryo, presumably pre-establish connectivity in the embryonic CNS when structures are still simple and distances relatively small (Bate, 1976; Hidalgo and Brand, 1997). Neurons developing during larval and pupal stages then send out their projections along the routes established by these pioneer neurons. Similarly, during embryonic and early larval development, the *Poxn*-neurons do not display an extensive outgrowth of neurites, but their projection pattern elaborates only during late third instar and pupariation. Moreover, most of the *Poxn*-neurons remain immature until the end of larval development, as evident from their colocalization with Prospero. Furthermore, most *Poxn*-neurons of third instar larval brains survive metamorphosis, and their number

increases only slightly during pupariation. Hence, the larval *Poxn*-neurons born during embryogenesis together with those that acquire Poxn expression or are born during larval stages form a scaffold of tracts. These projections refine and continue to differentiate during pupal development, and the *Poxn*-neurons finally form functional synapses in specific neuropil regions as part of the neural network of the adult brain.

4.2. Most *Poxn*-neurons of the dorsal cluster contribute to the formation of the ellipsoid body neuropil during metamorphosis

The projections from the *Poxn*-neurons of the DC that are present at the supraesophageal commissure in the larval brain, are early traces of the ellipsoid body neuropil. It has been previously shown that the major contributions to the ellipsoid body are projections of the large-field neurons or R-neurons (Hanesch *et al*., 1989). Fabian Schmid in our lab demonstrated that all enhancer trap lines that express Gal4 in sub-populations of the large-field neurons (Renn *et al*. 1999) are part of the dorsal Poxn expression domain in the male adult brain (Schmid, 2005). About four projections from the *Poxn*-neurons of the DC can be distinguished at the supraesophageal commissure of third instar wandering larvae. These projections are maintained during early stages of metamorphosis and appear to be the focal points that give rise to the ellipsoid body, which is formed by many additional axonal projections of the Poxn-expressing R-neurons and exhibits a perfect doughnut-like shape by 45 h APF. This suggests that Poxn is an important marker for the ellipsoid body throughout development.

In earlier studies using a suite of different ellipsoid body R-neuron markers, it was proposed that the initial traces of the ellipsoid body neuropil manifest themselves by 1-2 h APF while a complete ellipsoid body structure forms by 48 h APF (Renn *et al*., 1999).

Despite the lack of an earlier marker for ellipsoid body development like Poxn, these authors speculated that the neurons responsible for the formation of the ellipsoid body neuropil might already be present during early larval stages. In addition, they suggested that a small number of processes serve as scaffold for the formation of the ellipsoid body and that these processes provide pioneering cues for neurons born during later stages to extend their processes along the pre-established route (Renn *et al*., 1999). My studies thus corroborate their speculation by showing that the initial stages of ellipsoid body formation can be traced to early larval stages.

The large-field R-neurons form not only the ellipsoid body through their ring-like axonal processes, but also dendritic termini that are apparent as compact arbors at the lateral triangle, as previously visualized (Hanesch *et al*., 1989; Müller *et al*., 1997). These compact arbors can also be observed with the aid of the membrane-tethered CD8::GFP in the dendrites of the large-field neurons expressing the *Poxn-CD8::GFP* transgene.

The central complex of the adult brain is located between the large commissures of the optic foci and the commissure of the lateral horn on the posterior side and the medial lobes of the mushroom bodies and the antennal commissure on the anterior side (Nassif *et al*., 2003; Younossi-Hartenstein *et al*., 2003). The forerunners of these commissural bundles are present in the larval brain, but are much more closely spaced than in the adult because the central complex has not yet developed in between (Nassif *et al*., 2003; Younossi-Hartenstein *et al*., 2003). The axons that branch off, or are closely interconnected with, the medial lobe of the mushroom body in the larva are known to form the central core of the commissural system that further develops during metamorphosis (Nassif *et al*., 2003; Younossi-Hartenstein *et al*., 2003). The processes of the third instar larval *Poxn*-neurons of the DC colocalize with the medial lobe of the

mushroom bodies, thus invading these commissural bundles and forming a geometrically ordered matrix (Figure 24A). This interaction of the neurites of the *Poxn*-neurons with the medial lobe of the larval mushroom bodies, prefiguring the central commissure in the developing brain neuropil, might be crucial for the formation of the final projection pattern of the DC *Poxn*-neurons. During metamorphosis, the developing central complex separates the commissures by pushing the anterior bundles, i.e. the medial lobe of the mushroom bodies and the antennal commissure, away from the posterior bundles, i.e. the commissures of the optic foci and the commissure of the lateral horn (Younossi-Hartenstein *et al*., 2003). Therefore, the processes of the *Poxn*-neurons of the DC that colocalized with the medial lobe of larval mushroom bodies during late third instar are displaced from it during early pupal stages and no longer contact them in late pupal and adult brains.

The cerebral neuropils and various neurotransmitters employed by the different substructures of the central complex are quite conserved in arthropods (Strausfeld, 1998). Arthropods are considered to be an ideal taxon because many phylogenetic relationships can be inferred from these cerebral characters (Strausfeld, 1998). Thus, it has been postulated that there is a plausible phylogenetic relationship among neopteran insects with regard to ellipsoid body formation (Homberg *et al*., 1999). Similarly, during the formation of the ellipsoid body, the projections of the Poxn-expressing R-neurons transiently assume the distinct shape of a kidney-like structure between 20 h and 30 h APF. This transient form of the developing ellipsoid body is similar to the final form of the ellipsoid body in the brain of the cockroach *P. americana* (Loesel *et al*., 2002). Furthermore, the structural complexity of the central complex has been demonstrated to increase through successive instars in the beetle *Tenebrio* (Breidbach *et al*., 1992). Extending this observation of the central complex to the ellipsoid body, we might

propose that more complex organisms have a more complex ellipsoid body structure as well. Thus, the various transient morphologies of the ellipsoid body neuropil that we observe in *Drosophila* during early stages of pupal development resembles the final ellipsoid body structures in some low-order insect species (Loesel *et al*., 2002), but becomes more refined in subsequent pupal stages to perform more elaborate functions in the adult CNS of the fly.

In many insects, such as the locust, the honey bee, the sphinx moth, the housefly, the cockroach, the beetle, and the fruit fly, the GABA immunoreactive fibers of the central complex are restricted mainly to the lower division of the central body, termed ellipsoid body in fruit flies and beetles (Hanesch *et al*., 1989; Homberg *et al*., 1999, Loesel *et al*., 2002). Relatively few *Poxn*-neurons of the DC, in both larval and adult brains, produce the neurotransmitter GABA.

In the *Poxn* mutant, the prominent structure of the ellipsoid body is not observed. It is replaced by a few globular structures, which might be formed by projections of the Poxn-independent small-field neurons and the aberrant processes of the R-neurons. Since the survival and neuronal fate of the *Poxn*-neurons of the DC are independent of Poxn function, the observed phenotype in the *Poxn* mutant is most probably caused by the inability of the *Poxn*-neurons to properly target the correct neuropil regions.

The *roundabout* (*robo*) gene acts like a growth cone guidance receptor in *Drosophila* (Kidd *et al*., 1999; Keleman *et al*., 2005), and the Robo proteins, Robo2 and Robo3, convey pathfinding information (Nicolas and Preat, 2005). Although there are no reports of expression of these Robo proteins in the developing ellipsoid body during larval and pupal stages, $robo^{2}$ and $robo^{3}$ mutants display an abnormal ellipsoid body morphology in the adult brain (Nicolas and Preat, 2005). Thus, analysis of projection patterns of *Poxn*-neurons in *robo* mutants might provide insights into the Poxn function

in these neurons. Moreover, it has been shown in our lab that the activity of all known Gal4-enhancer trap lines expressed in the R-neurons of the ellipsoid body (Renn *et al.* 1999) depends on a functional Poxn protein (Schmid, 2005). Since these enhancer trap lines usually reflect the activity of one of the genes flanking the site of insertion, it is a strong indication that the transcription factor Poxn directly or indirectly controls the activity of such candidate genes in ellipsoid body R-neurons and controls through some of these gene functions the specific fate of these neurons and their function.

The central complex has also been described as a higher center for locomotion and orientation behavior in flies (Strauss, 2002). In particular the ellipsoid body has been proposed to regulate locomotor activity, step length adjustment, control of walking speed, on-target fixation, and spatial orientation memory (Strauss, 2002, Neuser *et al.*, 2008) although other parts of the central complex were also affected by the mutants studied by these authors and hence might contribute to, or be responsible for, the observed effects. Therefore, it would be interesting to analyze the locomotor and orientation performance of *Poxn* mutants rescued by the *Sbl107* transgene, which complements for all functions but the brain function of *Poxn,* in appropriate behavioral paradigms.

4.3. Are all *Poxn*-neurons of the ventral cluster ventral projection neurons?

Throughout development, the *Poxn*-neurons of the VC target analogous neuropil regions. They form processes that pass through the larval antennal lobes (LAL) at all stages, but no arborizations are apparent. At late third larval instar, they pass through the developing adult antennal lobe where they do begin to form dendritic arbors. Therefore, their function is most probably restricted to the adult brain. The arborizations at the adult

ALs are much more elaborate than those apparent during late third instar. Thus, as mentioned in section 4.1., in the early stages of development *Poxn*-neurons pre-establish a route and direct the later growing neurites to the correct neuropil compartments.

There are not many apparent arborizations between the cell bodies and the terminals till late third instar, as documented for the projection neurons that form the mACT (Ito *et al*., 1997). The neurites extend slightly in the developing adult antennal lobe only at late larval stages whereas in larval antennal lobes no such neurites can be visualized during third instar. The morphology of the projections that pass through the mACT also remains the same throughout all stages of development.

Arborization between cell bodies and terminals begins to increase substantially with the onset of pupariation. The increase in the formation of arbors at the developing adult antennal lobes correlates with the development of their glomerular structure (Jefferis *et al*., 2004). Maximal arborization is apparent around 50 h APF, which coincides with the time when the first signs of glial invasion of the antennal lobes become manifest (Jefferis *et al*., 2004). The terminals also exhibit intensive arborizations in the lateral horn region in late pupal stages, directly correlating with the timing of the elaboration of the lateral horn region (Ito *et al*., 1997).

On basis of positions of cell bodies, projection patterns, and colocalization with the expression of enhancer trap lines, *MZ699* and *GH146*, which defines the two non-overlapping subsets of vPNs that are presently known (Jefferies *et al.,* 2001; Lai *et al*., 2008), about 80% of the *Poxn*-neurons in each VC can be classified as vPNs (Werner Boll, unpublished results).

Incorporation of BrdU, administered during larval stages, shows that about 30 of approximately 75 neurons of each VC are labeled with BrdU and hence suggests that they are born after embryogenesis (in the following all numbers refer to one brain

hemisphere). Since 80% of the ventral Poxn cluster are vPNs, this result indicates that of the approximately 60 vPNs 30-45 are born during and 15-30 after embryogenesis because 20% of the *Poxn*-neurons of the VC in the adult brain could not be classified and hence about 15 might or might not be vPNs. It was recently shown by the MARCM technique that a postembryonic lineage consisted of about 50 vPNs, all of which were labeled by *MZ699* or *GH146* (Lai *et al*., 2008). Comparing these results, we have to take into account that they were obtained by the use of two different techniques. BrdU incorporation used by us labels cells that go through S-phase, while the MARCM technique depends on the recombination-induced segregation of the Gal4 driver and the $Gal80^{ts}$ repressor during mitosis and labels a clone. This difference in techniques is important if S-phase and mitosis are separated by a large time period when, for example, GMCs are arrested in the G2-phase during embryogenesis, as has been postulated for neuroblast lineages in the PNS (Prokop and Technau, 1994) and CNS (Truman and Bate, 1988; Champlin and Truman, 1998). If some *Poxn*-neurons were arrested in G2 and divide only in larvae, our number of *Poxn*-neurons born after embryogenesis would be underestimated and, accordingly, that of *Poxn*-neurons born during embryogenesis overestimated.

In addition, it is possible that uptake of BrdU by feeding larvae and its incorporation into DNA was delayed and S-phase activity during very early larval life was missed, which would also result in an underestimation of the vPNs born after embryogenesis. However, since the total number of neurons that express Poxn in each brain hemisphere increases only by 10 during the entire first instar (Table 1), we may ignore this last effect. We further disregard the trivial explanation that the observed numbers of *Poxn*-neurons labeled by BrdU is affected by the failure to detect the Poxn

and BrdU signals, which would result in a slight underestimation of the number of Poxn-expressing cells born after embryogenesis.

Thus, if none of the *Poxn*-neurons of the VC are arrested in G2 during embryogenesis, our results suggest that 30-45 Poxn-expressing vPNs of each VC are born during embryogenesis which implies, when combined with the 50 vPNs of the postembryonic vPN lineage (Lai *et al*., 2008), that there are at least 80 vPNs, which further implies that at least 20 vPNs of the postembryonic lineage do not express Poxn. On the other hand, of the 30-45 Poxn-expressing vPNs not labeled by BrdU at most about 18-33 might derive from cells arrested in G2 during embryogenesis. This conclusion is based on the assumption that the anterior and posterior clusters of Poxn-expressing cells in the embryonic brain correspond to the ventral and dorsal Poxn-expressing clusters on the adult brain, respectively. Our results show that the anterior Poxn-expressing cluster in the embryonic brain consists of 12 postmitotic neurons (Figure 17B and Table 1; Werner Boll, unpublished results). Thus, in the other extreme case, of the 60 vPNs that express Poxn about 48 are born after embryogenesis, which agrees nicely with the 50 vPNs of the postembyonic lineage (Lai *et al*., 2008). In addition, this case implies that about 12 Poxn-expressing vPNs are born during embryogenesis and that there are at least 60 vPNs. An analysis carried out by Werner Boll further showed that of the 6 vPNs labeled by *GH146* only 4 express Poxn. Therefore, at least a few vPNs do not express Poxn.

Werner Boll's results further showed that about 20 *Poxn*-neurons of the VC do not overlap with neurons marked by *MZ699*. Only 4 of these overlap with vPNs expressing *GH146*. If we assume that all *Poxn*-neurons of the ventral cluster in the adult brain contact the antennal lobe, as it appears, it follows that the remaining ≈ 16 *Poxn*-neurons

of the VC are vPNs that are not labeled by either of the two enhancer trap lines or are local interneurons.

In *Poxn* mutants, the projection pattern of *Poxn*-neurons is highly disturbed. In the absence of Poxn function, the projections of the VC neurons no longer pass through the larval and the developing adult antennal lobe and do not project through the mACT. As a consequence, the lateral brain regions are not targeted at all. The neurites of the VC sometimes seem to follow the inner antennocerebral tract, and sometimes they run more or less parallel to the neurites of the DC. The morphology of the VC *Poxn*-neurons is aberrant throughout development and leads to strongly reduced dendritic arborizations in the glomeruli of the adult antennal lobe, the complete absence of axonal projections in the mACT and of arborizations in the region of the lateral horn. Thus, although the neurons of the ventral Poxn cluster obviously differ in function from the dorsal Poxn cluster, superficially they exhibit the same kind of phenotype in the absence of the Poxn function: their survival and basic neuronal fate are independent of Poxn, while their ability to target the correct neuropil regions is strongly impaired.

Therefore, a possible function of the transcription factor Poxn in the brain might be the direct or indirect activation of genes that are important for pathfinding and, in the ventral cluster, for specification of the vPN fate. In both clusters Poxn might activate similar pathways that regulate their correct wiring in the brain. The phenotype of *Poxn* mutant brains resembles to a certain extent the defects observed in the dendritic targeting of neurons in the antennal lobe of *Dscam* mutants (Zhu *et al*., 2006). Dscam, a cell adhesion molecule is crucial for proper neuronal wiring (Schmucker *et al*., 2000). In *Dscam* mutants in which the expression of specific Dscam iso-forms is suppressed by RNAi, the antennal lobe glomeruli are not targeted to the same extent as in the wild type, the processes are more compact, and the axonal arborizations patterns are highly aberrant

(Hattori *et al*., 2007; Shi *et al*., 2007). Thus, as *Poxn* mutants manifest similar problems, Poxn might be involved in the control of dendritic and axonal pathfinding, potentially through cell surface adhesion molecules.

The morphological phenotype of these two groups of neurons, dorsal and ventral, is also reflected by an aberrant behavior of *Poxn* mutants. Previous work in our lab showed that *Poxn* mutant males do not initiate courtship towards receptive females in the dark (Boll and Noll, 2002; Krstic *et al*., 2009). Since *Poxn* mutant males rescued by the *Poxn* transgene, *PK6*, which rescues the *Poxn* function required for brain development but not that necessary for taste bristle development, initiate courtship in the absence of visual cues, it followed that the *Poxn*-neurons in the adult brain are involved in the processing of olfactory information (Boll and Noll, 2002). Dimitrije Krstic in our lab was able to phenocopy this effect by introducing the olfactory mutation $Or83b^2$ (Larsson *et al*., 2004) into a *Poxn* mutant whose brain function was rescued by *PK6*. Thus, he could demonstrate that the *Poxn* brain function is essential for the processing of olfactory information important in courtship (Krstic, 2009). Therefore, the courtship phenotype of *Poxn* mutant males can be directly correlated with the obvious morphological and implied functional defects of their vPNs. In the absence of Poxn function, these vPNs are not able to relay olfactory information to the lateral horn, one of the higher olfactory centers in the brain. Although this seems to be a likely explanation for the observed behavioral phenotype and its link to the processing of olfactory information, it does not rule out that *Poxn*-neurons of the DC, which so far have not been implicated in the processing of olfactory information, are involved in the processing of a pheromonal olfactory signal as well. It also remains to be tested whether the aberrant dendritic projections of *Poxn*-vPNs in the adult antennal lobe are essential for the integrity of the olfactory network in this neuropil, as it has been proposed that the interaction among

dendritic projections of different PNs might be important for the patterning of the adult antennal lobe (Jefferies *et al*., 2004).

5. References

Awasaki, T. and Kimura, K. I. (1997). *pox neuro* is required for development of chemosensory bristles in *Drosophila*. *J. Neurobiol*. **32**, 707 -721.

Awasaki, T. and Kimura, K. I. (2001). Multiple function of *poxn* gene in larval PNS development and in adult appendage formation of *Drosophila*. *Dev. Genes Evol*. **211**, 20-29.

Bainbridge, S. P. and Bownes, M. (1981). Staging the metamorphosis of *Drosophila melanogaster*. *J. Embryol. Exp. Morphol.* **66**, 57-80.

Bate, C.M. (1976). Pioneer neurones in an insect embryo. *Nature* **260**, 54-56.

Bearer, E. L. (2003). Overview of image analysis, image importing, and image processing using freeware. *Curr. Protoc. Mol. Biol.* **14**, 14-15.

Benton, R., Vannice, K. S., Gomez-Diaz, C., and Vosshall, L. B. (2009). Variant ionotropic glutamate receptors as chemosensory receptors in *Drosophila*. *Cell* **136**, 149-162.

Bodmer, R., Carretto, R., and Jan, Y. N. (1989). Neurogenesis of the peripheral nervous system in *Drosophila* embryos: DNA replication patterns and cell lineages. *Neuron* **3**, 21-32.

Boll, W. and Noll, M. (2002). The *Drosophila Pox neuro* gene: control of male courtship behavior and fertility as revealed by a complete dissection of all enhancers. *Development* **129**, 5667-5681.

Bopp, D., Jamet, E., Baumgartner, S., Burri, M., and Noll, M. (1989). Isolation of two tissue-specific *Drosophila* paired box genes, *Pox meso* and *Pox neuro*. *EMBO J*. **8**, 3447-3457.

Breidbach, O., Dennis, R., Marx, J., Görlach, C., Wiegandt, H., and Wegerhoff, R. (1992). Insect glial cells show differential expression of a glycolipid-derived, glucuronic

acid-containing epitope throughout neurogenesis: detection during postembryogenesis and regeneration in the central nervous system of *Tenebrio molitor* L. *Neurosci. Lett.* **147**, 5-8.

Campos, A. R., Rosen, D. R., Robinow, S. N., and White, K. (1987). Molecular analysis of the locus *elav* in *Drosophila melanogaster*: a gene whose embryonic expression is neural specific. *EMBO J.* **6**, 425-431.

Carlson, J. R. (1996). Olfaction in *Drosophila*: from odor to behavior. *Trends Genet.* **12**, 175-180.

Carmona, R., Macías, D., Guadix, J. A., Portillo, V., Pérez-Pomares, J. M., and Muñoz-Chápuli, R. (2007). A simple technique of image analysis for specific nuclear immunolocalization of proteins. *J. Microsc.* **225**, 96-99.

Champlin, D. T. and Truman, J. W. (1998). Ecdysteroid control of cell proliferation during optic lobe neurogenesis in the moth *Manduca sexta*. *Development* **125**, 269-277.

Choksi, S. P., Southall, T. D., Bossing, T., Edoff, K., de Wit, E., Fischer, B. E., van Steensel, B., Micklem, G., and Brand, A. H. (2006). Prospero acts as a binary switch between self-renewal and differentiation in *Drosophila* neural stem cells. *Dev. Cell* **11**, 775-789.

Chu-Lagraff, Q., Wright, D. M., McNeil, L. K., and Doe, C. Q. (1991). The prospero gene encodes a divergent homeodomain protein that controls neuronal identity in *Drosophila*. *Development* **2**, 79-85.

Collins, T. J. (2007). ImageJ for microscopy. *Biotechniques* **43**, 25-30.

Consoulas, C., Duch, C., Bayline, R. J., and Levine, R. B. (2000). Behavioral transformations during metamorphosis: remodeling of neural and motor systems. *Brain Res. Bull.* **53**, 571-583.

Consoulas, C., Restifo, L. L., and Levine, R. B. (2002). Dendritic remodeling and growth of motoneurons during metamorphosis of *Drosophila melanogaster*. *J. Neurosci.* **22**, 4906-4917.

Couto, A., Alenius, M., and Dickson, B. J. (2005). Molecular, anatomical, and functional organization of the *Drosophila* olfactory system. *Curr. Biol.* **15**, 1535-1547.

Dambly-Chaudière, C., Jamet, E., Burri, M., Bopp, D., Basler, K., Hafen, E., Dumont, N., Spielmann, P., Ghysen, A., and Noll, M. (1992). The paired box gene *pox neuro*: a determinant of poly-innervated sense organs in *Drosophila*. *Cell* **69**, 159 -172.

de Belle, J. S. and Heisenberg, M. (1994). Associative odor learning in *Drosophila* abolished by chemical ablation of mushroom bodies. *Science* **263,** 692-695.

de Bruyne, M., Clyne, P. J., and Carlson, J. R. (1999). Odor coding in a model olfactory organ: the *Drosophila* maxillary palp. *J. Neurosci*. **19**, 4520-4532.

de Bruyne, M., Foster, K., and Carlson, J. R. (2001). Odor coding in the *Drosophila* antenna. *Neuron* **30**, 537-552.

Doe, C. Q., Chu-LaGraff, Q., Wright, D. M., and Scott, M. P. (1991). The prospero gene specifies cell fates in the *Drosophila* central nervous system. *Cell* **65**, 451-464.

Dumstrei, K., Wang, F., Nassif, C., and Hartenstein, V. (2003). Early development of the *Drosophila* brain: V. Pattern of postembryonic neuronal lineages expressing DE-cadherin. *J. Comp. Neurol*. **455,** 451-462.

Eliceiri, K. W. and Rueden, C. (2005). Tools for visualizing multidimensional images from living specimens. *Photochem. Photobiol.* **81**, 1116-1122.

Fishilevich, E. and Vosshall, L. B. (2005). Genetic and functional subdivision of the *Drosophila* antennal lobe. *Curr. Biol.* **15**, 1548-1553.

Grenningloh, G., Rehm, E. J., and Goodman, C. S. (1991). Genetic analysis of growth cone guidance in *Drosophila*: fasciclin II functions as a neuronal recognition molecule. *Cell* **67**, 45–57.

Hallem, E. A. and Carlson, J. R. (2004). The odor coding system of *Drosophila*. *Trends Genet.* **20**, 453-459.

Hallem, E. A. and Carlson, J. R. (2006). Coding of odors by a receptor repertoire. *Cell* **125**, 143-160.

Halter, D. A., Urban, J., Rickert, C., Ner, S. S., Ito, K., Travers, A. A., and Technau, G. M. (1995). The homeobox gene repo is required for the differentiation and maintenance of glia function in the embryonic nervous system of *Drosophila melanogaster*. *Development* **121**, 317-332.

Hanesch, U., Fischbach, K. F., and Heisenberg, M. (1989). Neuronal architecture of the central complex in *Drosophila melanogaster*. *Cell Tiss. Res.* **257**, 343-366.

Hattori, D., Demir, E., Kim, H. W., Viragh, E., Zipursky, S. L., and Dickson, B. J. (2007). Dscam diversity is essential for neuronal wiring and self-recognition. *Nature* **449**, 223-227.

Heimbeck, G., Bugnon, V., Gendre, N., Keller, A., and Stocker, R. F. (2001). A central neural circuit for experience-independent olfactory and courtship behavior in *Drosophila melanogaster*. *Proc. Natl. Acad. Sci. USA* **98**, 15336-15341.

Heinze, S. and Homberg, U. (2007). Maplike representation of celestial *E*-vector orientations in the brain of an insect. *Science* **315**, 995-997.

Hidalgo, A. and Brand, A. H. (1997). Targeted neuronal ablation: the role of pioneer neurons in guidance and fasciculation in the CNS of *Drosophila*. *Development* **124**, 3253-3262.

Homberg, U. (1987). Structure and functions of the central complex in insects. In: Arthropod brain: its evolution, development, structure, and functions (Gupta AP, Ed.). New York, Wiley & Sons 347-367.

Homberg, U. (2002). Neurotransmitters and neuropeptides in the brain of the locust. *Microsc. Res. Techniq*. **56**, 189–209.

Homberg, U. (2008). Evolution of the central complex in the arthropod brain with respect to the visual system. *Arthropod Struct. Dev.* **37**, 347-362.

Homberg, U., Vitzthum, H., Müller, M., and Binkle, U. (1999). Immunocytochemistry of GABA in the central complex of the locust *Schistocerca gregaria*: identification of immunoreactive neurons and colocalization with neuropeptides. *J. Comp. Neurol.* **409**, 495–507.

Ilius, M., Wolf, R., and Heisenberg, M. (1994). The central complex of *Drosophila melanogaster* is involved in flight control: studies on mutants and mosaics of the gene *ellipsoid body open*. *J. Neurogenet.* **9**, 189-206.

Ito, K. and Hotta, Y. (1992). Proliferation pattern of postembryonic neuroblasts in the brain of *Drosophila melanogaster*. *Dev. Biol*. **149**, 134-148.

Ito, K., Sass, H., Urban, J., Hofbauer, A., and Schneuwly, S. (1997). GAL4-responsive UAS-*tau* as a tool for studying the anatomy and development of the *Drosophila* central nervous system. *Cell Tissue Res.* **290**, 1-10.

Ito, K., Suzuki, K., Estes, P., Ramaswami, M., Yamamoto, D., and Strausfeld, N. J. (1998). The organization of extrinsic neurons and their implications in the functional roles of the mushroom bodies in *Drosophila melanogaster Meigen*. *Learn Mem.* **5**, 52-77.

Jäger, R. and Fischbach, K. F. (1987). Some improvements of the Heisenberg-Böhl method for mass histology of *Drosophila* heads. *Dros. Inf. Serv*. **66**, 162-165.

Jefferis, G. S. X. E., Marin, E. C., Stocker, R. F., and Luo, L. (2001). Target neuron prespecification in the olfactory map of *Drosophila*. *Nature* **414**, 204-208.

Jefferis, G. S. X. E., Marin, E. C., Watts, R. J., and Luo, L. (2002). Development of neuronal connectivity in *Drosophila* antennal lobes and mushroom bodies. *Curr. Opin. Neurobiol.* **12**, 80-86.

Jefferis, G. S. X. E., Potter, C. J., Chan, A. M., Marin, E. C., Rohlfing, T., Maurer, C. R. Jr., and Luo, L. (2007). Comprehensive maps of *Drosophila* higher olfactory centers: spatially segregated fruit and pheromone representation. *Cell* **128**, 1187-1203.

Jefferis, G. S., Vyas, R. M., Berdnik, D., Ramaekers, A., Stocker, R. F., Tanaka, N. K., Ito, K., and Luo, L. (2004). Developmental origin of wiring specificity in the olfactory system of *Drosophila*. *Development* **131**, 117-130.

Keleman, K., Ribeiro, C., and Dickson, B. J. (2005). Comm function in commissural axon guidance: cell-autonomous sorting of Robo in vivo. *Nature Neurosci.* **8**, 156-163.

Kidd, T., Bland, K. S., and Goodman, C. S. (1999). Slit is the midline repellent for the robo receptor in *Drosophila*. *Cell* **96**, 785-794.

Kondoh, Y., Kaneshiro, K. Y., Kimura, K., and Yamamoto, D. (2003). Evolution of sexual dimorphism in the olfactory brain of Hawaiian *Drosophila*. *Proc R Soc Lond B* **270**, 1005–1013.

Kramer, J. M. and Staveley, B. E. (2003). GAL4 causes developmental defects and apoptosis when expressed in the developing eye of *Drosophila melanogaster*. *Genet. Mol. Res*. **2**, 43-47.

Krstic, D. (2009). Influence of *Pox neuro* on courtship behavior of the *Drosophila* male: dissection of sensory cues and neuronal network underlying olfactory pheromone processing in the adult brain. Ph.D. thesis, University of Zürich.

Krstic, D., Boll, W., and Noll, M. (2009). Sensory integration regulating male courtship behavior in *Drosophila*. *PLoS ONE* **4**, e4457.

Küppers, B., Sanchez-Soriano, N., Letzkus, J., Technau, G. M., and Prokop, A. (2003). In developing *Drosophila* neurones the production of gamma-amino butyric acid is tightly regulated downstream of glutamate decarboxylase translation and can be influenced by calcium. *J. Neurochem*. **84**, 939–951.

Lachmanovich, E., Shvartsman, D. E., Malka, Y., Botvin, C., Henis, Y. I., and Weiss, A. M. (2003). Co-localization analysis of complex formation among membrane proteins by computerized fluorescence microscopy: application to immunofluorescence co-patching studies. *J. Microsc*. **212**, 122-131.

Lai, S.-L., Awasaki, T., Ito, K., and Lee, T. (2008). Clonal analysis of *Drosophila* antennal lobe neurons: diverse neuronal architectures in the lateral neuroblast lineage. *Development* **135**, 2883-2893.

Laissue, P. P. and Vosshall, L. B. (2008). The olfactory sensory map in *Drosophila*. In: Brain Development in *Drosophila melanogaster* (Technau, G. M., ed.). Springer, New York, pp. 102-114.

Larsson, M. C., Domingos, A. I., Jones, W. D., Chiappe, M. E., Amrein, H., and Vosshall, L. B. (2004). *Or83b* encodes a broadly expressed odorant receptor essential for *Drosophila* olfaction. *Neuron* **43**, 703-714.

Lee, T. and Luo, L. (1999). Mosaic analysis with a repressible cell marker for studies of gene function in neuronal morphogenesis. *Neuron* **22**, 451-461.

Levine, R. B., Morton, D. B., and Restifo, L. L. (1995). Remodeling of the insect nervous system. *Curr. Opin. Neurobiol.* **5**, 28-35.

Li, L. and Vaessin, H. (2000). Pan-neural Prospero terminates cell proliferation during *Drosophila* neurogenesis. *Genes Dev*. **14**, 147-151.

Lin, H.-H., Lin, C.-Y., and Chiang, A.-S. (2007). Internal representations of smell in the *Drosophila* brain. *J. Biomed. Sci.* **14**, 453-459.

Liu, G., Seiler, H., Wen, A., Zars, T., Ito, K., Wolf, R., Heisenberg, M., and Liu, L. (2006). Distinct memory traces for two visual features in the *Drosophila* brain. *Nature* **439**, 551-556.

Loesel, R., Nässel, D. R., and Strausfeld, N. J. (2002). Common design in a unique midline neuropil in the brains of arthropods. *Arthropod Struct. Dev*. **31**, 77-91.

Manders, E. M., Stap, J., Brakenhoff, G. J., van Driel, R., and Aten, J. A. (1992). Dynamics of three-dimensional replication patterns during the S-phase, analysed by double labelling of DNA and confocal microscopy. *J. Cell Sci.* **103**, 857–862.

Manders, E. M. M., Verbeek, F. J., and Aten, J. A. (1993). Measurement of colocalization of objects in dual-colour confocal images. *J. Microsc.* **169**, 375–382.

Mariotta, L. (2007). Functional dissection of the *Poxn* brain enhancer in *Drosophila melanogaster*. Diploma thesis, Zürich.

Marin, E. C., Watts, R. J., Tanaka, N. K., Ito, K., and Luo, L. (2005). Developmentally programmed remodeling of the *Drosophila* olfactory circuit. *Development* **132**, 725-737.

Martin, J. R., Raabe, T., and Heisenberg, M. (1999). Central complex substructures are required for the maintenance of locomotor activity in *Drosophila melanogaster*. *J. Comp. Physiol. A* **185**, 277-288.

McGuire, S. E., Le, P. T., Osborn, A. J., Matsumoto, K., and Davis, R. L. (2003). Spatiotemporal rescue of memory dysfunction in *Drosophila*. *Science* **302**, 1765-1768.

McGuire, S. E., Mao, Z., and Davis, R. L. (2004). Spatiotemporal gene expression targeting with the TARGET and gene-switch systems in *Drosophila*. *Sci. STKE*. **12**, l6.

Menon, K.P., Sanyal, S., Habara, Y., Sanchez, R., Wharton, R. P., Ramaswami, M., and Zinn, K. (2004). The translational repressor Pumilio regulates presynaptic morphology and controls postsynaptic accumulation of translation factor eIF-4E. *Neuron* **44**, 663-676.

Müller, M., Homberg, U., and Kühn A. (1997). Neuroarchitecture of the lower division of the central body in the brain of the locust (*Schistocerca gregaria*). *Cell Tissue Res.* **288**, 159-176.

Nassif, C., Noveen, A., and Hartenstein, V. (2003). Early development of the *Drosophila* brain: III. The pattern of neuropile founder tracts during the larval period. *J. Comp. Neurol.* **455**, 417-434.

Neckameyer, W. S. and Cooper, R. L. (1998). GABA transporters in *Drosophila melanogaster*: molecular cloning, behavior, and physiology. *Invertebr. Neurosci.* **3**, 279-294.

Neuser, K., Triphan, T., Mronz, M., Poeck, B., and Strauss, R. (2008). Analysis of a spatial orientation memory in *Drosophila*. *Nature* **453**, 1244-1247.

Nicolas, E. and Preat, T. (2005). *Drosophila* central brain formation requires Robo proteins. *Dev Genes Evol.* **215**, 530-536.

Noll, M. (1993). Evolution and role of Pax genes. *Curr. Opin. Genet. Dev*. **3**, 595-605.

Okada, R., Awasaki, T., and Ito, K. (2009). Gamma-aminobuyric acid (GABA)-mediated neural connections in the *Drosophila* antennal lobe. *J. Comp. Neurol*. **514**, 74-91.

Pearson, K. (1909). Determination of the coefficient of correlation. *Science* **30**, 23-25.

Poeck, B., Triphan, T., Neuser, K., and Strauss, R. (2008). Locomotor control by the central complex in *Drosophila* – an analysis of the *tay* bridge mutant. *Dev. Neurobiol.* **68**, 1046-1058.

Popov, A. V., Peresleni, A. I., Ozerskii, P. V., Shchekanov, E. E., and Savvateeva-Popova, E. V. (2005). The role of the flabellar and ellipsoid bodies of the central complex of the brain of *Drosophila melanogaster* in the control of courtship behavior and communicative sound production in males. *Neurosci. Behav. Physiol.* **35**, 741-750.

Popov, A. V., Sitnik, N.A., Savvateeva-Popova, E.V., Wolf, R., and Heisenberg, M. (2003). The role of central parts of the brain in the control of sound production during courtship in *Drosophila melanogaster*. *Neurosci. Behav. Physiol.* **33**, 53-65.

Prokop, A. and Technau, G. M. (1994). BrdU incorporation reveals DNA replication in non dividing glial cells in the larval abdominal CNS of *Drosophila*. *Roux's Arch. Dev. Biol*. **204**, 54–61.

Python, F. and Stocker, R. F. (2002). Immunoreactivity against choline acetyltransferase, gamma-aminobutyric acid, histamine, octopamine, and serotonin in the larval chemosensory system of *Drosophila melanogaster*. *J. Comp. Neurol.* **453**, 157–167.

Renn, S. C. P., Armstrong, J. D., Yang, M., Wang, Z., An, X., Kaiser, K., and Taghert, P. H. (1999). Genetic analysis of the *Drosophila* ellipsoid body neuropil: organization and development of the central complex. *J. Neurobiol*. **41**, 189 -207.

Robinow, S. and White, K. (1988). The locus *elav* of *Drosophila melanogaster* is expressed in neurons at all developmental stages. *Dev. Biol*. **126**, 294-303.

Sakura, M., Lambrinos, D., and Labhart, T. (2008). Polarized skylight navigation in insects: model and electrophysiology of e-vector coding by neurons in the central complex. *J. Neurophysiol.* **99**, 667-682.

Schmid, F. (2005). Analysis of the *Poxn* function in the adult brain of *Drosophila melanogaster*. Diploma thesis, Zürich.

Schmucker, D., Clemens, J. C., Shu, H., Worby, C. A., Xiao, J., Muda, M., Dixon, J. E., and Zipursky, S. L. (2000). *Drosophila* Dscam is an axon guidance receptor exhibiting extraordinary molecular diversity. *Cell* **101**, 671-684.

Scholz, H., Ramond, J., Singh, C. M., and Heberlein, U. (2000). Functional ethanol tolerance in *Drosophila*. *Neuron* **28**, 261-271.

Shi, L., Yu, H. H., Yang, J. S., and Lee, T. (2007). Specific *Drosophila* Dscam juxtamembrane variants control dendritic elaboration and axonal arborization. *J. Neurosci*. **27**, 6723-6728.

Spletter, M. L., Liu, J., Liu, J., Su, H., Giniger, E., Komiyama, T., Quake, S., and Luo, L. (2007). Lola regulates *Drosophila* olfactory projection neuron identity and targeting specificity. *Neural Dev*. **2**:14.

Stocker, R. F. (1994). The organization of the chemosensory system in *Drosophila melanogaster*: a review. *Cell Tissue Res.* **275**, 3-26.

Stocker, R. F., Lienhard, M. C., Borst, A., and Fischbach, K. F. (1990). Neuronal architecture of the antennal lobe in *Drosophila melanogaster*. *Cell Tissue Res.* **262**, 9-34.

Stocker, R. F., Heimbeck, G., Gendre, N., and de Belle, J. S. (1997). Neuroblast ablation in *Drosophila* P[GAL4] lines reveals origins of olfactory interneurons. *J. Neurobiol.* **32**, 443-456.

Stockinger, P., Kvitsiani, D., Rotkopf, S., Tirián, L., and Dickson, B. J. (2005). Neural circuitry that governs *Drosophila* male courtship behavior. *Cell* **121**, 795-807.

Strausfeld, N. J. (1998). Crustacean–insect relationships: the use of brain characters to derive phylogeny amongst segmented invertebrates. *Brain Behav. Evol.* **52**, 186–206.

Strausfeld, N. J. (1999). A brain region in insects that supervises walking (Binder MD, Ed.). *Prog. Brain Res.* **123**, 273-284.

Strauss, R. (2002). The central complex and the genetic dissection of locomotor behavior. *Curr. Opin. Neurobiol.* **12**, 633-638.

Strauss, R. and Heisenberg, M. (1993). A higher control center of locomotor behavior in the *Drosophila* brain. *J. Neurosci*. **13**, 1852-1861.

Tissot, M. and Stocker, R. F. (2000). Metamorphosis in *Drosophila* and other insects: the fate of neurons throughout the stages. *Prog. Neurobiol*. **62**, 89-111.

Truman, J. W. (1990). Metamorphosis of the central nervous system of *Drosophila*. *J. Neurobiol.* **21**, 1072-1084.

Truman, J. W. and Bate, M. (1988). Spatial and temporal patterns of neurogenesis in the central nervous system of *Drosophila melanogaster*. *Dev. Biol*. **125**, 145-157.

Urbach, R. (2007). A procephalic territory in *Drosophila* exhibiting similarities and dissimilarities compared to the vertebrate midbrain/hindbrain boundary region. *Neural Dev*. **2**: 23.

Vitzthum, H., Müller, M., and Homberg, U. (2002). Neurons of the central complex of the locust *Schistocerca gregaria* are sensitive to polarized light. *J. Neurosci.* **22**, 1114-1125.

Vosshall, L. B. and Stocker, R. F. (2007). Molecular architecture of smell and taste in *Drosophila*. *Annu. Rev. Neurosci.* **30**, 505-533.

Vosshall, L. B., Wong, A. M., and Axel, R. (2000). An olfactory sensory map in the fly brain. *Cell* **102**, 147-159.

Wagh, D. A., Rasse, T. M., Asan, E., Hofbauer, A., Schwenkert, I., Dürrbeck, H., Buchner, S., Dabauvalle, M. C., Schmidt, M., Qin, G., Wichmann, C., Kittel, R., Sigrist, S. J., and Buchner, E. (2006). Bruchpilot, a protein with homology to ELKS/CAST, is required for structural integrity and function of synaptic active zones in *Drosophila*. *Neuron* **16**, 833-844.

Wilson, R. I. and Laurent, G. (2005). Role of GABAergic inhibition in shaping odor-evoked spatiotemporal patterns in the *Drosophila* antennal lobe. *J. Neurosci.* **25,** 9069-9079.

Witten, J. L. and Truman, J. W. (1998). Distribution of GABA-like immunoreactive neurons in insects suggests lineage homology. *J. Comp. Neurol.* **398**, 515–528.

Woods, D. F. and Bryant, P. J. (1991). The discs-large tumor suppressor gene of *Drosophila* encodes a guanylate kinase homolog localized at septate junctions. *Cell* **66**, 451-464.

Wu, C.L., Xia, S., Fu, T.F., Wang, H., Chen, Y. H., Leong, D., Chiang, A.S., and Tully, T. (2007). Specific requirement of NMDA receptors for long-term memory consolidation in *Drosophila* ellipsoid body. *Nature Neurosci.* **10**, 1578-1586.

Wu, J. S. and Luo, L. (2006). A protocol for dissecting *Drosophila melanogaster* brains for live imaging or immunostaining. *Nature Protoc.* **1**, 2110-2115.

Xiong, W. C., Okano, H., Patel, N. H., Blendy, J. A., and Montell, C. (1994). repo encodes a glial-specific homeo domain protein required in the *Drosophila* nervous system. *Genes Dev.* **8**, 981-994.

Younossi-Hartenstein, A., Nguyen, B., Shy, D., and Hartenstein, V. (2006). Embryonic origin of the *Drosophila* brain neuropile. *J. Comp. Neurol.* **497**, 981-998.

Younossi-Hartenstein, A., Salvaterra, P. M., and Hartenstein, V. (2003). Early development of the *Drosophila* brain: IV. Larval neuropile compartments defined by glial septa. *J. Comp. Neurol.* **455**, 435-450.

Zito, K., Fetter, R. D., Goodman, C. S., and Isacoff, E. Y. (1997). Synaptic clustering of Fascilin II and Shaker: essential targeting sequences and role of Dlg. *Neuron* **19**, 1007-1016.

Zhu, H., Hummel, T., Clemens, J. C., Berdnik, D., Zipursky, S. L., and Luo, L. (2006). Dendritic patterning by Dscam and synaptic partner matching in the *Drosophila* antennal lobe. *Nature Neurosci.* **9**, 349-355.

Acknowledgments

It is a privilege to acknowledge with gratitude all the support and encouragement I have received from all the people who have assisted me in completing the project. First and foremost, with due reverence I would like to thank my supervisor Prof. Markus Noll for providing me the opportunity to work under his supervision. I am extremely indebted for his patient guidance. His valuable suggestions have helped me to instill scientific attitude to discern and unwind the intricacies of *Drosophila* neural biology and motivated me to persistently strive for perfection. The experience I gained under his stewardship will be a cherishing memory throughout my life.

A special word of thanks to Werner Boll for his guidance smothered with constant encouragement and motivation, which helped me to enshrine the importance of constant perseverance in untangling the most perplexing problems. He taught me all the basics of *Drosophila* neurogenetics and constantly helped me to develop the aptitude to think, analyze carefully and ratiocinate. The everyday discussions with him were priceless and always very enlightening. He always showed benevolent and helpful attitude to solve my scientific and other quotidian problems especially with german translations.

I also thank Markus and Werner for editing my thesis and providing valuable suggestions.

I sincerely thank Prof. Reinhard F. Stocker, and Prof. Konrad Basler for being a part of my thesis committee, and for providing helpful suggestions to improve my scientific work. The scientific discussions during the committee meetings were always instrumental in instigating new ideas for unwinding the intricacies surrounding the complex *Drosophila* brain.

Thanks are due to the past and present members of the Noll group for their unconditional help, practical guidance, and nice company during my stay in the lab.

I would also like to thank Prof. Walter Schaffner, Prof. Bernhard Dichtl, and their lab members for numerous insightful scientific discussions during progress and literature seminars.

I would always be grateful to all my friends especially Vaibhav for standing by me in all ups and downs, and for building my confidence whenever I felt low. I would also like to thank Annina, Jasmin, Sandra, Nikunj, Ashok, Manoj, Manuel, Jyoti, Akshay, Namit and Amit for the many enjoyable moments I had with them.

Last but not the least; I would like to express deep gratitude to my parents and my brother, Vikas for their unconditional love, affection, and wholesome support. They have always been encouraging me through all my endeavors and boosting my morale to fight back whatsoever problems thwarted my way. I lost my father in 2009, and after that it has been a difficult journey for the whole family. I would like to thank them for there patience and strong will that kept me going. It would have not been possible for me to complete this thesis without there assistance and moral support at every turn of my life.

At the end, I would like to acknowledge the providence of Almighty God and am immensely grateful for his protection and favor.

CURRICULUM VITAE

PERSONAL DATA

First name and surname: Shilpi MINOCHA

Date of Birth: 18th of October 1982

Place of birth: New Delhi, India

Nationality: Indian

EDUCATION

07.2006- present

Ph.D. Student
Molecular Life Science Ph.D. program
Institute of Molecular Biology
University of Zürich, Switzerland

Project Supervisor: Prof. Markus Noll
Topic of Research: Role of *Poxn* during development of *Drosophila* brain: fate determination of ellipsoid body large-field neurons and ventral projection neurons.

09.2005-06.2006

Research Assistant
International **C**entre for **G**enetic **E**ngineering and **B**iotechnology, New Delhi, India

Project Supervisor: Dr. Amit P. Sharma
Topic of research: "Structural/ functional/ computational studies on peptides, proteins and genes of direct relevance to human pathogens and human diseases particularly Malaria".

2003-2005

Master of Science with Honors
Main subject: Molecular Biology and Biotechnology
Department of Plant Molecular Biology and Biotechnology
University of Delhi, South Campus, India

Percentage obtained: 76.9% (A+) University Topper.

Diploma Thesis Project Supervisor: Prof. Akhilesh Kr. Tyagi
Topic of Research: **"Analysis of single nucleotide polymorphisms for chromosome 11 in *japonica* and *indica* (PB1 and IR64) rice"**. Duration (April 2004 – May 2005).

2000- 2003

Bachelor of Science with Honors
Main subject: Microbiology
Ram Lal Anand College
University of Delhi, South Campus, India

Percentage obtained: 73.5% (A+) University Topper

PRACTICAL TRAINING

DNA/RNA Based Techniques: DNA/ RNA extraction and purification from bacteria and plants, Polymerase chain reaction (Real-time PCR, RT-PCR, PCR-RFLP, Inverse), Transformation/Transfection, Restriction digestion and cloning.
Protein Based Techniques*:* Protein profiling using SDS-PAGE 1D/2D, Isoelectric focusing, Western Blotting, *In vitro* Kinase Assay, Isolation of recombinant protein using Ni-NTA bead and GST bead columns, Chromatography – size exclusion and TLC, Autoradiography, X-ray crystallography and fluorography.
Cell and Tissue culture*:* Isolation of sub-cellular components, cell fractionation, sectioning and staining of plant tissue, Androgenesis, Somatic Embryogenesis, Transfection and Organogenesis.
Microbiological Techniques*:* Isolation and enrichment for bacterial/fungal growth, maintenance and preservation of culture, Ame's Test, screening for drug resistance.
Bioinformatics*:* BLAST, ENSEMBL, NCBI, SWISS-PROT, ExPASY, UNIX Programming (Phred, Phrap, Consed and PolyPhred), MegAlign, ClustalW, Windows XP/Vista, Adobe Illustrator/Photoshop.
Others*:* ELISA, Immunoprecipitation, TLC/DLC, Confocal Microscopy.

AWARDS AND ACHIEVEMENTS

2005
- Qualified Graduate Aptitude Test in Engineering (GATE) with 94.48 percentile conducted by conducted by the Indian Institutes of Technology and the Indian Institute of Science, Bangalore.
- Award of Lectureship (Net) Awarded by Human Resource Development Group, Council of Scientific & Industrial Research, India.
- Junior Research Fellowship awarded by University Grants Commission, India.
- South Campus Post-Graduate Scholarship for scoring highest marks during Masters.
- Best Female Student award for outstanding performance in studies and co-curricular activities.

2004
- All India Post-Graduate Scholarship for scoring highest marks during Bachelors.
- Rotary Scholarship excellence in extra co-curricular activities.
- Sonia Ashta Award for best biology student.
- Best Pass student for getting highest marks in the university.

2003
- First prize in Annual Quiz Competition, Microbiology Society of Delhi University.
- First prize in Poster making, Microbiology Society of Delhi University.
- Vice-President of the Mikrobiologika Society (Student's Academic Society for Microbiology).

ORAL PRESENTATIONS

- Talk at CALZONE - Colloquium for life science PhD students organized by Young European Biotech Network Switzerland (YEBN Switzerland).
- Talk at 12th European *Drosophila* Neurobiology Conference (Neurofly 2008) at University of Würzburg, Germany (6^{th}-10^{th} September 2008).
- Talk at Developmental Biology Research groups Lunch Seminars at Institute of Molecular Biology, University of Zürich (5^{th} December 2008).
- Invited talk at Biozentrum Universität Basel (16^{th} December 2008) organized by Prof. Heinrich Reichert.
- Invited Talk at Biozentrum, Universität Fribourg in Department of Biology (16^{th} June 2008) organized by Prof. Reinhard F. Stocker.

POSTER PRESENTATIONS:

- Janelia Farm Research Campus (HHMI, Washington) for the conference on "Functional Anatomy of the Arthropod Central Complex & Motor System" (11^{th} – 14^{th} May, 2008).
- For two consecutive years at the Molecular Life Sciences PhD students retreat (2006 and 2007).
- Annual Swiss *Drosophila* Meeting in University of Bern (April 26, 2008).
- Institute of Molecular Biology Retreat (11.01.-13.01.2008) held in Stoos (Morschach).
- 21^{st} European *Drosophila* Research Conference, Nice-Acropolis, France (18^{th} November-21^{st} November, 2009).

INTERESTS AND ACTIVITIES:

Painting, Swimming, Traveling, Learning languages